UNIVERSITY OF PAVIA – IUSS SCHOOL FOR ADVANCED STUDIES PAVIA

Department of Brain and Behavioural Sciences (DBBS)
Master of Science Degree in Psychology, Neuroscience, and Human Sciences

SPIKE-TIMING-DEPENDENT PLASTICITY AT CEREBELLAR GOLGI CELL SYNAPSES

Supervisor: **Prof Lisa Mapelli**

Co-supervisor: **Dr Eleonora Pali**

Master's thesis written by

Tuba Özcan, **501466**

Academic year 2023/2024

Index

Abstract

The precise timing of action potentials, known as spike-timing, is crucial for enhancing information storage and computational efficiency in neuronal networks, supporting long-term synaptic plasticity mechanisms. The cerebellum is renowned for its role in coordinating precise timing during complex sensory and motor behaviours. At the input stage of the cerebellar cortex, Golgi cells (GoCs) function as the main inhibitory interneurons that govern the spatiotemporal reconfiguration of cerebellar inputs on a millisecond timescale. They receive excitatory signals from parallel fibres (PFs) on their apical dendrites and from mossy fibres (MFs) on their basal dendrites. However, the functional implications of segregating inputs across these two distinct dendritic projections, and their effects on GoC synaptic plasticity, remain to be elucidated. Recently, a multicompartmental GoC model predicted that this anatomical arrangement, coupled with the specific N-methyl-D-aspartate receptors (NMDARs) localization on basal dendrites, could be instrumental in driving spike-timing dependent plasticity (STDP) at MF-GoC synapses. Based on these predictions, our study aimed to validate the existence of STDP at MF-GoC synapses. Whole-cell patch-clamp recordings were performed on acute cerebellar slices from GlyT2 transgenic mice. Stimulus pairs of MFs and PFs were applied with specific and fixed phase differences (±10, ±25, ±50, ±100 ms) at 4 Hz for 60 iterations. The involvement of NMDAR was evaluated using NMDAR antagonists (D-APV, 100 μM and 7-Cl Kyn, 50 μM). Consistent with model predictions, we observed bidirectional Hebbian STDP at MF-GoC synapses driven by NMDAR activation. Specifically, spike-timing dependent long-term potentiation (st-LTP) occurred when MF preceded PF stimulation, while spike-timing dependent long-term depression (st-LTD) occurred in the reversed order. Notably, the ±25 ms phase difference was found to be the most effective for inducing STDP. Overall, these findings demonstrate how temporally correlated PF and MF inputs are finely integrated in GoC basal dendrites to promote st-LTP or st-LTD, with high temporal precision. MF-GoC STDP may thus represent a novel plasticity mechanism for modulating GoC activity, thereby enhancing our understanding of timing and learning processes occurring within the cerebellar granular layer.

Key words: cerebellum, Golgi cells, spike timing-dependent plasticity, N-methyl-D-aspartate receptors, mossy fibres, parallel fibres

Acknowledgements

I would like to express my sincere gratitude to my supervisor, Prof Lisa Mapelli, for trusting me and welcoming me into her research laboratory. Her support allows me to write my thesis on a topic that I am passionate about. I would like to extend my heartfelt thanks to my co-supervisor, Dr Eleonora Pali. Her knowledge, guidance, and willingness to share her expertise were instrumental in the completion of this work.

Many thanks to my family for supporting me every step of my journey: my mother Hacer, my father Sadullah and my brothers Furkan and Buğra. I am lucky to have them as my family.

And many thanks to Lapo for making Pavia a home for me; it would have been much harder without his trust and support. I am also grateful to his family, Alessandra, and Franco for being my second family in Italy.

Lastly, I would like to thank my friends in Pavia - İrem, Bilgesu, and Merve - for accompanying me on this journey, and to my friend in Türkiye, Büşra, for believing in me and being my support system from afar.

Preface

This master's thesis is carried out in partial fulfilment of the requirements for the degree of Master of Science in Psychology, Neuroscience and Human Sciences at the University of Pavia and IUSS School of Advanced Studies. The goal of the student is to present solid neurophysiological research of STDP performed onto GoCs, from the literature review to the discussion of the results.

The thesis is separated into several parts; the introduction part provides the theoretical background for the experiment by the presentation of the historical investigation, theories and anatomy of cerebellum. Furthermore, it covers GoCs, STDP, and how STDP operates specifically onto GoCs. Later, the aim of study is presented. In the method part, the experimental design is explained step by step, giving a brief description of the whole-cell patch-clamp technique and its use in STDP research. The outcome of the research is provided in the result part. Then the results are discussed, and lastly the overall conclusion is presented.

A. Introduction

The introduction is divided into four different chapters. Each chapter includes the main components of this study aiming to provide necessary theoretical grounding. The first chapter begins with the history behind the cerebellum and presents the main cerebellar theories. The second chapter is based on the anatomical description of the cerebellum, which is the region of interest of this study. The third chapter is focused on GoC, a specific inhibitory cell type located in the granular layer of the cerebellar cortex and the target component of this investigation. The fourth chapter provides an overview on synaptic plasticity and how it operates in the cerebellum, with a focus on a peculiar type of synaptic plasticity called spike-timing dependent plasticity (STDP). The last part of the chapter presents work on how STDP occurs in cerebellar GoCs.

CHAPTER 1: HISTORY OF THE CEREBELLUM

1.1 Dissection Studies

The cerebellum derives from Latin and literally means “little brain”, since it is a tiny portion of the brain that accounts for only 10% of the entire brain volume (Kandel et al., 2000, p.832). However, its distinction from the cerebrum as a separate structure, attracted the attention of early philosophers since antiquity. The Roman physician Galen (A.D. 129/130-200/2001) was the first anatomist who systematically investigated the cerebellum of various animals, excluding humans, to define its functioning. According to Galen, the cerebellum was like a pump that regulates the flow of ‘*animal spirit’* (i.e., the liquid controlling muscle movements) (Valera, 2013). Additionally, he proposed that the central portion of the cerebellum, later called ‘*vermis*’, had particular importance for memory. In the Renaissance, Galen’s view of the cerebellar anatomy and functioning was revisited by Andreas Vesalius (1514-1569) in his book *De humani corporis fabria* (1543). He used a new methodology for the dissection of the human brain (Valera, 2013). In his comparative studies across vertebrates, he emphasised that the folding and fissures of the cerebellum are significantly less variable than those in the cerebral cortex (Glickstein et al., 2009). Instead, he refrained from making assumptions regarding cerebellar functions without having any experimental evidence (Glickstein et al., 2009; Catani and Sandrone, 2015, p. 133). Later, Varolio (1543-1575) characterised the cerebellar role in controlling sensory functions, including unconscious sensibility, and its connections with the pons (Glickstein et al., 2009). Using the same method, Thomas Willis (1664) identified the three main structures that connect the cerebellum with other brain areas, namely inferior, middle, and superior cerebellar peduncles (Catani & Sandrone, 2015, p. 134). Moreover, he identified that the cerebellum was crucial for vital involuntary actions, including respiration. Then, cerebellectomy studies performed on pigeons showed that removing the cerebellum did not lead to the animal death but resulted in crucial impairments of the equilibrium and movements (Catani & Sandrone, 2015, p.135).

During the 17th century, Malpighi (1628-1694) studied the organisation of the white fibres and the cerebellar cortex (Valera, 2013). Then, Raymond de Vieussens (1641–1716)

recognized a grey area of glandular substance later named as cerebellar nuclei by Félix Vicq dÁzyr (1746 –1794) (Glickstein et al., 2009). In the 18th century, the major divisions of the cerebellar anatomy were well described in Vincenzo Malacarne's (1744-1816) book *'Il Cervelletto'* (1776), representing the first work devoted solely to the cerebellum. In this book, he named each lobe and lobule of the cerebellum providing a detailed anatomical description.

I.2 Lesion Studies

At the beginning of the 19th century, lesion studies on animals were the most efficient approach to correlate specific functions to given brain regions. During this time, Alessandro Volta developed electrochemical batteries to generate electricity (Catani & Sandrone, 2015, p. 135). Following this discovery, Luigi Rolando (1773-1831) applied a certain amount of electricity to a cerebellar tissue and observed that limb movements were immediately triggered (Catani & Sandrone, 2015, p. 135). Thus, he concluded that the cerebellum must be strongly involved in the initiation of movements. On the other hand, Pierre Flourens (1794-1867) observed that cerebellar ablation did not result in the lack of movement but rather in altered motor coordination. Therefore, for the first time, the distinction between the generation and coordination of movement was made. Specifically, he posited that the production of movement occurred in the spinal cord and medulla oblongata, while the motor coordination occurred in the cerebellum (Glickstein et al., 2009). Then, Luciani (1840-1919) defined three main deficiencies following cerebellar lesions based on the alteration in the continuity of movement: asthenia, atonia, and astasia (D'Angelo et al., 2011; Glickstein et al., 2009). Later, Babinski (1857-1932) described in detail dysdiadochokinesia symptoms as the inability to perform rapid, alternating voluntary movements. Then, Holmes (1876-11965), studying the soldiers who had cerebellar stroke during the First World War, characterised ataxia and its symptoms (Glickstein et al., 2009; Valera, 2013).

From an anatomical perspective, evolutionary improvements were made by Bolk (1866-1930) in his comparative anatomy studies, leading to the division of the cerebellum into four main regions: the anterior lobe, the posterior vermis, and the two cerebellar hemispheres. A significant contribution by Bolk was his observation that the continuity of folia chains of the vermis and cerebellar hemispheres is consistent across animals and

humans. Afterwards, Larsell (1886-1964) recognized ten transverse units in the vermis defined as cerebellar lobules (Glickstein et al., 2009).

1.3 Cytoarchitecture and Physiology

At the end of the 19th century, following advancements in histological techniques and electrophysiological recordings, studies of the cerebellum were focused on the characterization of its cytoarchitecture and circuitry. Jan Evangelista Purkinje (1787-1869) provided early insights into individual elements of the nervous system, supporting the emerging neuron doctrine (Catani & Sandrone, 2015, p.139; Glickstein et al., 2009). Specifically, Purkinje characterised a peculiar type of cerebellar neuron that would later be called with his name (i.e., Purkinje cells). Then, Camillo Golgi (1843-1926) implemented the black reaction for staining neurons, ensuring the detailed visualisation of the entire neuron. He published his book titled "*Sulla fina anatomia del cervelletto umano"* (1874) where he described the cerebellar cytoarchitecture and cell connectivity (Figure 1.1). He also identified the primary cellular components of the cerebellum including Purkinje cells (PCs), stellate cells, granule cells (GrCs), and GoCs. Specifically, he provided detailed descriptions of GoCs defining them as 'big nervous cells' and intriguingly noting that their axonal plexus did not extend beyond the cerebellum, unlike PC axons which indeed represent the sole output of the entire cerebellar cortex (D'Angelo et al., 2011). Of particular interest is the reticular theory of neural organisation proposed by Golgi, suggesting that the nervous system forms a continuous network composed of axons. In contrast with the reticular theory, Santiago Ramon y Cajal (1852-1934) formulated the neuron doctrine. According to this doctrine, the brain and spinal cord are composed of discrete units called neurons communicating through synapses (Glickstein et al., 2009). Although the neuron doctrine was not substantiated until the advent of electron microscopy in the 1960s, both Golgi and Cajal were awarded the Nobel Prize in 1906 for their groundbreaking contributions to neuroscience (Glickstein et al., 2009; Catani & Sandrone, 2015, p.139).

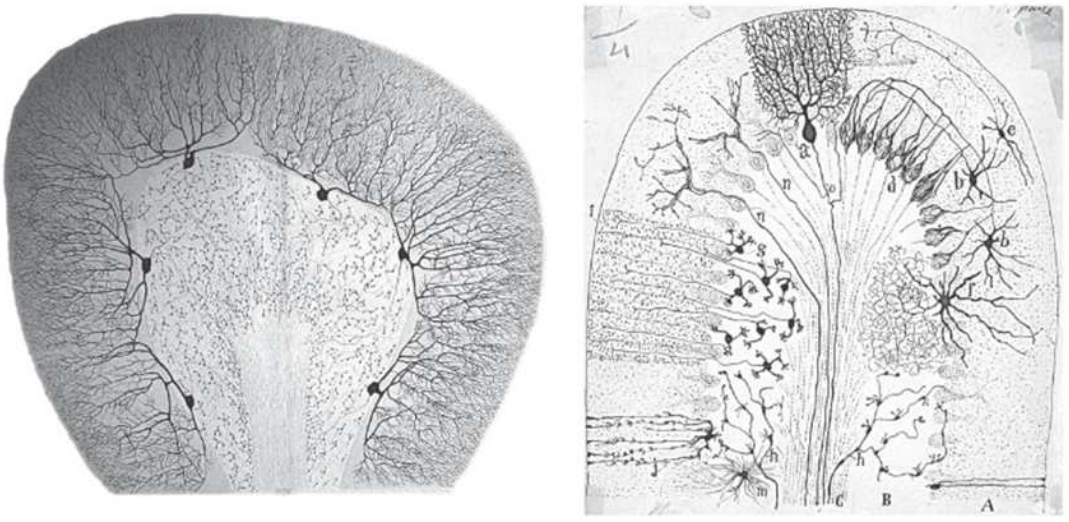

Figure 1.1. **Different representations of cerebellar cytoarchitecture.** Left: Camillo Golgi's representation of the cerebellar cells organised in a syncytium in a parasagittal section of a cerebellar folium (Golgi, 1903–1929). Right: Santiago Ramón Cajal's version representing neurons displayed as single units (Cajal, 1911) (Catani & Sandrone, 2015, p. 138).

Cajal continued expanding the knowledge of cerebellar cell types (Figure 1.1, right) by identifying additional cells such as Lugaro and unipolar brush cells (UBCs) and meticulously studying the cerebellar glomeruli within the granular layer (D'Angelo et al., 2011). Moreover, he characterised the two primary input fibres to the cerebellar cortex; the first is MFs, and the second is climbing fibres (CFs) with an origin in the inferior olivary nuclei (ION).

1.4 Cerebellar Theories

In 1928, Jelgersma proposed that PCs detect discrepancies between intention and execution, triggering corrective signals to the cerebral cortex for high-level coordination or to the spinal cord for low-level coordination (Glickstein et al., 2009). His insights on the formation of temporary connections during the learning process of cerebellar coordination anticipated later theories of cerebellar plasticity (Glickstein et al., 2009). Later, in the 1960s, a comprehensive work related to cerebellar functioning and structure was published in the book titled "*The Cerebellum as a Neural Machine"* (Eccles et al., 1967). The investigation of the

inhibitory and excitatory properties of various cerebellar neurons and their interactions led to a comprehensive understanding of the cerebellar cortex. Specifically, Eccles shed light on the inhibition of GrCs by GoCs, representing the first identification of a central inhibitory mechanism in the cerebellum (Eccles et al., 1964; D'Angelo et al., 2011). Subsequently in 1973, he proposed that the cerebellum has a large computational capacity due to its structure and physiology, acting as a timing machine (Eccles, 1973; D'Angelo et al., 2011). During the same period as Eccles, David Marr (1969) and James Albus (1971) developed computational models of cerebellar motor function. Marr proposed that PF inputs could be stored as a strengthening of synaptic weights, thereby modifying the GrC to PC connections under the simultaneous activation of the CFs (Glickstein et al, 2009). Later, Albus (1971) revised this assumption, suggesting that the simultaneous CF and PF activation would instead lead to a weakening in synaptic weights between the PF and PC synapses. Both Marr and Albus proposed that the cerebellum acts like a perceptron, a type of pattern recognition system. Specifically, the input network, performing sparse expansion recoding, enhances the pattern discrimination capacity of the PC that, in turn, receives the teaching signal from the CF (Albus, 1971; Kawato et al., 2021).

In revising Marr's and Albus's Motor Learning Theory, Ito et al. (1974) proposed that the cerebellum operates as a feedforward control system, predicting and adjusting movements without relying on feedback from the actual outcome. Instead of using feedback, it compares signals representing desired movements with signals representing performed movements as sensory error. Ito investigated the adaptation of vestibulo-ocular reflex (VOR) as a model for cerebellar control, involving compensatory eye movements with head movements, requiring the activation of the vestibular system (Ito, 2013). In this context, CFs carry visual error signals that modulate the synaptic weights between PF and PC synapses, crucial for the adaptive VOR during motion.

The cerebellum is renowned for its rapid information processing on a millisecond timescale. This capability led Ivry and Keele (1989) to propose that the cerebellum functions as a distinct component of the motor control system, specifically governing the timing. However, the timing processes within the cerebellum extend beyond motor functions; they also support perceptual and cognitive systems whenever temporal prediction is required. This broadens the cerebellum's role to include predictive processing across various domains. Churchland and Sejnowski (1992) further advanced this understanding with their hypothesis

that the brain constructs an internal virtual reality to cope with the timing demands of a dynamic environment. According to this perspective, the cerebellum anticipates sensory states to facilitate precise motor planning through predictive mechanisms (D'Angelo, 2018). Building on these insights, contemporary views have reshaped cerebellar theories to emphasise a continuous interaction between the cerebellum and the cerebral cortex. This interaction establishes an internal loop characterised by both feedback and feedforward connections (Figure 1.2). These connections are dynamic and capable of being updated in real-time, allowing the cerebellum to refine motor commands, based on sensory input, and anticipate outcomes. Thus, the cerebellum not only contributes to motor control but also integrates predictive processing and error correction, enhancing its role in adaptive and precise movement coordination.

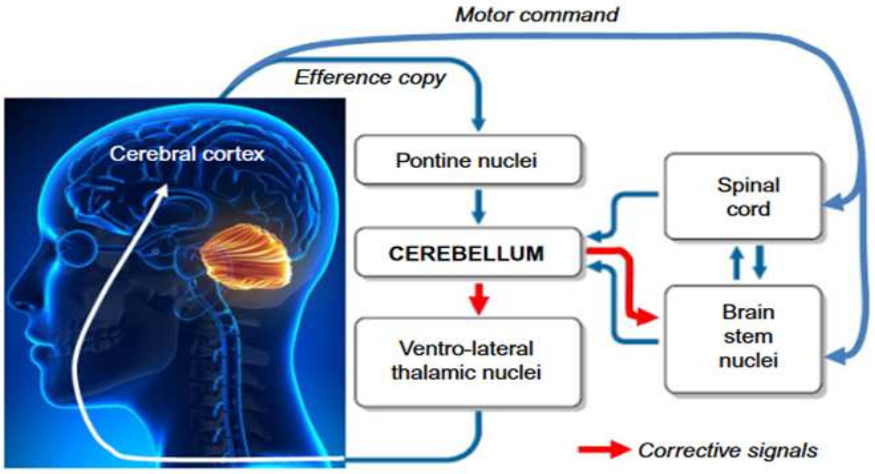

Figure 1.2 Macro-circuit connections of the cerebellum. Representation of the loops formed by the cerebellum with the cerebral cortex, brainstem, and spinal cord. Efference copy through pontine nuclei refers to a copy of motor commands which are then elaborated by cerebellar internal forward model to predict the sensory consequences of movement. When errors occur, or when there is novelty, meaning deviations from the forecast, the cerebellum issues corrective signals. These signals can directly impact movement, either through the brainstem or by altering the motor plan itself through the cortex. When deviations from the forecast persist, the cerebellum adapts by adjusting the internal forward model through plasticity (D'Angelo, 2018).

Then, Doya et al. (1999) explored in detail the concept of learning identifying three distinct types of learning occurring in the different brain regions: unsupervised, supervised, and reinforced learning. According to this assumption, cerebellar circuitry constructs an internal model of the environment to facilitate predictive control, characterised by a dual input system akin to supervised learning. In contrast, the cerebrum appears to engage in unsupervised learning independently of external guidance (Kawato et al., 2021).

Ito (2008) applied non-motor aspects of the cerebellum into the feedforward control model, suggesting a generalised cerebellar model extending the theory of motor functioning to sensory and cognitive processing. According to Ito, the cerebellum processes both movements and thoughts in an analogous manner, using similar internal models (Ito, 2008; D'Angelo, 2018).

Currently, advances in computational theories of the cerebellum are yielding promising results in the field of robotics and brain modelling. As our understanding deepens and these theories evolve, they not only enhance our comprehension of cerebellar motor and non-motor functions but also hold enormous potential for understanding their impact in pathological conditions (D'Angelo, 2018).

CHAPTER 2: CEREBELLUM

2.1. Gross Anatomy of the Cerebellum

The cerebellum has undergone evolutionary development in the vertebrate lineage of chordates, with origins dating back to early fishes, amphibians, and reptiles (Coolidge, 2020, p. 155). Despite accounting for just 10% of the total brain volume, the cerebellum contains around 69 billion neurons, more than half of all neurons in the brain (Kandel et al., 2000 p. 832; Singh, 2021). When considering this intriguing feature, it is evident that the conventional view of the cerebellum as purely a neuronal machine involved in sensorimotor control is outdated. Evolution has favoured the development of the cerebellum as a secondary brain structure that supports and complements the cerebrum in both sensorimotor and higher-order functions (Coolidge, 2020, p. 155).

In terms of its location, the human cerebellum is located in the posterior *cranial fossa*, anteriorly to the *pons* and the *medulla oblongata* (Kandel et al., 2000 p. 832). Conversely, in rodents, the cerebellum is located dorsal to the brainstem. Additionally, it borders rostrally with the quadrigeminal plate, and is in contact ventrally with both the 4th ventricle and the brainstem (Schröder et al., 2020, p. 157). The cerebellum is connected to the brainstem through three major bundles of fibres, known as cerebellar peduncles, which serve as conduits to facilitate the passage of both afferent and efferent cerebellar projections with different brain areas. Specifically, the *superior peduncle* connects the cerebellum to the midbrain, the *middle peduncle* to the *pons*, and the *inferior peduncle* to the *medulla oblongata* (Kandel et al., 2000, p.833).

2.1.1 Anatomical subdivisions of the cerebellum

Considering the transverse axis, the cerebellum is separated into three distinct lobes: the *anterior lobe,* the *posterior lobe*, and the *flocculonodular lobe*. The *primary fissure* separates the anterior lobe from the posterior one, while the *posterolateral fissure* divides the flocculonodular lobe from the other two lobes.

When observing the mammalian cerebellum from a dorsal view, three main cerebellar regions can be distinguished: i) a medial zone, the vermis, ii) an intermediate zone, the paravermis, and iii) two lateral zones, the cerebellar hemispheres (Figure 2.1A).

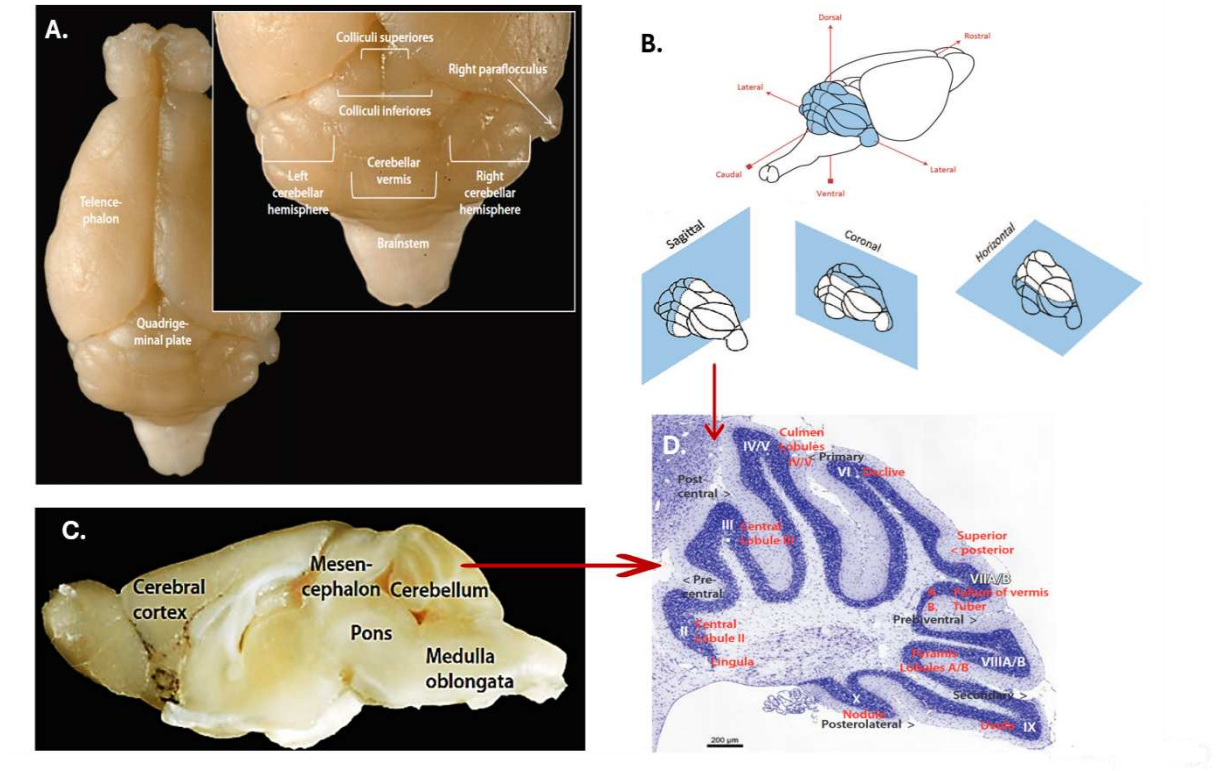

Figure 2.1 Anatomical subdivision of the mouse cerebellum. A, representation of the dorsal view of a mouse cerebellum, positioned posteriorly to both telencephalon and quadrigeminal plate of the mesencephalon, and anteriorly to the brain stem. The cerebellar vermis and the two hemispheres are shown in the inset (adapted from the book Neuroanatomy of a mouse brain: An Introduction written by Schröder et al., 2020). **B,** the image depicts the whole brain showing the ventral-dorsal, lateral and rostral-caudal views of the mouse cerebellum (adapted from Valera, 2013). **C,** lateral view of a mouse brain indicating the location of the pons and medulla oblongata with respect to the cerebellum (adapted from Schröder et al., 2020). **D,** the image illustrates a cerebellar sagittal slice of a mouse depicting ten different cerebellar lobules (adapted from Schröder et al., 2020).

Following an intricate folding process, shallower fissures further subdivide the cerebellar vermis into 10 lobules (Figure 2.1D). These lobules have been designated with specific names that vary between rodents and humans. In rodents, they are denoted by Roman numerals I-X, whereas humans have distinct names assigned to them (Figure 2.2). The anterior zone of the vermis contains the following five lobules: lobule I (*lingula* i.e., designation for humans), lobule II and III (*central lobules*), lobules IV and V (*culmen*). The central zone contains two lobules: lobules VI (*declive*), and lobule VII, further subdivided into lobule VIIa (*folium*) and *lobule* VIIb (*tuber*). The posterior zone contains two lobules: lobule VIII (*pyramid*) and lobule IX (*uvula*). Lastly, the nodular zone contains the lobule X (*nodulus*) (Figure 2.2). Each lobule of the vermis laterally extends to constitute each of the two cerebellar hemispheres (Figure 2.2).

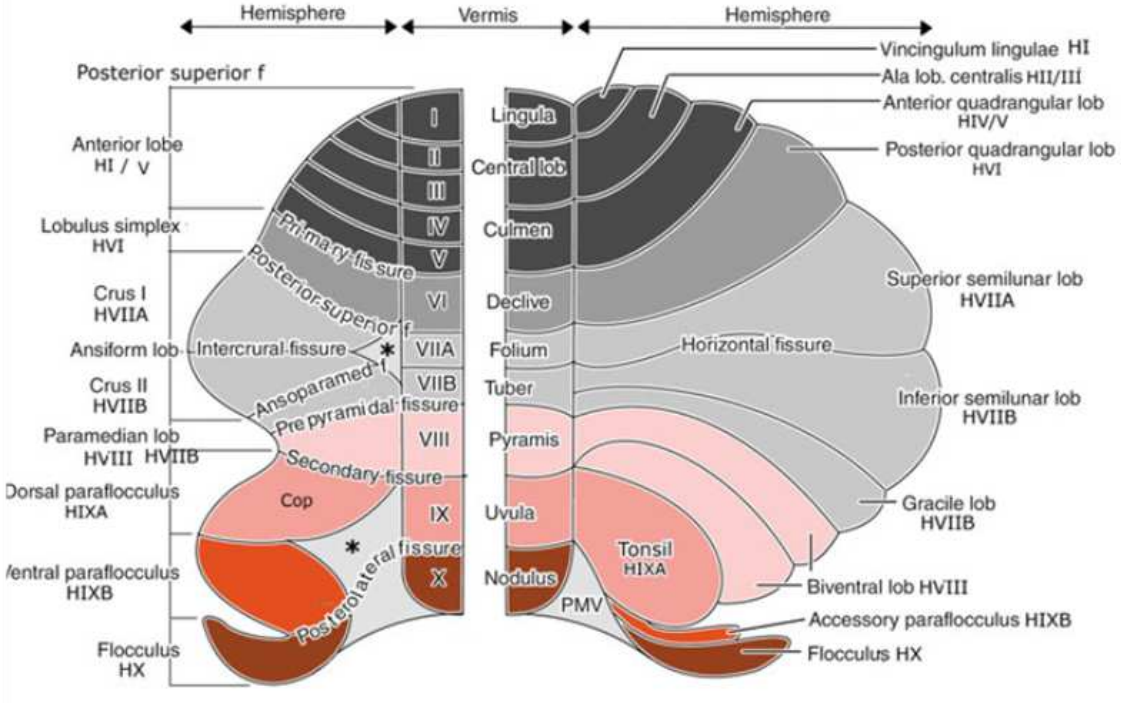

Figure 2.2 Comparison between the mouse (*left* panel) and human cerebellum (*right* panel) of the anatomical nomenclature. The image illustrates Larsell's (1952) numbering system for the lobules of the vermis and hemispheres. The homology of the lobules is indicated using the same colour. Asterisks denote areas devoid of cortex in the centre of the ansiform lobule and the paraflocculus. Abbreviations: Cop copulapyramidis, PMV posterior medullary velum (Voogd & Marani, 2016).

2.1.2 Functional subdivisions of the cerebellum

The cerebellum is subdivided into three distinct regions based on their functional role and phylogeny: the *vestibulocerebellum* (archicerebellum), the *spinocerebellum* (paleocerebellum) and the *cerebrocerebellum* (neocerebellum). Each region receives projections from different areas of the nervous system and projects back via the deep cerebellar nuclei (DCN) (D'Angelo, 2018).

The vestibulocerebellum is phylogenetically the oldest region of the cerebellum, and the only one that can also be observed in fishes and lower amphibians. It comprises a flocculonodular lobe and the *lingula*. It receives inputs homolaterally from primary vestibular afferent fibres of the cranial nerve VIII, visual inputs from the superior colliculi, and eventually inputs from the visual cortex via pontine nuclei. Additionally, it projects to the medial and lateral vestibular nuclei. In mammals, the vestibulocerebellum is involved in controlling balance, gait, and eye movements (Kandel et al., 2000, p. 834; D'Angelo, 2018).

The spinocerebellum contains the vermis and the two paravermis. The vermis receives visual, auditory, vestibular, and somatic inputs from the head and proximal body parts (Kandel et al., 2000, p.834) Then, the vermis, through the fastigial nucleus, projects to the cortical and brain stem regions related to the medial descending system (comprising reticular nucleus, vestibular nucleus, and red nucleus) to control proximal muscles of the limbs and the head (Kandel et al., 2000, p.843). On the other hand, the two adjacent paravermis structures receive input projections from the spino-olivary system and then project, through the interposed nucleus, to both lateral corticospinal and rubrospinal systems (Kandel et al., 2000, p.842). The somatotopic organisation of the spinocerebellar system has been well-characterised and it comprises two neural maps of the body located on the anterior and posterior folia. In both maps, vermis represents the head and trunk while paravermis represents the limbs and distal muscles (Kandel et al., 2000, p. 842).

Eventually, the cerebrocerebellum is the phylogenetically latest part of the mammalian cerebellum and it comprises two cerebellar hemispheres and the posterior lobe (Kandel et al., 2000, p.834). The cerebrocerebellum receives many inputs from the cerebral cortex via the middle cerebellar peduncle. This pathway is known as the cortico-ponto-cerebral pathway. Then, the cerebrocerebellum directs its inputs, via the superior cerebellar peduncle, to the

cerebral cortex including motor, premotor and prefrontal cortices through the dentate nuclei. This pathway is known as cerebellar-thalamocortical pathway. Taken together, these two pathways are thought to generate a loop between the brain and the cerebellum sustaining a continuous information flow. In terms of function, the cerebrocerebellum is not only involved in motor planning, but also in higher functions, including attention, language, executive function, and social cognition (Schmahmann & Sherman, 1998; Timmann et al., 1999; Timmann & Daum, 2007; Manto, 2008; Strata, 2015; Sokolov et al., 2017; D'Angelo, 2018; Stoodley & Tsai, 2021; Chao et al., 2023).

2.2 Inputs of the Cerebellum

The cerebellum receives a large amount of information from the cerebral cortex, enabling a feedback loop associated with planning and execution. Indeed, there are forty times more axons projecting to the cerebellum than departing from it (Kandel et al., 2000 p. 832). The origins of all the cerebellar inputs are the ION, and a group of precerebellar nuclei comprising hindbrain and spinal nuclei. The axons of all the neurons located in the precerebellar nuclei that enter the cerebellum give rise to MFs, while the axons of the neurons located in the ION entering the cerebellum generate CFs (Schröder et al., 2020, p. 154). CFs and MFs represent the two main afferent fibre systems projecting to the cerebellum.

2.2.1 Precerebellar nuclei and mossy fibres

MFs are one of the two types of fibre entering the cerebellum from diverse parts of the nervous system. Five main distinct regions that provide inputs to MFs can be identified: i) the pontine nuclei and the tegmental pontine reticular nucleus are involved in vision, planning and execution; ii) the spinal cord and cuneate provide proprioceptive signals; iii) the vestibular nucleus plays a role in balance, gait and eye movements; iv) the lateral reticular nucleus and red nucleus are involved in coordination; v) DCN can provide feedback corollary discharge signals that may be involved in associative learning (Hull & Regehr, 2022).

MFs spread across the cerebellar granular layer that represents the input stage of the cerebellar cortex. Each MF can branch into multiple folia, and each branch gives then rise to specialised structures known as cerebellar rosettes, which are central components of cerebellar glomeruli. A single MF can produce up to several hundreds of rosettes. Within the glomerulus, each rosette represents the presynaptic element characterised by multilobed grooves to establish excitatory synaptic contacts with dendrites of tens of GrCs (Palay & Cahan-Palay, 1974). Completing the cerebellar glomerulus are the axons of GoCs and their basal dendrites, which receive input from MFs and ascending axons of GrCs (Cesana et al. 2013). Eventually, the intersection of each MF bouton with GrC dendrites and GoCs axonal/dendritic synapses are enveloped by a glial cell. Overall, this specialised structure is known as *glomerulus* (Mapelli et al., 2014; Hull & Regehr, 2022). Additionally, MFs make synapses with UBCs (Hull & Regehr, 2022). MFs show continuous discharges at 10-30 Hz even during rest (Albus, 1971), and generally MF inputs consist of localised bursts of activity (D'Angelo, 2018).

2.2.2 Inferior olive nuclei and climbing fibres

CFs originate from neurons in the ION giving rise to the olivocerebellar tract (Luo & Sugihara, 2016). The ION is divided into several distinct subnuclei including principal olive, dorsal and medial accessory olive nuclei. Fibres projecting to the ION originate from the cerebral cortex, the red nucleus, the spinal cord, and some brain stem nuclei (Valera, 2013). The olivocerebellar tract reaches the cerebellum through the inferior cerebellar peduncle. Then, each olivocerebellar axon gives rise to several CFs that run in different longitudinal compartments based on the molecular expression profile of PCs (Luo & Sugihara, 2016). Each CF branch makes strong contacts with just one single PC in a modular manner (Hull & Regehr, 2022).

In terms of their physiology, the neurons of ION show spontaneous firing frequency at 10 Hz (Llinás & Yarom, 1986) that is synchronised by dentro-dendritic gap junctions between neighbouring neurons (Luo & Sugihara, 2016). Excitatory inputs to the ION, originating from the somatosensory and vestibular system, may reset this rhythm to evoke firing. An action potential or a brief burst occurring in the CFs trigger a complex spike response in the targeted

PCs. Complex spikes are characterised by multiple after-discharges and occur at an average frequency of about 1 Hz (Eccles et al. 1967; Kitazawa et al., 1998; Dean at al., 2010).

2.3 Outputs of the Cerebellum

The DCN and the vestibular nucleus constitute the sole output of the entire cerebellar cortex (Jaeger, 2021). The vestibular nucleus receives projections solely from the flocculonodular lobe (vestibulocerebellum), while the other lobes of the cerebellum project directly to the DCN. The DCN comprises three main parts: the interposed, lateral (dentate), and medial (fastigial) nuclei, with the interposed nuclei further divided into anterior (emboliform) and posterior (globose) parts. It receives collaterals from cerebellar inputs and is targeted exclusively by PC axons (Kandel et al., 2000, p. 833). It is organised topographically, with each nucleus receiving projections from a functionally distinct part of the cerebellar cortex and appears suggesting different functional roles (Takahashi & Shinoda, 2021). A significant portion of the DCN does not directly project onto motoneurons, but instead projects to the red nucleus or via the thalamus to the motor cortex. This indicates that the DCN projections are more involved in integrative functions such as motor coordination and modulation of movement rather than the direct execution of movements (Valera, 2013). DCN neurons constitute a heterogeneous population including glutamatergic, gamma-aminobutyric acid (GABA)ergic and glycinergic neurons (D'Angelo, 2018). DCN neurons display spontaneous autorhythmic activity (Hull & Regehr, 2022).

2.4 Cytoarchitecture of the Cerebellum

The cerebellum comprises a white matter core covered by an outer layer of grey matter defined as the *cerebellar cortex*. The distinctive tree-like appearance of the white matter is called *arbor vitae.* The white matter core contains the DCN, each positioned bilaterally (Schröder et al., 2020, p. 157). Compared to irregular convolutions of the cerebral cortex, the surface of the cerebellum shows finely organised grooves called *folia*. The cerebellar cortex captures attention due to its stereotyped and geometrically organised neural circuits (Kandel et al., 2000 p. 832). It is divided into three layers that, from the outermost to the innermost, are: the molecular layer, the Purkinje cell layer, and the granular layer (Fig.

2.3). Schematically, the cerebellar cortex shows a central "trisynaptic arc" in which the inputs from MFs excite GrCs that, in turn, excite PCs through their axons, the PFs. PCs, in turn, are the sole output of the entire cerebellar cortex with their axons projecting to the DCN. In addition, distinct local interneurons can be found within the cerebellar cortex at various levels: i) granular layer interneurons include inhibitory GoCs, inhibitory Lugaro cells and excitatory UBCs; ii) Purkinje cell layer interneurons include inhibitory candelabrum cells, and iii) molecular layer interneurons (MLIs) include inhibitory basket and stellate cells.

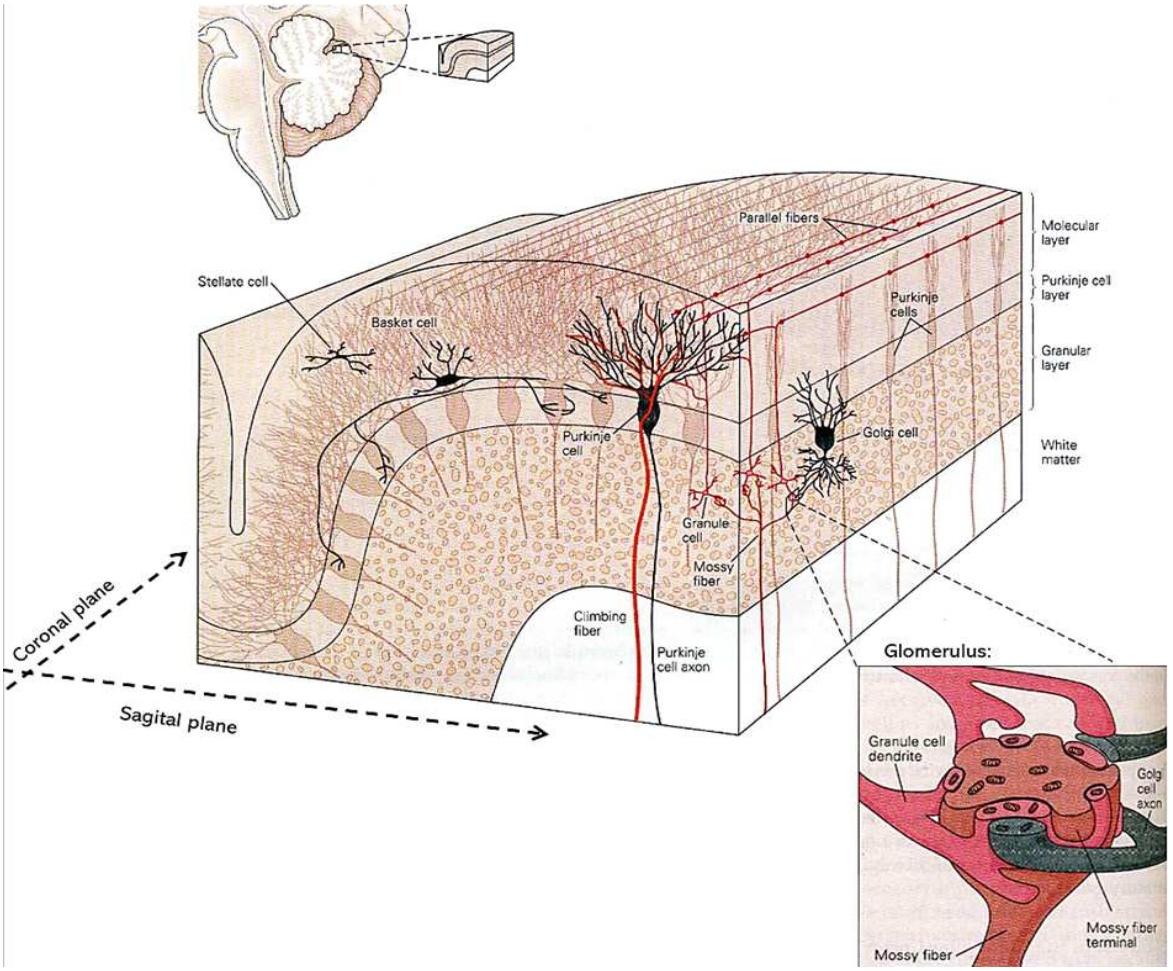

Figure 2.3 The three-layered organisation of the cerebellar cortex. An illustration of the human cerebellum. showing a magnified view of the cerebellar cytoarchitecture. The dendrites of Purkinje cells spread sagittal into the molecular layer. The axons of granule cells, named parallel fibres, run through the coronal plane contacting many Purkinje cells longitudinally. Molecular layer interneurons, including stellate and basket cells, are also

depicted. Except for the climbing fibres, the mossy fibres and granular cells, all the other neurons illustrated are inhibitory (adapted from Kandel et al., 2000, p. 836).

2.5 Granular Layer

The granular layer represents the input stage of cerebellar processing. It integrates a multitude of sensory, motor, and contextual information (Badura & De Zeeuw, 2017). It possesses a specialised architecture meticulously designed to facilitate precise information processing (D'Angelo & De Zeeuw, 2009; Sudhakar et al., 2017). When MFs reach the granular layer, they give rise to distinctive structures called rosettes, which constitute the central elements of the cerebellar glomeruli. Rosettes consist of presynaptic components with multilobed grooves where dendrites from various GrCs are located. The axons of GoCs and their basal dendrites complete the cerebellar glomerulus (Figure 2.3). The terminals of GoC axons intertwine with the dendrites of GrC within the rosette grooves, while the basal dendrites of GoCs receive input from MFs and ascending axons of GrCs.

2.5.1 Granule cells

GrCs are the most numerous cell types in the entire brain. They possess a small soma, and, on average, four short dendrites each terminating with a characteristic claw-shaped branching in the mossy fibre rosettes (Albus, 1971). On the other hand, GrC ascending axons contact the basal dendrites of GoCs in the granular layer before extending into the molecular layer, where they give rise to PFs that run parallel to the longitudinal axis of the cerebellar folium (Valera, 2013). In the molecular layer, PFs make excitatory synapses with PCs, GoC apical dendrites and MLIs.

In terms of physiology, GrCs are excitatory glutamatergic neurons differing from the predominant inhibitory interneurons found in the cerebellar cortex. Unlike other cerebellar neurons that display autorhythmic activity, GrCs, together with UBCs, are the only cell type that are silent at rest. In response to burst activity of MFs, GrCs show regular repetitive firing. Additionally, GrCs show resonance in the theta frequency band, akin to GoCs (D'Angelo & De Zeeuw, 2009; D'Angelo, 2018). It is worth noting that GrCs express a specific type of GABA receptor (GABAR) called extra synaptic α6-containing $GABA_A$, which has higher

affinity compared to the classical α1-containing $GABA_A$ receptors. This heightened sensitivity to GABA allows GrCs to respond strongly to GABA spillover within the glomerulus (Mapelli et al., 2014). Additionally, the continuous spontaneous spiking activity of GoCs keeps GrCs hyperpolarized, limiting their firing in response to MF inputs (Valera, 2013; Mapelli et al., 2014; Prestori 2019).

2.5.2 Unipolar Brush cells and Lugaro cells

UBCs are glutamatergic interneurons located in the granular layer of the vestibulocerebellum. They have a single short dendrite characterised by a brush-like appearance, typically receiving input from a single MF terminal. On the other hand, UBCs have axonal branches constituting an intrinsic-MF terminal that contact GrCs and other UBCs. They are silent at rest as GrCs and show bursts, rebounds, and a late-onset activity in response to MF stimulation (D'Angelo, 2018). Inhibition from GoCs and PCs plays a crucial role in further shaping UBC activity (Hull & Regehr, 2022).

Based on their morphology and physiology, Lugaro cells are distinct glycinergic/GABAergic interneurons of the granular layer (Lugaro, 1894). Lugaro cells are primarily found in the posterior lobus (VII and X) (Dieudonné & Dumoulin, 2000). They can be categorised into two groups based on the shape and location of their soma: large Lugaro cells, located in the deeper granular layer with fusiform or triangular soma, and small Lugaro cells, located beneath Purkinje cell layer (Prestori et al., 2019). The dendrites of Lugaro cells extend in two opposite directions from their soma, running parallel to the Purkinje cell layer parasagittally. The axons of Lugaro cells can reach the molecular layer, where they form a local and transverse plexus running parallel to PFs. These transverse fibres preferentially contact apical dendrites of GoCs regulating their activity (Hirono, 2016; D'Angelo, 2018; Prestori et al., 2019). Moreover, Lugaro cells receive strong inhibitory inputs through PC axon collaterals and excitatory inputs through MFs (Prestori et al., 2019)

2.6 Purkinje Cell Layer

The Purkinje cell layer is located above the granular layer and comprises the large cell bodies of PCs. PC axons are the sole output of the entire cerebellar cortex, projecting to the DCN. PC output is entirely inhibitory (Palay & Cahan-Palay, 1974).

2.6.1 Purkinje cells

PC, one of the largest and most complex neurons in the central nervous system, plays a crucial role in cerebellar neural processing (D'Angelo, 2018). In rodents, the soma of PCs is around 15 μm in diameter. Each PC dendritic branch originates from a couple of dendritic trunks, which contribute to their intricate morphology (Eccles et al., 1967; Play & Chan-Palay, 1974). PCs can effectively process information due to their complex dendritic structure and synaptic organisation. Indeed, PCs show a huge dendritic arborization, with dendrites that spread widely in the sagittal plane and thin out in the coronal plane (Harvey & Napper, 1991). These dendrites, electrically active and capable of complex synaptic integration, receive approximately 200 thousand synapses from PFs and a single synapse from CFs (Grangeray et al., 2016). PF inputs are conveyed to PC spines located in their thin branches, while CFs synapses are conveyed directly to smooth dendrites showing thorny spines. Additionally, inhibitory synapses from MLIs impinge onto dendritic shafts (Palay & Chan-Palay, 1974). On the other hand, PCs possess myelinated axons that form collaterals that can contact other PCs, Lugaro cells, basket cells and GoCs. Specifically, PCs exhibit two different axonal plexuses: one located within the Purkinje cell layer, and a second one located deeper in the granular layer (Valera, 2013).

PCs show a spontaneous firing frequency ranging from 20 to more than 100 Hz (Cerminara et al., 2015). This heightened activity is believed to offer computational benefits, albeit at an increased energetic expense (Hull & Regehr, 2022). Besides their intrinsic pacemaking, PCs have a rich repertoire of electro-responsiveness including burst pauses and rebound firing (Grangeray et al., 2016; D'Angelo, 2018). Moreover, ephaptic signalling, a phenomenon when the current flowing across neuronal membranes generates large extracellular signals that influence nearby neuron firing, has been demonstrated to impact PC activity. This occurs through several mechanisms. Firstly, the presynaptic specialisation of basket cells, known as *pinceau,* sustains a pinceau-mediated inhibition on PCs. Secondly, a recent study highlighted ephaptic coupling among PCs, where a single PC generates large ephaptic signals that rapidly excite nearby PCs, promoting synchronised firing (Han et al., 2018). Lastly, CFs can inhibit firing in nearby PCs through ephaptic-mediated extracellular hyperpolarization (Hull & Regehr, 2022).

Abnormal firing rates of PCs can affect firing patterns in DCN neurons, potentially contributing to disorders such as ataxias and autism (Grangeray et al., 2016). Recent cerebellar research indicates that synchronous firing within distinct neuronal populations is a key mechanism to control neural coding in the cerebellum (Person & Raman, 2012). Indeed, multiple circuit mechanisms facilitate the synchronisation of spikes among specific classes of cerebellar neurons. Feedforward inhibitory synapses, observed between MLIs and PCs restrict the integration time window of their targets, thereby regulating spike-timing. Additionally, recurrent inhibitory connections between PCs, MLIs, and GoC contribute to population synchrony, further enhancing coordinated firing patterns (Hull & Regehr, 2022).

2.6.1.1 Complex and simple spikes in PCs

Simple spikes represent the intrinsic pacemaking activity of PCs or can be driven by PF inputs. As PF synapses on PCs lead to a brief excitatory postsynaptic potential (EPSP), the summation of several PF inputs on the proximal axons of PC is required to induce their firing (Grangeray et al., 2016). In contrast, complex spikes of PCs are driven by low-frequency CF activity (1-3 Hz). CF stimulation induces a prolonged voltage-gated calcium conductance in the soma and dendrites of PCs, resulting in prolonged depolarization, characterised by an initial large amplitude spike followed by a high frequency burst (Figure 2.4A). The low frequency of complex spikes alone cannot encode the magnitude of a behavioural response or stimulus. Instead, they are thought to play a role in the timing of peripheral events or function as a trigger for behavioural responses. A timing control can be achieved through synchronised activity of ION neurons in response to a sensory stimulus. ION neurons are known to be electronically coupled through dendritic synapses, enabling them to fire synchronously. These synchronous inputs from ION neurons to CFs result in complex spikes occurring simultaneously in multiple PCs (Kandel et al., 2000, p. 840; D'Angelo, 2018; Figure 2B).

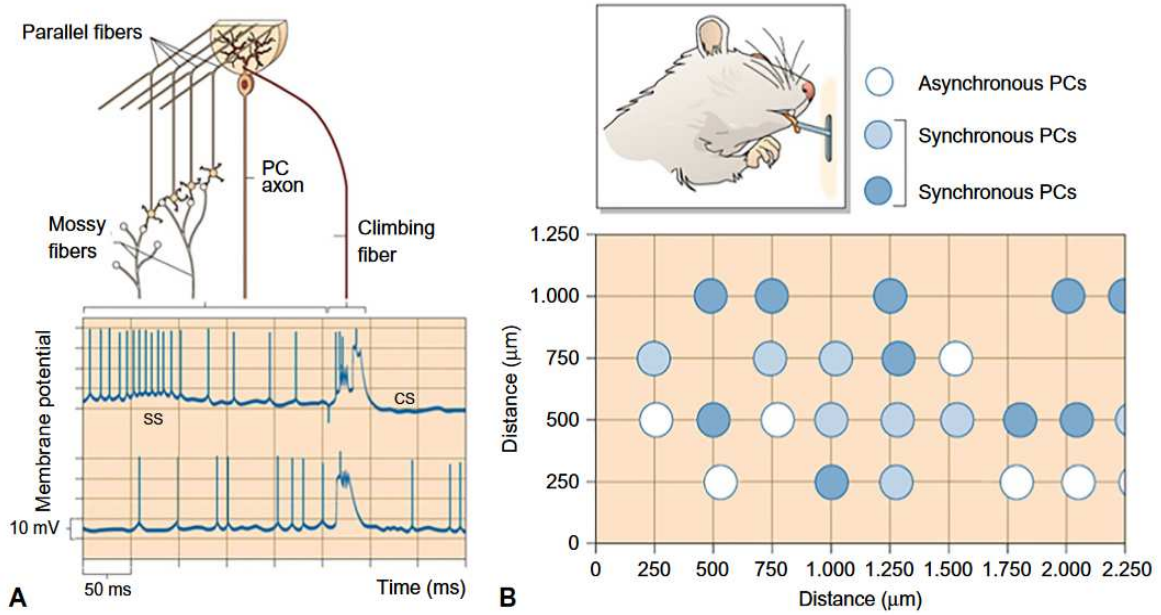

Figure 2.3 The activity of Purkinje cells (PCs). A, the picture shows simple spike (SS) and complex spike (CS) activity of a given PC in response to parallel and a single climbing fibre activity, respectively. B, the picture shows that sensory stimuli, such as licking, trigger synchronous firing of PCs in distinct clusters (D'Angelo, 2018).

The membrane potential of PCs exhibits bistability, alternating between up and down states (Rokni et al., 2009). The hyperpolarized state (down state) is characterised by the absence of simple spike firing, while the depolarized state (up state) involves spontaneous PC firing at high frequencies, even in the absence of any synaptic input (Williams et al., 2002). Hyper- or depolarizing current during the down state would shift the membrane potential to the up state, whereas the same current during an up-state shifts it to the down-state (Rokni et al., 2009). Additionally, inputs from CFs and GrCs can induce state transitions in PCs (Jacobson et al., 2008).

2.6.1.2 Parasagittal microzones

A cerebellar module is recognised as the fundamental operational unit of the cerebellum, consisting of a group of PCs that receive common CF inputs. These PCs project to a specific region of the DCN which, in turn, receives collaterals from the same ION axons

that constitute those CFs reaching the CF zone of PCs. These olivo-cortico-nuclear circuitry forms the core structure of individual cerebellar modules (Apps et al., 2018). Therefore, PCs are organised into parasagittal microzones each serving as discrete processing modules. Although microzones may differ in their external connections, their internal circuitry is consistent throughout the entire cerebellum (Dean et al, 2010).

Furthermore, PCs exhibit a range of molecular and physiological properties that correspond to microzonal organisation. This includes different expression patterns of Aldolase C (Aldoc or "zebrin II"), which contribute to the formation of parasagittal zebra stripes in the cerebellar cortex (Oscarsson, 1979; Hull & Regehr, 2022).

2.6.1.3 Impact of GrC axonal contacts on PC firing: the beam-like and patch-like theory

The longitudinal projection pattern of PFs differs from the transverse projection pattern of MFs (Luo & Sugihara, 2016). This discrepancy between the functional mosaic-like organisation of the cerebellar cortex and the structural longitudinal organisation of the PF system has sparked debate regarding how information is processed in response to MF inputs (Cohen & Yarom, 1998). The traditional "Beam Theory" proposes that GrC activation by MFs excites PCs in a beam-like manner (Braitenberg & Atwood, 1958; Eccles et al., 1967), while MLIs provide off-beam inhibition, limiting the activated region (Eccles et al., 1967). Supporting this theory, studies have demonstrated that MF input induces field potentials in the molecular layer beyond the MF termination area (Garwicz & Andersson, 1992), whisker stimulation modulates PCs located transversely (Bosman et al., 2010), and there is synchrony in the simple spike firing during natural inputs (De Zeeuw et al., 1997). However, some *in vivo* studies have reported that MF inputs or peripheral inputs evoked activity in only patches of PCs (Cramer et al., 2013). Cohen and Yarom (1998) demonstrated that PF stimulation evokes a narrow beam of activity, propagating along the PFs, while MF stimulation elicits a circular, non-propagating patch of synchronised activity in PCs. Thus, the alternative ‘Radial Theory’ suggests that the ascending axon, rather than PFs, predominantly influences PC firing, defining the functional module of the cerebellar cortex. However, the precise way PCs respond to MF inputs remains unclear. Both patch-like and beam-like patterns of PC

excitation may coexist, albeit with different dynamic properties (D'Angelo et al., 2010; Cramer et al., 2013).

2.7 Molecular Layer

The molecular layer constitutes the outermost layer of the cerebellar cortex and contains the cell bodies of inhibitory interneurons collectively known as MLIs. These MLIs include stellate and basket cells, which are interspersed among GrC axons and the dendritic arborization of PCs (Kandel et al., 2000; p. 838; D'Angelo et al., 2016).

2.7.1 Molecular layer interneurons

Basket and stellate cells are GABAergic interneurons that provide feedforward inhibition to PCs (Watanabe, 2016). Despite their anatomical distinction and location, both display pacemaking activity. Basket cells are in the basal one-third of the molecular layer and target the soma and axon initial segment of PCs. Conversely, stellate cells are in the distal two-thirds of the molecular layer and target the dendrites of the PCs. MLIs are activated by a glutamate spillover from CF to PC synapses and are also directly and strongly excited by PFs. These two cell types exert distinct effects on PCs: basket cells rapidly and profoundly affect PC spiking, while stellate cells provide dendritic inhibition that counterbalances the PF excitation, although not directly affecting PC spiking (Watanabe, 2016). Specifically, basket cells form specialised *pinceau* structures on the initial segment of PCs, inhibiting PC firing by rapid *ephaptic signals* (Blot & Barbour 2014, reviewed in Hull & Regehr, 2022). On the other hand, PFs activate stellate cells, which, in turn, exert a feedforward inhibition on PCs, resulting in a delayed inhibition limiting the PC excitation to the onset of excitatory inputs (Liu & Dubois, 2016). Furthermore, MLIs are interconnected via gap junctions that allow current flow between the neighbouring cells, with a critical role in temporal synchronisation (Liu & Dubois, 2016). Conversely, MLIs do not inhibit GoCs despite their proximity (Hull & Regehr, 2022).

CHAPTER 3: GOLGI CELLS

3.1 A Brief History of Golgi Cells

GoCs was identified as the 'big nerve cell' of the cerebellum by Camillo Golgi (1874), following his discovery of the black reaction which enabled the visualisation of a detailed neuronal structure for the first time (Galliano et al., 2010).

Camillo Golgi described GoCs as neurons showing an irregularly round or polygonal soma and long extensions (Figure 3.1). Golgi also emphasised the impressive axonal plexus of GoCs which has become a morphological criterion for their recognition (Galliano et al., 2010). Santiago Ramon y Cajal further investigated the detailed morphological characteristics of GoCs. Cajal described the orientation and extension of the axonal plexus and dendrites of GoCs that depart from the soma in any direction. GoC apical dendrites reach the molecular layer where they contact PFs, while the axonal plexus of GoCs is restricted to the granular layer (Palay & Chan- Play, 1974). Additionally, Cajal identified for the first time the glomerulus structure where MF, GoC basal dendrites/axons and GrC dendrites intertwine to form crucial synaptic interactions (Galliano et al., 2010). Later in 1960, Eccles discovered the inhibitory nature of GoCs and characterised both GoC *feedforward* and *feedback inhibition* onto GrCs (Eccles *et al*., 1964).

The investigation of GoCs also contributed significantly to the development of cerebellar theories. In Eccles' *beam theory* (see Chapter 2), it was proposed that the feedback and feedforward inhibition by GoC onto GrCs enhances the spatial discrimination of cerebellar inputs. According to Marr's motor learning theory, PCs learn motor pattern representations conveyed by MF and CF. The capacity of PCs to learn these patterns increases as the number of inputs reaching PFs increases. Thus, GoCs intervene by limiting GrC activity through their inhibitory control (Galliano et al., 2010). A codon refers to a subset of activated MFs that convey signals to a GrC, and codon size refers to the number of GrCs activated by a beam of MFs. Marr proposed that the function of GoC inhibition is to regulate MF inputs reaching PCs via PFs, thereby influencing the *codon size* (Marr, 1969; Albus, 1971).

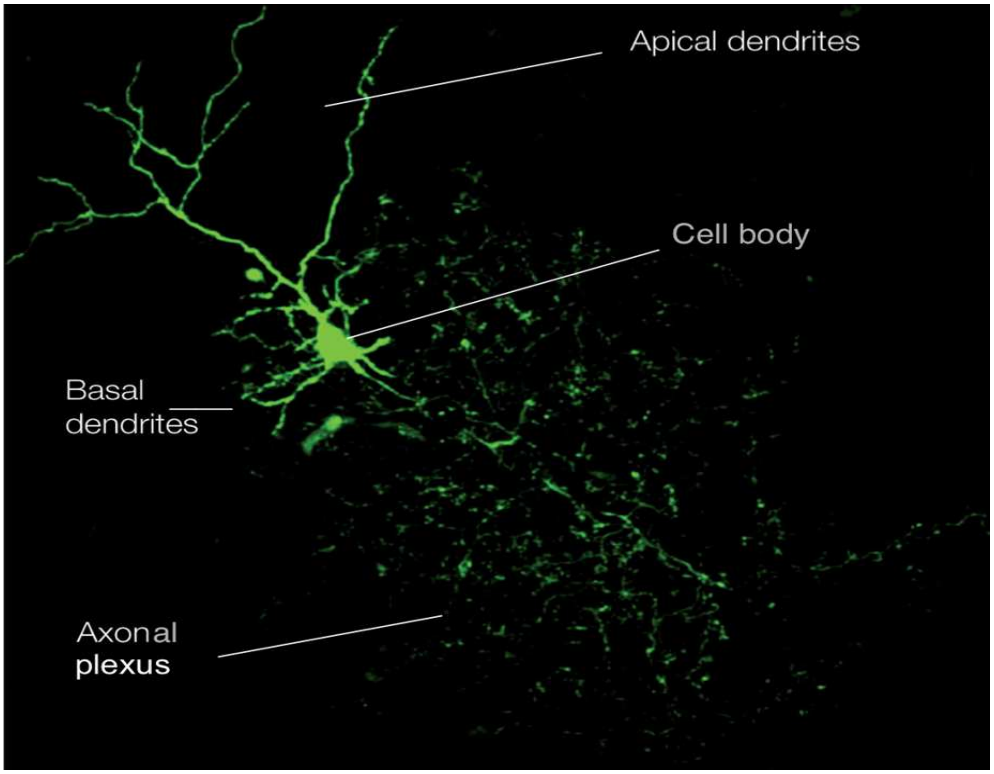

Figure 3.1 Confocal image of a Golgi cell. The image depicts a Golgi cell filled with AlexaFluo in an acute cerebellar slice. Its cell body, dendritic arborizations and axonal plexus are indicated (adapted from D'Angelo, 2008).

3.2 GoC Subtypes and Morphology

GoCs are the prominent interneurons distributed widely across the granular layer. While the majority of GoCs (80%) use both GABA and glycine as neurotransmitters, a subset exclusively employs either GABA (20%) or glycine (5%). In the vestibulocerebellum, GoCs make glycinergic synapses onto UBCs (Dieudonne, 2016). GoCs exhibit heterogeneous soma shapes and can be divided into five distinct subtypes based on their molecular expression (Geurts et al., 2003; Simat et al., 2007): i) the first subset of GoCs express metabotropic glutamate receptor 2 (mGluR2) and neurogranin and exhibits large polygonal soma; ii) another subset of GoCs express mGluR2 but lacks neurogranin and exhibits large polygonal soma; iii) a different subset of GoCs expressing the same markers of the second group, is located in the upper portion of the granular layer and exhibits with small polygonal soma;

iv) a subset of GoCs exclusively expressed neurogranin and displays a large polygonal soma; v) lastly, a distinct subset with exclusive neurogranin expression features a polygonal soma. Neurogranin was found to label GABAergic GoCs selectively, whereas mGluR2 was detected almost exclusively in GoCs with a dual neurotransmitter phenotype (Simat et al, 2007). Currently, no differentiation of GoC subtypes has been established based on their intrinsic electrophysiological properties, warranting further investigations (Forti et al., 2006; Galliano et al., 2010; D'Angelo et al., 2013).

In rodents, GoCs are multipolar neurons with four to ten dendrites emanating from their large soma (10–20 μm in diameter) (Barmack & Yakhnitsa, 2008). GoCs are characterised by their thick dendrite-like axons which bifurcate to send collaterals. These axonal collaterals form an extensive axonal plexus throughout the granular layer, leading the divergence of a single GoC input onto numerous GrCs (Dieudonne, 2016). The axonal terminals of GoCs are organised parasagittally, with a mediolateral extent of 180 μm, as reported in mice. Furthermore, axonal fields of GoCs overlap extensively and converge into a single glomerulus (Barmack & Yakhnitsa, 2008).

The dendrites of GoCs are classified in two distinct classes, basal and apical dendrites, according to their proximity to the GoC soma (Szoboszlay et al., 2016). The basal dendrites are confined into the granular layer where they make synaptic contact with MFs within the glomeruli (Palay & Chan-Palay 1974; Cesana et al. 2013). Conversely, one to four dendrites of GoCs extend into the molecular layer where they bifurcate into apical branches that ascend to the pial surface, perpendicular to PFs.

The confinement of GoC apical dendrites within the same zebrin II compartment as their soma seems to imply a parasagittal modular organisation of GoCs, like that of PCs. This restriction of GoC dendrites to specific compartments may facilitate localised patterns of inhibition, tailored to specific patterns of MF activity (Sillitoe et al., 2008).

The dendrites of GoCs show active properties (Rudolph et al., 2015) and a differential distribution of voltage-gated calcium channels (VGCC) which affects signal propagation along the dendrites (Masoli et al., 2020). It has been found that dendritic voltage-gated sodium channels enable somatic action potentials to activate voltage-gated calcium channels (VGCC) across the dendritic length. R-type and T-type VGCCs are primarily situated distally,

where they enhance synaptic inputs and support burst firing. Conversely, N-type channels are predominantly located near the soma, regulating spontaneous firing frequency and firing pattern through their interaction with Ca^{2+}-activated potassium channels. Thus, VGCCs exhibit distinct distributions and serve specialised roles within the different dendritic compartments of GoCs (Rudolph et al., 2015). Additionally, Masoli et al. (2020) simulated dendritic processing of GoCs in a multicompartment neuron model. In this model, dendrites express a diversified set of Ca^{2+}, Na^{+} and K^{+} ionic channels that could affect the dendritic integration of signals. Specifically, due to different distribution of Na^{+} channels in the apical and basal dendrites, basal dendrites exhibit stronger electrical coupling with the axon initial segment, compared to apical dendrites. On the other hand, Ca^{2+} channels are localised differently: high-threshold Ca^{2+} channels are in basal dendrites and axonal initial segment, while low-threshold Ca^{2+} channels are in distal dendrites and soma. Overall, the dendritic processing of excitatory inputs onto GoC has been demonstrated to be asymmetric (Masoli et al., 2020).

3.3 Excitatory Inputs onto GoCs

GoCs receive three types of excitatory glutamatergic inputs from (Figure 3.2): i) MFs which contact the basal dendrites of GoCs within the glomerulus (Cesana et al., 2013) ii) ascending axons of GrCs which contact the soma and dendrites of GoCs (Cesana et al., 2013); iii) PFs of GrCs which contact apical dendrites of GoCs in the molecular layer (Vos et al. 1999a). Synaptic transmission from MFs to GoCs involves α-amino-3-hydroxy-5-methyl-4-isoxazolepropionic acid receptors (AMPARs) and the NMDARs, whilst synapses from PFs to GoCs incorporate kainate receptors in addition to AMPARs and NMDARs (Cesana et al., 2013). Additionally, GoCs dendrites possess mGluR2 receptors. Following an intense activation of both GrCs and GoCs, these GoC receptors are thought to potentiate an inward rectifier K^{+} response current reducing the response of GoCs (Watanabe & Nakanishi, 2003). Instead, it is noteworthy that there is no direct contact between CFs and GoCs (Galliano et al. 2013; Dieudonne, 2016).

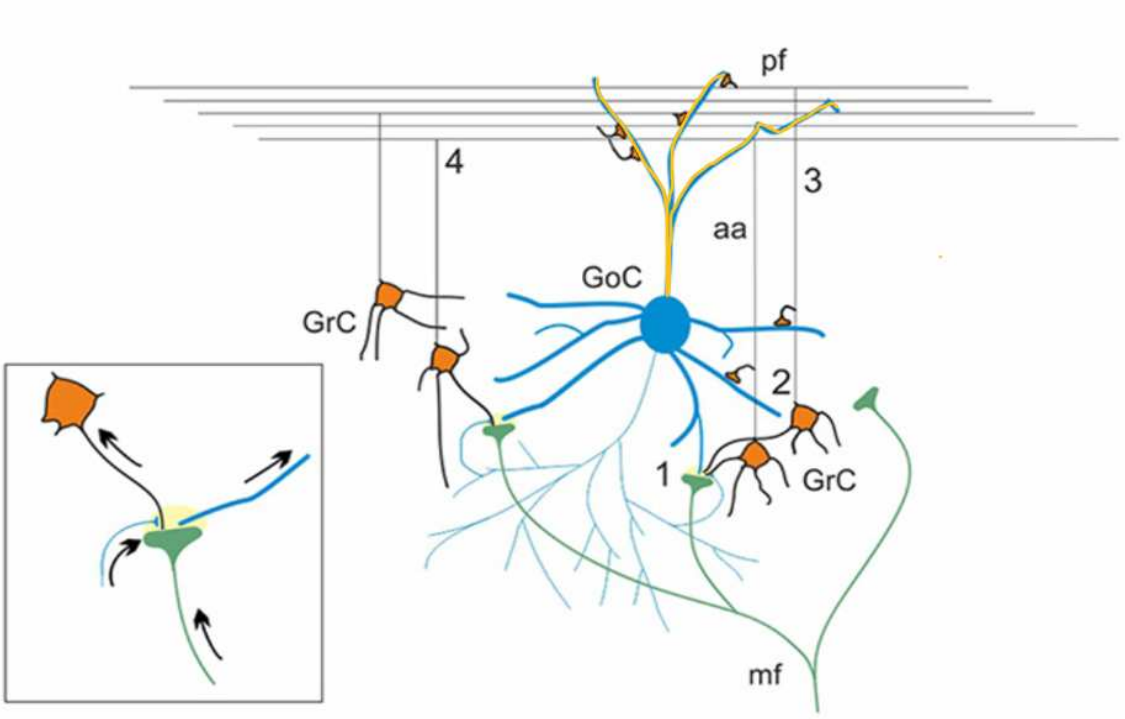

Figure 3.2. Schematic of GoC excitatory inputs. (1), MF- GoC monosynaptic pathway; (2), MF-GrC-GoC disynaptic pathway via GrC aa; (3), short and (4) long MF-GrC-GoC through PFs in the molecular layer. The inset shows synaptic contacts within the cerebellar glomerulus. In blue, Golgi cell (GoC); in green, mossy fibre (mf); in orange, granule cell (GrC); ascending axon (aa); parallel fibre (pf*)* (adapted from Locatelli et al., 2021).

3.4 Inhibitory Inputs onto GoCs

A well-characterised inhibition onto GoCs originates from Lugaro cells, which supply a combination of glycinergic and GABAergic signals via their axonal plexus in the molecular layer (Dieudonne, 2016). *In vivo* studies have demonstrated that Lugaro cells, due to their location, can shunt the apical dendrites of GoCs and participate in the synchronisation of GoCs along the PF beam (Vos et al. 1999b). However, the interaction between GoCs and Lugaro cells has been observed solely in the presence of serotonin release (Dumoulin et al., 2001, as reviewed in Hull & Regehr, 2012). The existence of MLIs inhibition onto GoCs has been a matter of debate; however, optogenetic studies have recently shown that axons of both stellate and basket cells do not functionally innervate Golgi cells (Hull & Regehr, 2012; Eyre & Nusser, 2016). This suggests that PCs and GoCs, despite sharing the same source of

excitatory inputs from GrCs, are independently modulated by distinct inhibitory mechanisms. The major inhibition onto GoC derives from other GoCs (Hull & Regehr, 2012). This occurs through GABAergic synaptic connections and gap junctions among GoC apical dendrites in the molecular layer. This electrical coupling between GoCs is thought to sustain synchronous GoC spiking and to produce low frequency oscillations in the theta-band (Dugue et al., 2009; Hull & Regehr, 2022). Additionally, GoC gap junctions allow spiking desynchronization in response to MF activation (Vervaeke et al., 2010; as reviewed in Hull & Regehr, 2022).

3.5 Outputs of GoCs

GoCs play a critical role in regulating information processing within the granular layer, and acute ablation of GoCs is known to cause ataxia (Watanabe et al.,1998). They are the only source of inhibition for billions of GrCs. Overall, GoCs performed three different kinds of inhibition onto GrCs: *feedforward, feedback,* and *lateral* inhibition. Specifically, the broader extension of GoC axons provides the basis for lateral inhibition in the granular layer (D'Angelo, 2008).

MFs stimulate GoC basal dendrites and subsequently GoC exert inhibition onto GrCs via their axons, generating a feedforward inhibition (MF → GoC → GrC) (Cesana et al., 2013; Prestori et al., 2019). Phasic and tonic inhibition are the two main pathways via which the feedforward inhibition mechanism functions (Mapelli et al., 2014). Phasic inhibition is characterised by $GABA_A$ receptor-mediated inhibitory postsynaptic events (Armano et al., 2000). These events narrow the time window for synaptic integration, thereby improving the accuracy of spike-timing in GrCs. Precisely, phasic inhibition, which is orchestrated by the feedforward circuit, lasts for 4-5 ms in response to a single MF input or brief bursts, and effectively restricts GrC responses to 1-2 spikes. Conversely, tonic inhibition lowers GrC membrane resistance and consequently lowers their excitability. This occurs through extra synaptic $GABA_A$ receptors that are activated when GABA levels are low (Hamann et al., 2002; Farrant & Nusser, 2005; Mapelli et al, 2009). GrC excitability is controlled by tonic inhibition allowing the neuron to distinguish significant information from background activity (Duguid et al., 2012; Mapelli et al., 2014). Regarding the feedback inhibition (PF→GoC→GrC), GrCs activated by MFs stimulate GoC apical dendrites in addition to

stimulating PCs through PFs. Consequently, even though being activated by MFs, GrCs reduce their capacity to activate PCs (Mapelli et al., 2014; Prestori et al., 2019). The activation of GoC apical dendrites, in turn, leads to the inhibition of GrCs located around the GoC axonal plexus within the glomerulus. This gives rise to the lateral inhibition which occurs when the response of a given neuron to a stimulus is inhibited by the excitation of neighbouring interneurons. Moreover, *ex vivo* research demonstrated that the lateral inhibition in the granular layer gives rise to a centre-surround organisation of GrC activity (Mapelli & D'Angelo, 2007).

3.6 Electrophysiological Properties

GoCs exhibit a diverse array of electrophysiological responses, including pacemaking (Dieudonne, 1998; Forti et al., 2006), burst response followed by a pause, phase reset, rebound excitation (Vos et al., 1999a, b; Solinas et al., 2007a, b), population synchrony (Ros et al., 2009; Dugue et al., 2009) and, ultimately, resonance in the theta frequency band (Solinas et al. 2007a, b).

GoCs are known to display autorhythmic activity at around 1-10 Hz in acute cerebellar slices (Dieudonne, 1998; Forti et al., 2006). It has been found that the pace-making depends on the action of four ionic currents: slow inward-rectifier H-current (I_H), persistent Na^+ current (I_{Na-p}), Ca^{2+} dependent K^+ current mediated by SK-type channels (I_{K-AHP}), and K^+ current mediated by M-type channels ($I_{K\text{-}slow}$). I_H is involved in keeping the membrane potential in a range that allows the interaction of other Na^+ and K^+ currents to generate pacemaking activity (Figure 3.3/A).

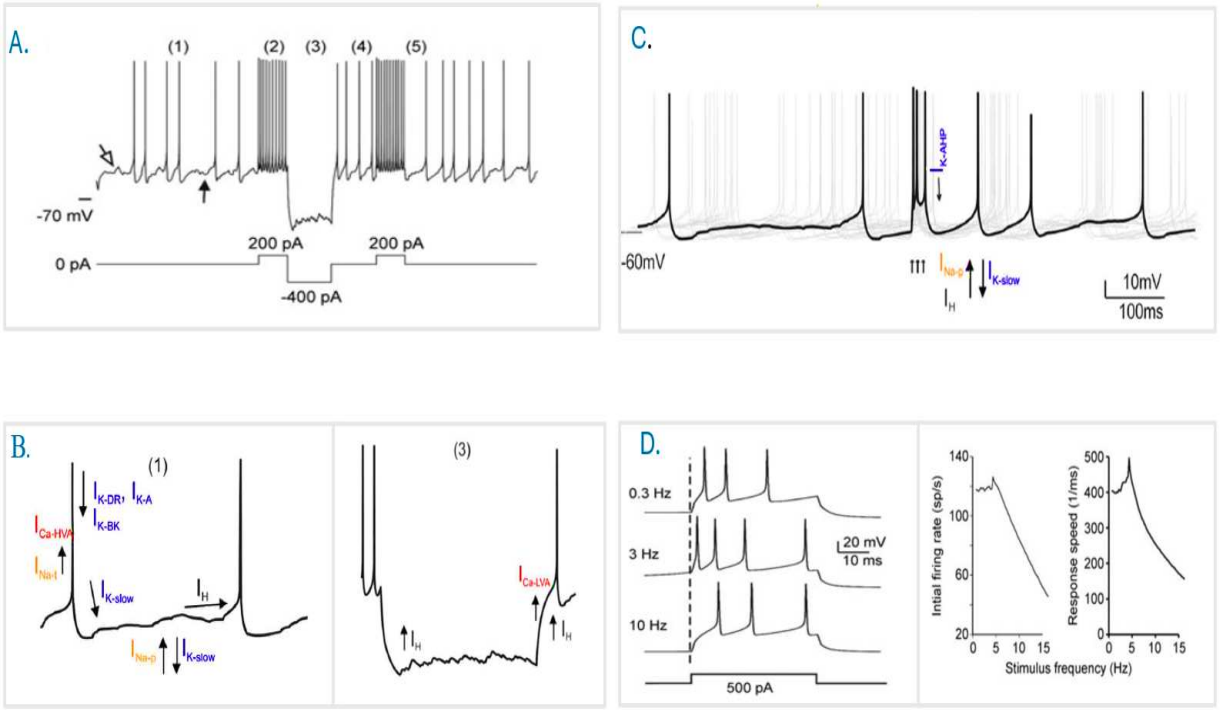

Figure 3.3 The electrophysiological properties of Golgi cells. A Representation of Golgi cell pace-making activity at 1-10 Hz (1). In response to depolarization GoC exhibits high frequency discharge with frequency adaptation (2). In response to hyperpolarization, GOC exhibits sagging inward rectification (3) followed by rebound excitation (4). Lastly, in response to a burst of activity GoC exhibits a silent pause (5). **B** Representation of ionic currents underlying low frequency GoC pacemaking (1), and sagging inward rectification (3**) C** Representation of ionic mechanisms underlying silent pause followed by a burst. **D** Representation of GoC activity showing faster and higher frequency spikes at the resonant frequency of 6 Hz when stimulated with repeated pulses. Transient Na^+ current (I_{Na-t}; yellow), persistent Na current (I_{Na-p}; yellow), and resurgent Na current (I_{Na-r}; yellow). High-voltage-activated Ca^+ current (I_{Ca-HVA}; red), and low-threshold activated Ca^+ current ($I_{Ca-LVA;}$ red). In purple colour, Ca-dependent K^+ current of the BK-type (I_{K-BK}; purple), Ca^+-dependent K^+ current of the SK-type channels (I_{K-AHP}; purple), delayed-rectifier K^+ current ($I_{KV;}$ purple), slow K^+ current of the M-type channels (I_{K-slow}; purple), fast-inactivating K current of the A-type (I_{K-A}; purple), and slow inward-rectifier H-current (I_H; black) (adapted from D'Angelo et al., 2013 and Galliano et al, 2010).

3.6.1 Neural entrainment

GoCs possess spontaneous rhythmic discharge at low frequencies both in awake and anaesthetised animals (Vos et al., 1999b; Holtzman et al., 2006). *In vivo* research also shows that GoC firing frequency is in phase with oscillation of local field potential recorded in the granular layer (Dugue et al., 2009; D'Angelo et al., 2013). Furthermore, GoCs display resonance around their oscillation frequency, which allows them to amplify responses within the theta-frequency band (Solinas et al., 2007a, b).

The feedback inhibition exerted by GoCs onto GrC can entrain both cells to a common rhythm, with GrCs firing occurring just before GoCs. This common rhythm also extends to the length of PFs, resulting in a global synchronisation (Vos et al., 1999a). As a conclusion, GoCs affect the timing of GrC spikes. Moreover, gap junctions among GoCs sustain GoC synchronisation (Vos et al., 1999a; Holtzman et al., 2006; as reviewed in Galliano et al., 2010). Eventually, GoCs display rhythmic entrainment resembling the UP-DOWN states typical of neocortical activity (Ros et al. 2009; as reviewed in Galliano et al., 2010).

3.7 The impact of GoCs on cerebellar microcircuit activity

The role of GoCs in cerebellar information processing can be summarised as follows (Galliano et al, 2010; D'Angelo, 2011). First, GoC feedforward inhibition enables the granular layer to generate a time-windowing effect limiting the duration and intensity of GrC responses to MF inputs (D'Angelo & De Zeeuw, 2009). This inhibition operates through two mechanisms: phasic and tonic inhibition. Tonic inhibition relies on the neurotransmitter spillover inside the glomerulus, extending its influence on GrCs. Further, inhibition regulates the gating of the MF-GrC relay during prolonged input bursts, thereby affecting GrC input resistance and spike threshold. Thus, phasic and tonic inhibition cooperate to modulate GrC responsiveness to excitation (Mapelli et al., 2014). Secondly, GoC feedback inhibition provides homeostatic control, as local excitation in the granular input layer triggers GoCs inhibition. Thirdly, GoCs contribute to sustain oscillations within the granular layer. Through feedback inhibition, GoCs support the oscillatory behaviour of GrCs, with their inhibition extending over a large population of GrCs. Gap junctions among GoCs further contribute to

these oscillations (Maex & De Schutter, 1998; Solinas et al; 2007a; Dugue et al., 2009). Lastly, the granular layer response to MF burst exhibits a centre-surround organisation mediated by lateral inhibition from GoCs, with excitation centred in the core and inhibition located in surrounding areas (Mapelli & D'Angelo, 2007).

CHAPTER 4: SYNAPTIC PLASTICITY

4.1 History and Definition of Synaptic Plasticity

Throughout history, philosophers and psychologists have engaged in a timeless debate, pondering whether the mind is shaped by experience or not, and, if so, to what extent learning mechanisms play a role in it. This dichotomy is framed as the nature and nurture debate, whose origin dates to Aristotle. He precisely suggested that the mind can be considered as a *tabula rasa* - 'a blank state'- that can be shaped solely by experience. He also emphasised repetition and causality among events as key factors for mental representations. Early psychological studies on learning reinforced this view, which had been conceptualised by the empiricists like John Locke and David Hume. In addition, William James, known as the father of American psychology, wrote on how habits are formed, and mentioned *the plasticity of organic materials* as the basis for habit formation (James, 1890). He also defined repetition, intensity and competition as key elements for creating associations (Markram et al., 2011). Over time, it has become evident that the extent of the mind's freedom is limited, and learning is constrained by temporal and spatial factors. While the philosophical debate persists, contemporary neuroscience has reached a consensus that the brain is a dynamic system shaped by experience within the constraints of its intrinsic nature.

A single neuron is bombarded with thousands of inputs every instant. The intriguing question is how the neuron selects which information to prioritise as salient among them and what neuronal mechanism underlies this selection process. In other words, how a neuron, embedded in a neural network, becomes finely tuned to specific information (Markram et al., 2012).

According to classical views on synaptic transmission, synapses are thought to facilitate the transmission of information between neurons (or from neurons to muscles), with synaptic connections remaining stable once established during brain development (Byrne, 1997). Ramon y Cajal (1911) was one of the pioneers who linked memory and learning to structural plasticity. He proposed that long-term memories do not require the formation of new neurons, but rather the growth of new connections between existing neurons. For the first time, Sherrington (1897) coined the term *'synapses'* to describe the connections between

neurons, although he did not mention its relationship with learning. Then, Tanzi (1893) introduced the concept that associative memories and motor skills may rely on the facilitation of existing connections. Tanzi's student, Ernesto Lugaro (1898), was the first to use the term *'plasticity'* to elucidate synaptic modifications. By the 1930s, chemical synapses had been investigated, revealing that information flowed from presynaptic axons to postsynaptic dendrites, before being integrated in the soma. Then, Eccles' studies focused on individual connections and short-term synaptic plasticity (STSP). Eccles proposed the idea that an action potential (AP) propagating down to the axon would briefly be reflected into dendrites (Eccles & Sherington, 1931).

In the 1940s, Warren McCulloch and Walter Pitts pioneered the concept of recurrent neural network inspired by the early studies on synaptic facilitation. A recurrent neural network is a neural network with an internal memory that can use its prior inputs to make accurate predictions. These investigations proposed that once information is introduced, it reverberates within the system rather than rapidly dissipating. The breakthrough in the field occurred with the conceptualization by Donald Hebb, alongside Konorski (1948). Hebb (1949) introduced the concept of what is now known as *Hebbian plasticity* in his book titled "The Organization of Behavior". Here is an excerpt:

> "*Let us assume that the persistence or repetition of a reverberatory activity (or "trace") tends to induce lasting cellular changes that add to its stability. ... When an axon of cell A is near enough to excite a cell B and repeatedly or persistently takes part in firing it, some growth process or metabolic change takes place in one or both cells such that A's efficiency, as one of the cells firing B, is increased*" (p. 62).

Then, Shatz (1992) succinctly captured the Hebbian postulate in his renowned statement "*cells that fire together wire together*", implying a causal link between simultaneous events. However, this statement only partially encapsulates the concept of Hebbian plasticity, as Hebb's original postulate also incorporates the direction of activation. Additionally, Hebb posited that a group of co-activated neurons would give rise to what is known as "*Hebbian assemblies"*, where precepts and thoughts find representation. These linked assemblies would generate *phase sequences,* reflecting different thought processes. However, Hebb's postulate did not address the precise timing of inputs; rather, it emphasised the temporal ordering of activity when elucidating phase sequences in the assemblies (Hebb, 1949).

Currently, synaptic plasticity refers to the activity-dependent modification in synaptic transmission strength or in the efficiency at existing synapses. This process is essential to lead the brain to convert transient experiences into enduring memory engrams (Citri & Malenka, 2008). On the other hand, non-synaptic plasticity includes changes in neuronal intrinsic properties regardless of synaptic connection parameters.

Synaptic plasticity manifests into two distinct forms with respect to its resource of allocation: homosynaptic and heterosynaptic plasticity (Byrne, 1997). Homosynaptic plasticity, also referred to as input-specific or associative plasticity, occurs at synapses directly involved in the activation of a cell during the induction process. This type of plasticity requires presynaptic activation of a given synapse for its induction. Conversely, heterosynaptic plasticity denotes changes in synaptic strength at synapses that are not directly stimulated. Both forms of plasticity may coexist and can complement each other (Chistiakova et al., 2014).

In 1964, Eric Kandel and Ladislav Tauc conducted pioneering studies on synaptic plasticity at the cellular level, focusing their investigations on the marine snail *Aplysia*. By pairing EPSPs with a conditioning stimulus, they observed long-lasting enhancement of the EPSP. Kandel and Tauc's studies on Aplysia laid the foundation for understanding the molecular mechanisms underlying synaptic plasticity, earning them the Nobel Prize in Physiology or Medicine in 2000 (Markram et al., 2012).

Experimental evidence for long-term synaptic plasticity was provided by Bliss and Lømo in 1973. They applied a repeated brief high-frequency stimulation (100 Hz) known as tetanus (Douglas & Goddard, 1975) to the perforant path fibres of hippocampal dentate gyrus, leading to a long-lasting potentiation of GrCs that persisted for hours. This phenomenon differed significantly from previously observed short-term potentiation and post-tetanic potentiation (Gerard, 1930; Bliss & Lømo, 1973). Although long-term synaptic potentiation (LTP) had been documented, there was still a lack of evidence for long-term synaptic depression (LTD). Hebb did not explicitly address synaptic depression (Hebb, 1949). In the field of machine learning, it became apparent that Hebbian rule lacked constraints to limit the increase of synaptic weight. This introduces the covariance learning rule and the concept of weight normalisation to mitigate this limitation (Markram et al., 2011). In 1973, Stent proposed an inverse mechanism to the Hebbian learning rule. According to this mechanism, not only coincident activities of pre- and postsynaptic neurons strengthen synaptic

connections (as Hebb suggested), but also anti-coincident activities (i.e., when postsynaptic neurons fires before the postsynaptic) should weaken these connections. This suggested that reversing the typical Hebbian combination of pre- and postsynaptic activations results in the induction of LTD rather than LTP. When coincident activity leads to LTD and anti-coincident activity leads to LTP, this phenomenon is termed as *anti-Hebbian plasticity.* Then, Levy and Steward (1979) contributed to the field by exploring *depotentiation,* which is the reversal of previously enhanced synaptic strength. This process is triggered by the activation of a weaker pathway without the need of pairing pre- and post-synaptic acitvity (Markram et al., 2011).

4.2 Short-Term Synaptic Plasticity

STSP refers to the transient changes in synaptic strength or efficiency that lasts from hundreds to thousands of milliseconds. It plays a crucial role in regulating the properties of synaptic transmission, thereby influencing the dynamics of circuit activity. STSP is thought to underlie sensory adaptations, transient changes in behaviour, and working memory at the behavioural level (Citri & Malenka, 2008).

The molecular mechanisms underlying STSP relate to the quantal hypothesis proposed by Bernard Katz. Specifically, Katz proposed that neurotransmitter release occurs in discrete packets known as quanta (Katz, 1969). During neurotransmission, depolarized presynaptic terminals lead to the opening of VGCC. The intracellular Ca^{2+} influx triggers the fusion of synaptic vesicles with the presynaptic membrane, leading to the neurotransmitter release into the presynaptic cleft; this process is called *exocytosis* (Zucker & Regehr, 2002). The work of Katz has shown that synapses are dynamic linkages with adaptable characteristics rather than static transmission elements. STSP involves both postsynaptic and presynaptic mechanisms that modulate neurotransmitter release and Ca^{2+} influx. These mechanisms can induce either synaptic facilitation or depression. Presynaptic mechanisms of STSP rely on changes in the probability of neurotransmitter release, with higher release probability leading to depression and lower release probability leading to facilitation. On the other hand, postsynaptic mechanisms entail desensitisation of the receptors.

STSP also occurs through paired-pulse stimulation, where the interval between stimuli may determine the sign of plasticity. Stimuli delivered within a short time interval (less than

20 ms) often result in paired-pulse depression caused by the inactivation of voltage-dependent sodium or VGCCs, or a temporary depletion of the readily releasable pool of vesicles at the presynaptic terminal. Conversely, longer interstimulus intervals (20- 500 ms) often lead to paired-pulse facilitation, attributed to residual Ca^{2+} buildup in the presynaptic terminal (Zucker & Regehr, 2002; Citri & Malenka, 2008).

4.3 Hebbian Long-Term Synaptic Plasticity

Long-term synaptic plasticity involves changes in synaptic strength that can persist from minutes to hours and even years. It has been considered as the molecular mechanism underlying learning and memory (Martin et al., 2000). While primarily investigated in the hippocampus, it is now recognized to be prevalent throughout diverse brain regions, each with multiple and distinct underlying mechanisms (Citri & Malenka, 2008). Recently, the molecular mechanisms driving long-term synaptic plasticity have been well-characterised. At the molecular level, long-term synaptic plasticity comprises three different phases: induction, expression and consolidation. Induction is associated with initial stimulation triggering Ca^{2+} influx changes, which activate intracellular signalling pathways. Expression involves structural changes in dendritic compartments, lastly consolidation involves stable changes and maintenance of a certain synaptic weight because of protein synthesis (Lüscher & Malenka, 2012).

Long-term synaptic plasticity manifests as LTP or LTD. Considering LTP, it refers to the persistent strengthening of synaptic connection in response to prolonged stimulation. LTP can be rapidly generated and further strengthened and maintained through repetition. Traditionally, LTP is induced by high-frequency stimulation (tetanus) of the presynaptic afferents, or by pairing low-frequency stimulation of presynaptic afferents with large postsynaptic depolarization (>30 mV; Caporale & Dan, 2008). LTP shows three main properties: cooperativity, associativity, and input specificity (Nicoll et al, 1988). Cooperativity implies that LTP can be induced by the simultaneous activation of a critical number of synapses. Associativity refers to the ability to strengthen a weak input when it is activated concurrently with a strong input, reflecting the Hebbian rule. Lastly, input specificity implies that LTP is elicited solely at active synapses and not at adjacent, inactive synapses reaching the same postsynaptic cell (Citri & Melanka, 2008). On the other hand, LTD reflects a

persistent weakening of synapses. Homosynaptic LTD has been identified in hippocampus and cerebral cortex in 1990s (Citri & Malenka, 2008). A typical protocol for eliciting LTD involves pairing prolonged repetitive low-frequency stimulation of presynaptic afferents (~900 stimuli at 1 Hz) with small postsynaptic depolarization (<30 mV; Dudek & Bear, 1992; Mulkey & Malenka, 1992). A study demonstrated that, delivering 900 pulses at 1 Hz on the Shaffer collateral projection, produced a depression of excitatory postsynaptic potential in CA1 neurons, which persisted for over an hour. Overall, the study highlighted that: i) the effect depended on the stimulation frequency, as 900 pulses at 10 Hz caused no lasting change, and at 50 Hz, synaptic potentiation was usually observed; ii) the depressed synapses still supported LTP in response to high-frequency tetanus; iii) the effects of conditioning stimulation could be prevented by applying NMDAR antagonists.

4.3.1 The role of intracellular calcium changes in long-term synaptic plasticity

The factors governing the direction of long-term synaptic plasticity at the molecular level were elucidated in the 1980s, providing a comprehensive understanding of Hebbian long-term synaptic plasticity. First, Bienenstock, Cooper and Munro (1982) introduced a new learning rule known as 'the BCM rule'. They demonstrated that low-frequency activity in the postsynaptic neuron during presynaptic pairing would induce LTD, while high frequencies lead to LTP (Markram et al., 2011). Later, ionotropic glutamatergic NMDAR were identified as *coincidence detectors* of presynaptic and postsynaptic activity, requiring presynaptic glutamate release immediately followed by postsynaptic depolarization (Figure 4.1) (Mayer et al., 1984).

LTP induction typically requires the activation of ionotropic glutamatergic NMDARs and AMPARs, localised on dendritic compartments. AMPARs are permeable to Na^+ and K^+ ions, while NMDARs are permeable to Ca^{2+}, in addition to Na^+ and K^+. When the postsynaptic membrane is close to its resting potential, NMDAR channels are obstructed by Mg^{2+} ions (Fig. 4.1). Consequently, the activation of AMPARs primarily contributes to the inward current responsible for generating EPSPs following presynaptic activation. Then, the membrane depolarization sustained by AMPAR activation allows Mg^{2+} to unblock from the NMDAR channel, thereby enabling Ca^2 influx and further facilitating membrane depolarization (Fig. 4.1). Therefore, NMDARs act as a coincidence detector being activated

only when glutamate is bound, and the postsynaptic neuron is depolarized. Then, the resulting Ca^{2+} influx through NMDARs activates various kinases, including calcium/calmodulin-dependent protein kinase II (CaMKII) and protein kinase A (PKA) (Malenka & Bear, 2004; Sjöström et al., 2008: Nicoll, 2017; Lisman, 2017).

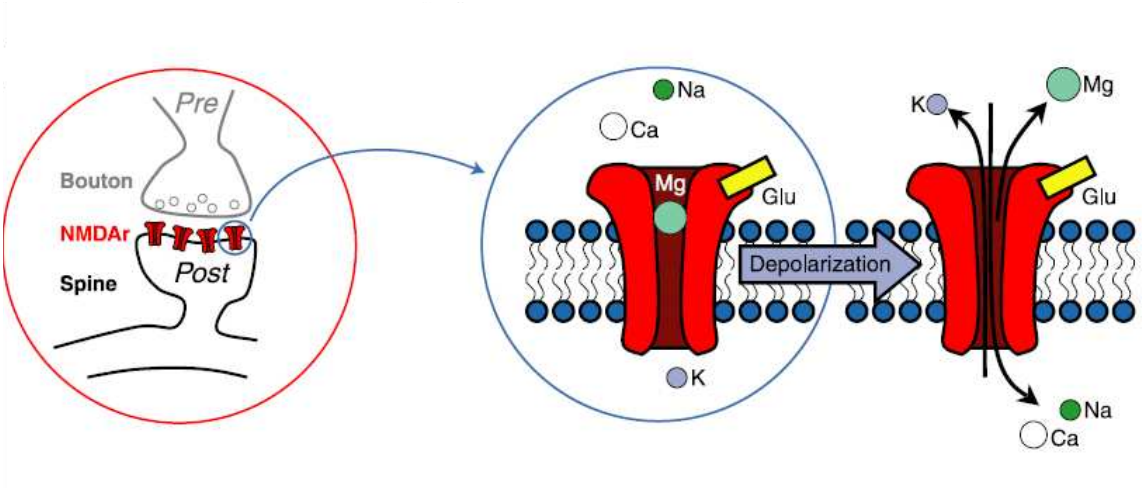

Figure 4.1 NMDA receptor channel unblock. Representation of the mechanism of NMDAR unblock showing that upon reaching a sufficient level of membrane depolarization, the NMDA receptor becomes unblocked, leading to Ca^{2+} influx (adapted from Sjöström et al., 2008).

While LTP and LTD have distinct induction protocols and effects, they share several common molecular mechanisms acting in different ways. The BCM rule suggests that intracellular Ca^{2+} level in the postsynaptic cell appears to define the sign of long-term synaptic plasticity. Lower-level membrane potentiation in the postsynaptic cell results in a modest Ca^{2+} influx leading to LTD, while higher-level membrane potentiation leads to a large Ca^{2+} influx leading to LTP. Specifically, activation of CaMKII by a large Ca^{2+} influx induces LTP induction, whereas recruitment of phosphatases such as protein phosphatase1 (PP1) and calcineurin by a modest Ca^{2+} increase is necessary for LTD induction (Caporale & Dan, 2008). Both processes involve alterations in AMPAR trafficking, either through insertion or removal from the postsynaptic membrane. Calcium signalling plays a crucial role in initiating these changes, with NMDARs and mGluRs serving as key sources of Ca^{2+} (Lisman, 2017). Both LTP and LTD are necessary to optimise the information storage in a neural network and

are thought to complement each other rather than functioning reversely (Malenka, 1994; Martin et al., 2000).

4.3.2 The role of timing and neuronal backpropagation in long-term synaptic plasticity

In the 1980s, Levy and Steward conducted a study on burst-induced synaptic plasticity, focusing on temporal asymmetry. They examined how granule cells in the hippocampal dentate area responded to strong ipsilateral and weak contralateral projections from the entorhinal cortex. They found that the timing sequence of strong and weak inputs from these different pathways critically influenced synaptic plasticity in the target cells. Specifically, strong stimulation preceding weak stimulation (by up to 20 ms) induced LTD in the weaker input pathway, while the reverse order induced LTD. Although they did not explore the precise timing effects of individual spikes, their findings suggested that the associative signal resided in the postsynaptic cell or a component thereof, supporting the principles of Hebbian theory. This signal could manifest as the cell discharge or as a significant and local dendritic depolarization, which, in turn, regulated individual synapses (Levy & Steward, 1983; Markram et al., 2011).

Until the late 1990s, experimental methodologies did not allow precise control of presynaptic stimulation. In 1991, Sakmann and Neher were awarded the Nobel prize in Physiology or Medicine for their research on ion channels and the invention of the patch-clamp technique, which revolutionised the field (Sakmann & Neher, 1984). This method facilitated investigations of synaptic plasticity at the ionic level, paving the way for the discovery of backpropagating action potential (bAP) role in this process.

Apical dendrites of pyramidal neurons exhibit voltage-gated Na^+ channels and VGCCs (Huguenard et al 1989; Regehr et al., 1993). As researchers began to focus on the role of postsynaptic activity in synaptic plasticity, Stuart and Sakmann (1994) challenged the traditional view of dendrites as passive elements (Huguenard et al 1989; Regehr et al., 1993). Building on previous findings that indicated active conductance in dendrites, they recorded from both the soma and the apical dendrite of cortical pyramidal cells. Their research revealed that an AP could propagate from the soma to dendrites (Stuart & Sakmann, 1994), suggesting

that this retrograde signalling might underlie Hebbian plasticity by directly activating VGCCs or enhancing synaptic Ca^{2+} influx. Markram and Sakmann (1995) later demonstrated that homosynaptic plasticity is tightly coupled to the precise timing of spikes emitted by the pre- and postsynaptic neurons, within a few tens of milliseconds. In 1997, the concept of STDP was established for the first time. The precise timing of postsynaptic backpropagating APs (bAPs; post) relative to EPSPs (pre) determined the sign of plasticity. When the presynaptic spike preceded the postsynaptic activation by less than 10 ms, LTP was induced. Conversely, when the presynaptic spike followed the postsynaptic activation by less than 10 ms, LTD occurred even if the induction frequency remained the same as for LTP (Markram et al., 1997). This highlighted the role of bAP as an associative signal that facilitates the induction of long-term synaptic plasticity (Magee & Johnston, 1997). Recently, the backpropagation of spikes has been recognised as a crucial mechanism underlying Hebb's rule, allowing neurons to detect the timing of presynaptic activation relative to their overall activity. The investigation of bAPs led to the identification of STDP as a fundamental Hebbian learning rule (Markram et al., 1997; Magee & Johnston, 1997). Therefore, neurons that fire together do not always wire together, timing is also essential (Markram et al., 2011).

4.4 Spike Timing Dependent Plasticity

STDP is a form of long-term synaptic plasticity that relies on the temporal relationship between the activity of presynaptic and postsynaptic neurons (Markram et al., 1997), that, in turn, controls the transition between st-LTP and st-LTD (Markram et al., 1997; Song et al., 2000; Caporale & Dan, 2008; Sgritta et al., 2017).

STDP involves the repeated EPSP-AP pairings within a specific time window, usually less than 100 milliseconds (Dan & Poo, 2004). This time window represents the temporal interval between the presynaptic and postsynaptic activity and can be either positive or depending on the causality between these two events. Specifically, a positive value indicates that presynaptic activity precedes postsynaptic activity (pre-before-post), while a negative value indicates the reverse (post-before-pre). The time window varies among different brain regions (Shouval et al., 2010). The relationship between the time window and plasticity changes is represented in an STDP timing curve, which serves as a synapse-specific representation of learning rules (Shouval et al., 2010). The temporal order and the time

interval between pre- and postsynaptic activity dictate the sign and magnitude of synaptic changes, respectively (Sgritta et al., 2017; Caporale & Dan, 2008; Song et al., 2000; Markram et al., 1997).

STDP is considered as Hebbian when causality is involved (Hebb, 1949). This means that pre-before-post activity leads to st-LTP, and post-before-pre activity leads to st-LTD. Conversely, when the opposite timing occurs, it is referred to as anti-Hebbian STDP. In both Hebbian and anti-Hebbian STDP, the backpropagation of postsynaptic spikes into dendrites is a necessary molecular mechanism. If this backpropagation does not occur, it is classified as non-Hebbian STDP (Sgritta et al., 2017). Different forms of STDP have been identified across various brain regions (Dan & Poo, 2004). STDP serves as a cellular mechanism for associative learning and behavioural conditioning. The correlation between spike-timing and the resultant change in synaptic strength is similar to that observed in classic conditioning experiments although in different time scales. This suggests that STDP reflects a fundamental neurophysiological manifestation of the principle of causality which underlies the temporal organisation of mental states (Froemke et al., 2010a,b).

4.4.1 Mechanisms of STDP induction

The molecular mechanisms underlying STDP typically rely on NMDARs and Ca^{2+} influx in the postsynaptic neuron, like those involved in long-term synaptic plasticity. Given the importance of timing for STDP, it is worth mentioning the distinct temporal kinetics between NMDARs and AMPARs and their role in long-term synaptic plasticity mechanisms. NMDARs have much slower kinetics than AMPARs, reaching peak conductance later and remaining open for 50-100 ms, whereas AMPARs remain open for only tens of milliseconds (Shouval et al, 2010: Lüscher & Malenka, 2012). During the pairing of postsynaptic bAPs and EPSPs, AMPARs are responsible for the initial depolarization and play a role in regulating the induction threshold and magnitude of LTP. In contrast, NMDARs are key for regulating Ca^{2+} influx based on postsynaptic depolarization levels. The timing of NMDARs unblock relative to a postsynaptic bAP appears to be crucial to determine the sign of STDP (Fuenzalida et al., 2010). In pre-before-post stimulation, bAP defines st-LTP time windows by facilitating the unblocking of Mg^{2+} from the NMDAR channel, leading to a strong Ca^{2+} influx (Lüscher & Malenka, 2012). Conversely, in post-before-pre stimulation, EPSPs coincide with the

afterdepolarization phase (AHP) of bAPs, resulting in a moderate level of Ca^{2+} influx. This low Ca^{2+} influx activates different signalling cascades that lead to st-LTD (Caporale & Dan, 2008). At synapses where st-LTD does not depend on NMDARs such as the PF-PC synapse, the induction of st-LTD is thought to depend on the activation of postsynaptic metabotropic glutamate receptor mGluRs and a Ca^{2+} influx through VGCC. This activation further triggers inositol 1,4,5-trisphosphate receptors (IP3) receptors signalling pathway (Bender et al., 2006).

Lastly, the involvement of neuromodulators is also crucial for the induction of STDP, as they modulate the synaptic activation of glutamate receptors (Brzosko et al., 2019). In the case of st-LTD, elevated postsynaptic Ca^{2+} levels can induce the synthesis of endocannabinoids, which function as a regulatory mechanism in the presynaptic neuron (Hashimotodani et al., 2007).

4.5 Plasticity in the Cerebellum

Synaptic plasticity studies have primarily focused on the hippocampus, which is associated with declarative memory. In contrast, the cerebellum has traditionally been associated with non-declarative procedural memory and motor learning. Given its crucial role in timing, learning, and prediction, research on plasticity has recently shifted attention towards the cerebellum.

Over the past two decades, various forms of plasticity have been identified in different cerebellar circuits (Hansel et al., 2001; Mapelli & D'Angelo, 2007; D'Angelo & De Zeeuw, 2009: Gao et al., 2012; D'Angelo, 2014), extending far beyond long-term synaptic plasticity at the PF-PC synapse proposed in the Motor Learning Theory (Marr, 1969; Albus, 1971). Indeed, long-term synaptic plasticity and intrinsic synaptic excitability have been shown to be distributed across the DCN, molecular layer, and granular layer, thereby sustaining cerebellar computation and learning (D'Angelo, 2014; Mapelli et al., 2015; Figure 4.2).

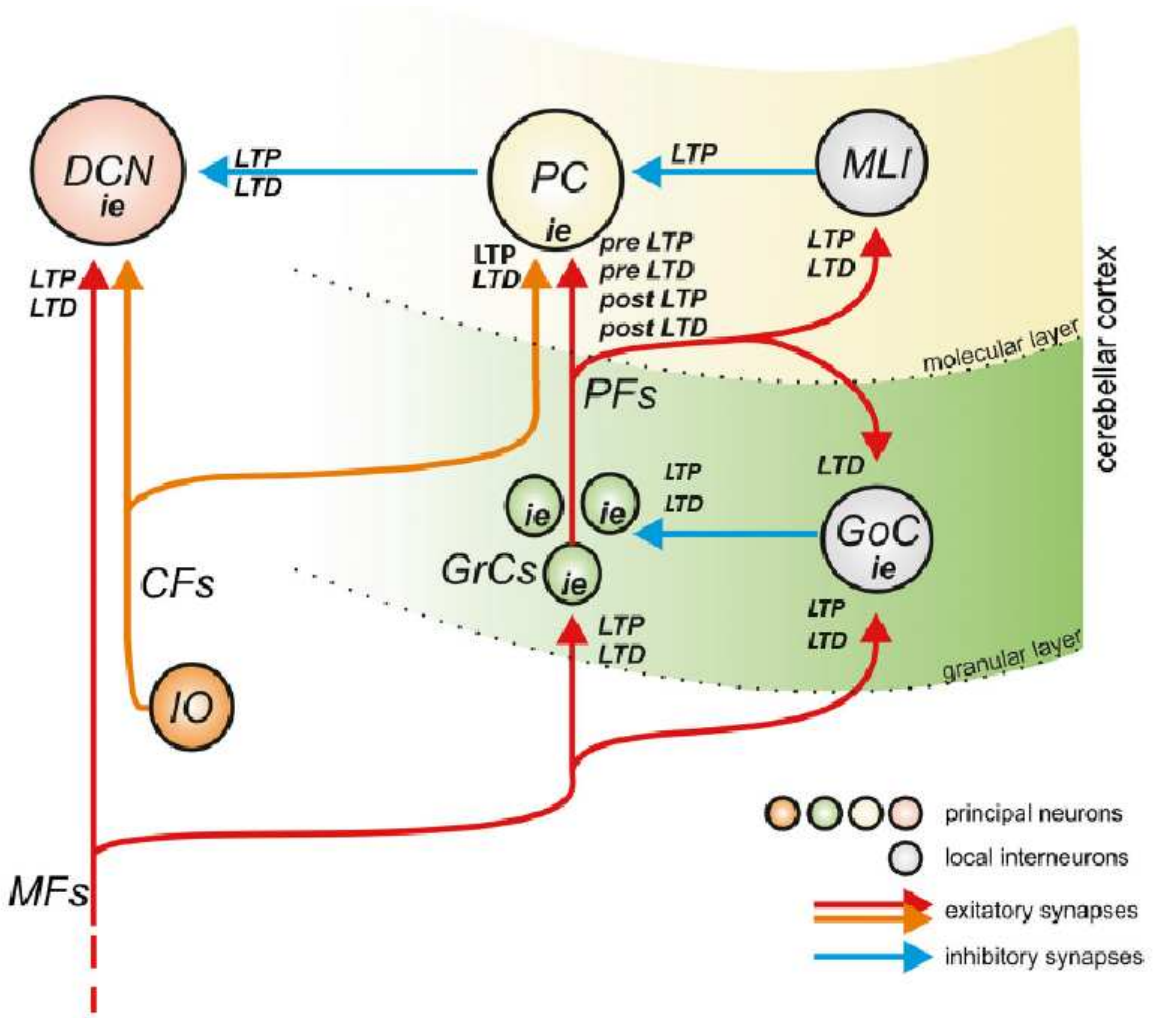

Figure 4.2 The distribution of synaptic plasticity in the cerebellum. The scheme shows the key hubs of synaptic plasticity in the cerebellum: granular layer, molecular layer and deep cerebellar nuclei (DCN). Mossy fibres (MFs) make excitatory synapses (red arrow) onto granule cells (GrCs), while both molecular layer interneurons (MLI) and Golgi cells (GoCs) make inhibitory connections (blue arrows) onto GrCs and PCs, respectively. Additionally, excitatory synapses from climbing fibres (CFs) onto DCN and Purkinje cells (PCs) are depicted. LTP: long-term potentiation; LTD, long-term depression ie: intrinsic excitability (adapted from Mapelli et al., 2015).

4.5.1 Synaptic Plasticity in the Molecular Layer

According to the Motor Learning Theory, PF-PC LTD driven by CF signals is considered sufficient for regulating cerebellar learning. However, recent studies have demonstrated various forms of plasticity between different cell types in the molecular layer,

indicating that cerebellar learning is based on a variety of different plasticity mechanisms (Bell et al.,1997; Hansel et al., 2001; Gao et al., 2012; D'Angelo, 2014).

Both postsynaptic and presynaptic forms of LTP and LTD have been observed at PF-PC synapses. Additionally, LTD has been demonstrated at CF-PC synapses. Long-term synaptic plasticity has also been observed at PF-MLI synapses and MLI–PC synapses (Mapelli et al., 2015). Lastly, LTP of intrinsic excitability has been found in PCs (as reviewed in D'Angelo, 2014).

Regarding postsynaptic LTD at the PF- PC synapse, it can be induced by paired stimulation of PFs and CFs, involving complex signal transduction pathways. PFs release glutamate which acts on both mGluRs and AMPARs, initiating a second messenger system in the postsynaptic side. CFs contribute to plasticity by generating widespread Ca^{2+} transients via complex spikes. This occurs when CFs release glutamate at their terminals, activating AMPARs and inducing strong depolarization in PCs. Furthermore, Ca^{2+} influx is facilitated by VGCCs and calcium-induced calcium release (CICR), alongside NMDARs activation by CFs. Simultaneously, an increase in intracellular Ca^{2+} concentration, and diacylglycerol (DAG), mediated by mGluR signalling cascade, activates Protein kinase C (PKC), which functions as the coincidence detector between PF and CF activity. PKC phosphorylates GluR2 subtypes of AMPARs, leading to their desensitisation and internalisation via endocytosis, ultimately leading to PF-PC LTD synapses. However, CF activity does not appear to be essential for LTD; intense PF stimulation or gradual summation of Ca^{2+} signals through multiple PF activations can also induce LTD. Extrinsic factors such as nitric oxide (NO), released from PFs due to brief PF burst stimulations, have been shown to promote postsynaptic LTD at PF-PC synapses (D'Angelo, 2014).

Synaptic plasticity occurs bidirectionally at PF-PC synapses, including both LTP and LTD. This bidirectional plasticity observed at PF-PC synapses contrasts with the typical pattern observed in hippocampal connections, suggesting an inverse BCM rule. In this context, low levels of Ca^{2+} lead to LTP, while high levels of Ca^{2+} lead to LTD (Gao et al., 2012). Bidirectional plasticity is also evident presynaptically at PF- PC synapses and it is independent of CF activation. Presynaptic LTP is induced by low-frequency stimulation of PFs, likely involving presynaptic Ca^{2+} influx and NO production, which regulate the release probability of glutamate. Endocannabinoids also contribute to presynaptic LTP at PF-PC synapses. High-frequency bursts may evoke endocannabinoid release activating cannabinoid1

(CB1) receptors in PF terminals. This suppresses Ca^{2+} sensitive adenylyl cyclase 1 (AC1), reduces cyclic α-amino-3-hydroxy-5-methyl-4-isoxazolepropionic acid (AMP), and attenuates PKA activity. Therefore, retrograde regulatory mechanisms in presynaptic LTP control plasticity at PF-PC synapses (D'Angelo, 2014; Mapelli et al., 2015).

Another form of plasticity in the molecular layer is LTD at CF-PC synapses, induced by brief tetanization of CFs, leading to a reduction in the slow component of the complex spike. This alteration may lead to a prolonged pause in complex spikes due to changes in afterhyperpolarization (Hansel & Linden, 2000). LTD at CF-PC synapses further modulates the postsynaptic expression of LTD and LTP at PF-PC synapses (Coesmans et al., 2004).

Long-term synaptic plasticity occurs at PF-MLI synapses as well as at MLI-PC synapses. MLIs establish feedforward loops in the molecular layer (PF-MLI-PC) which may synergistically influence PF-PC synapses via PF-MLI LTD. PF-PC LTD may coincide with LTP at PF-MLI and MLI-PC synapses, enhancing PC responses, while PF-PC LTP may coincide with LTD at the same synapses, reducing PC responses (Gao et al., 2012; Mapelli et al., 2015).

Lastly, intrinsic plasticity has been reported in PCs. Intrinsic plasticity refers to changes in neuronal electrical properties, such as modifications in ion channel expression and membrane properties. These changes can be induced by either neuronal spiking activity or synaptic inputs (Gao et al., 2012). In PCs, intrinsic plasticity is promoted by PF LTP, which subsequently inhibits further LTP induction through Ca^{2+} signalling in dendritic spines. This mechanism is believed to function as a regulatory mechanism at weaker, non-potentiated synapses (Mapelli et al, 2015).

4.5.2 Synaptic Plasticity in the DCN

The DCN, serving as the sole output of the entire cerebellum, holds a strategic position within the cerebellar circuitry for integrating plasticity (Mapelli et al., 2015). Recent suggestions propose that plasticity within the cerebellar cortex could operate on shorter timescales, storing transient memories that can be later transferred downstream and consolidated through plasticity at the DCN level (Mapelli et al., 2015).

Neurons in the DCN form synapses with MF collaterals. Stimulation of PCs leads to robust post-inhibitory rebound spike bursts in DCN cells, driving long-term plastic changes at MF-DCN synapses. Moreover, high-frequency bursts of MFs can induce synapse-specific MF- DCN LTP, which is crucial for associative learning tasks (Pugh & Raman, 2006). During eyelid conditioning, the firing rate of PCs decreases upon the presentation of the conditioned stimulus, resulting in DCN disinhibition and the generation of a blink.

At PC-DCN synapses, both LTP and LTD have been observed, depending on the activation of NMDARs and the increase in postsynaptic intracellular Ca^{2+} concentrations. A closed-loop robotic system, incorporating long-term plasticity at PF-PC, MF-DCN, and PC-DCN synapses, can simulate the adaptation of the VOR (Wang et al., 2008; D'Angelo, 2014). PF-PC synapses rapidly learn contextual information to correct movement errors, while PC-DCN and MF-DCN synapses store this information. This arrangement provides remarkable flexibility, preventing PF-PC synaptic weights from saturating, enabling rapid readaptation (Casellato et al., 2015).

4.5.3 Synaptic Plasticity in the Granular Layer

The Motor Learning Theory overlooked granular layer plasticity, assuming that the balance between inhibitory and excitatory signals in this layer is predetermined and static (Marr, 1969; Albus; 1971). However, it is now recognized that the granular layer plays a crucial role in regulating the timing, geometry, and coding of inputs that need to be conveyed to PCs (D'Angelo, 2014). Therefore, recent studies have shed light on many forms of synaptic plasticity in the granular input layer (Mapelli & D'Angelo, 2007; D'Angelo & De Zeeuw, 2009).

4.5.3.1 Plasticity at the MF-GrC synapse

LTP at MF-GrC synapses is orchestrated by a sophisticated interplay of intracellular calcium dynamics and multiple signalling pathways. Central to this process are NMDARs, which mediate Ca^{2+} influx. This influx is further amplified by the action of metabotropic glutamate receptors 1 (mGluR1s) via the IP3 pathway. Additionally, the activation of VGCCs

triggers membrane depolarization and the generation of repetitive spike discharges, crucial for LTP induction. Moreover, CICR amplifies and sustains these Ca^{2+} signals, consolidating long-term plastic changes at synapses.

Long-term synaptic plasticity at MF-GrC synapses involves NMDA-dependent bidirectional plasticity (Gall et al, 2005; Mapelli et al.,2015; Mapelli et al., 2022). According to the BCM rule, low-frequency bursts and mild membrane depolarization promote LTD by limiting Ca^{2+} influx, while high-frequency bursts and strong membrane depolarization enhance LTP (Gall et al., 2005). Furthermore, MF-GrC synaptic plasticity is regulated by neuromodulators. Activation of a7-nicotinic acetylcholine receptors (nAChRs) by the cholinergic system enhances MF-GrC LTP, altering the Ca^{2+} synaptic plasticity relationship. Under nicotine exposure, brief MF bursts that typically induce LTD can instead lead to LTP (Prestori et al., 2013). NO also modulates LTP-LTD balance. At high frequency of MF stimulation, there is a consistent release of NO in the granular layer, which depends on NMDAR and NO activity (Maffei et al., 2003; Mapelli et al., 2017).

Additionally, MF-GrC LTP modifies intrinsic electroresponsiveness, enhancing GrC firing, by reducing spike threshold through persistent modifications in Na^{+} and K^{+} currents (Nieus et al., 2006; D'Angelo, 2014). GoC-mediated inhibition further regulates membrane depolarization at the MF-GrC relay, influencing NMDAR unblocking through shunting inhibition, synaptic plasticity induction, and postsynaptic Ca^{2+} influx (Mapelli & D'Angelo, 2007). Additionally, GoC tonic and phasic inhibitions onto GrCs play a key role in modulating their intrinsic excitability (Armano et al., 2000).

4.5.3.2 Plasticity in the GoC network

GoCs are the main source of inhibition onto GrCs, playing an essential role in modulating the spatiotemporal processing of inputs within the granular layer (see Chapter 3). As a consequence of GoC lateral inhibition, LTP and LTD exhibit a centre-surround organisation within the granular layer, where more active centres tend to generate LTP, while less active surrounds determine LTD (Mapelli et al, 2015). This control is essential for regulating plasticity at MF- GrC relay and the spatiotemporal reconfiguration of inputs within the granular layer (D'Angelo & De Zeeuw, 2009; Locatelli et al., 2021).

Long-term synaptic plasticity also occurs at excitatory synapses onto GoCs (Robberechts et al., 2010; D'Angelo, 2014; Locatelli et al., 2021). LTD at PF - GoC synapses in the molecular layer is driven by the activation of mGluR2 receptors in response to high-frequency bursts of PF activity (Robberechts et al., 2010). Additionally, long-term synaptic plasticity at MF-GoC synapses relies on postsynaptic membrane depolarization (Locatelli et al., 2021). MF theta burst stimulation (TBS) delivered at a depolarized potential induces LTD at MF-GoC synapses, whereas TBS delivered at hyperpolarized potential leads to LTP, indicating the existence of a voltage dependence plasticity mechanism at the MF-GoC relay. The induction of LTP and LTD involves T-type and L-type VGCCs activation, together with NMDAR unblocking. Specifically, LTP requires the activation of T-type channels, activated at lower membrane potentials (positive to -70 mV), in addition to NMDARs. Conversely, LTD requires only L-type VGCCs, activated at higher membrane potentials (positive to -30 mV). These findings suggest that MF enables different forms of plasticity depending on membrane potential of the cell (Locatelli et al., 2021).

A computation model analysed the impact of distributed synaptic plasticity within the granular layer (Garrido et al., 2013). This model demonstrated that during MF bursts, the timing of the first spike in GrCs is primarily governed by the strength of MF-GrC connections. GrC-GoC synaptic connections regulate spike emission when GrC activity is high. Specifically, LTP at MF- GrC synapses reduces GrC reaction times. In the model, increasing the weights at MF-GoC synapses anticipated GoC firing and subsequent inhibition on GrCs, thereby shortening the time window for GrC firing. Overall, the temporal precision of the first GrC spike emitted is modulated by excitatory synapses onto GoCs, which involves plastic changes at both MF-GoC and PF-GoC synapses.

4.6 STDP in the Granular Layer

The granular layer of the cerebellum exhibits rapid temporal dynamics, operating within tens of milliseconds, potentially facilitating various forms of STDP (Garrido et al., 2013; Locatelli et al., 2021). A recent study has demonstrated the existence of Hebbian STDP occurring at MF-GrC synapses in the theta frequency range (4-10 Hz). Additionally, STDP was abolished by either randomised EPSP-AP pairings or high intracellular Ca^{2+} buffering,

and it was reversed to anti-Hebbian STDP by activation of the $GABA_A$ receptors (Locatelli et al., 2021).

4.6.1 Prediction of STDP at the MF- GoC synapse

A recent study using a detailed multi-compartmental model of GoC simulated the integration of excitatory inputs on apical and basal dendrites of GoCs (Masoli et al., 2020). This simulation suggested that precisely correlated MF-PF inputs can drive STDP at MF-GoC synapses.

When PF input precedes MF input, this latter falls in the AHP region of the bAP elicited by PF stimulation. This results in a minor membrane depolarization in basal dendrites. In this scenario, NMDAR channels fail to effectively unblock, resulting in LTD. Conversely, when PF input follows MF input, this latter coincides with the rising phase of the backpropagating PF-AP, causing a significant membrane depolarization of basal dendrites. This facilitates NMDAR activation, leading to LTP (Masoli et al., 2020).

B. Rationale and Aim

Rationale

The cerebellum, characterised by its uniform neural circuitry and high cell density, has been recognized as a timing, learning, and prediction machine within the brain (Mapelli et al., 2015). Not surprisingly, various forms of long-term synaptic plasticity have been explored in cerebellar circuitry, including the granular layer, a key hub for cerebellar plasticity (Gao et al. 2012; D'Angelo, 2014; Mapelli et al., 2015). This layer is notable for its role in fast, sub-milliseconds information processing contributing significantly to the cerebellum's timing function (D'Angelo & De Zeeuw 2009; Garrido et al., 2013). GoCs, inhibitory interneurons located in the granular layer, play a pivotal role in the spatiotemporal processing of cerebellar inputs. Characterised by apical and basal dendrites with distinct electrophysiological properties, GoCs receive excitatory synapses from PFs on their apical dendrites and from MFs on their basal dendrites (Rudolph et al., 2015; Prestori et al.,2019; Masoli et al., 2020). With their large soma and long extensions, GoCs regulate GrC signalling ensuring that the information is properly integrated, timed and patterned before being conveyed to PCs, the sole output of the cerebellar cortex (D'Angelo & De Zeeuw 2009). GoCs are essential for both accurate motor timing and coordination, indeed their ablation results in ataxia, a neurological condition consisting of lack of voluntary muscle coordination (Watanabe et al., 1998). Despite their importance, the mechanisms governing the plasticity at GoC excitatory synapses have been unexplored.

STDP is a form of long-term synaptic plasticity where the precise time window between presynaptic activity and postsynaptic depolarization determines the direction and strength of the plasticity (Markram et al., 1997, 2011; Bi & Poo; 1998; Dan & Poo, 2004; Caporale & Dan, 2008). Typically, STDP at excitatory synapses involves NMDARs, which act as coincidence detectors, requiring both presynaptic glutamate release and postsynaptic depolarization for their activation. NMDARs are also Ca^{2+} permeable, regulating the amount of intracellular Ca^{2+} influx and thus, according to the BCM rule, the plasticity sign (Malenka & Bear, 2004; Gall et al., 2005; Caporale & Dan, 2008; Song et al., 2010; Sgritta et al., 2017). In Hebbian plasticity, active dendritic properties and dendritic backpropagation influence the

postsynaptic signal, either enhancing or limiting NMDAR activation (Sjöström et al., 2008). In the granular layer, NMDAR-dependent Hebbian STDP has been observed at MF-GrC synapses (Sgritta et al., 2017). STDP is a promising candidate to explain the plasticity at MF-GoC synapses. Indeed, a recent computational study developed a detailed multicompartmental model of GoCs predicting that temporal correlated MF-PF inputs can drive STDP at MF- GoC synapses, under NMDARs activation (Casena et al., 2013; Masoli et al., 2020).

Aim

Given the vital role of GoC inhibitory function in cerebellar information processing and spatiotemporal reconfiguration of inputs within the granular layer, it is crucial to understand the mechanisms governing plasticity at cerebellar GoC synapses.

Recently, a detailed multicompartmental model of GoC has predicted that temporally correlated MF-PF inputs can drive STDP at MF-GoC synapses when NMDARs are activated (Masoli et al., 2020). To experimentally validate these predictions, we performed whole-cell patch-clamp recordings in acute coronal slices of the cerebellum from GlyT2 transgenic mice. We repeated MF-PF stimulus pairs with specific phase differences (±10, ±25, ±50, ±100 ms) at a frequency of 4 Hz for 60 iterations.

Our investigation aims to elucidate the functional significance of segregating inputs onto two distinct sets of dendritic projections—apical and basal dendrites. By doing so, we seek to uncover the intricate role of dendritic communication in governing both input processing and plasticity in GoCs. Ultimately, through this investigation, we aim to shed light on a novel plasticity mechanism that might allow GoCs to control learning and computation within the cerebellar granule cell layer, with high temporal precision.

C. Materials and Method

5.1 Materials

In line with the international guidelines of the European Union Directive 2010/63/EU, all animal manipulations and research procedures were approved by the Italian Health Office (authorization no. 638/2017-PR)/article 1, comma 4 of the D. Lgs. n. 26/2014) and the University of Pavia's Ethical Committee.

5.1.1 Animals and housing

Experimental procedures were carried out on 16-21 days old (P0 = day of birth) GlyT2-eGFP mice of either sex heterozygous for the bacterial artificial chromosome insertion of eGFP. The insertion of eGFP was performed under the control of the glycine transporter type 2 gene (Zeilhofer et al., 2005). To retain their heterozygotes, GlyT2-eGFP mice were bred on the C57BL/6 genetic background. All mice were grouped and housed in an artificially lit room with free access to water and food. The standardised 12:12 hour light-dark cycle, and a constant temperature and humidity were maintained throughout the study.

5.1.2 Slice preparation and maintenance

GlyT2-eGFP mice were anaesthetised with halothane (Sigma-Aldrich) and were sacrificed by quick decapitation under deep anaesthesia. The cerebellum was isolated using a well-established protocol (Forti et al., 2006; Cesana et al., 2013). Following the isolation, the cerebellum was fixed on the Leica VT1200S vibroslicer stage (Leica Biosystems) using cyano-acrylic glue. The 220 μm thick acute brain sections were cut in the coronal orientation, with an ice cold (2–3ºC) cutting solution containing the following: potassium gluconate 130 mM, KCl 15 mM, ethylene glycol-bis (β-aminoethyl ether) N,N,N',N'-tetraacetic acid (EGTA) 0.2 mM, N-2-hydroxyethyl piperazine-N-2-ethanesulphonic acid (Hepes) 20 mM, glucose 10 mM, pH 7.4 with NaOH (Dugué et al., 2005). Right after slices were obtained, they were quickly placed into an oxygenated bicarbonate-buffered (Krebs) solution that contained the

following: NaCl 120 mM, KCl 2 mM, $MgSO_4$ 1.2 mM, $NaHCO_3$ 26 mM, KH2PO_4 1.2 mM, $CaCl_2$ 2 mM, glucose 11 mM (pH 7.4 when equilibrated with 95% O_2–5% CO_2), and the slices were incubated in a submerged chamber at 32°C for at least 1 hour. Throughout the recordings, slices were kept in the recording chamber, mounted on the stage of an upright microscope (Olympus), and were continuously perfused with oxygenated Krebs' solution (1.5 ml/min) maintaining the temperature at 32°C with a Peltier feedback device (TC-324B, Warner Instrument Corp.).

5.1.3 Pharmacological application

During all experiments, 1 μM strychnine hydrochloride (Sigma-Aldrich) as glycinergic receptor antagonist and 10 μM SR 95531 (6-imino-3-(4-methoxyphenyl)-1(6H)-pyridazine butanoic acid hydrobromide, gabazine; Abcam) as $GABA_A$ receptor antagonist were added to the Kreb's solution to constantly block inhibitory synaptic transmission. During certain experiments, the Krebs' solution was supplemented with 50 μM 7-chlorokynurenic acid sodium salt (7-Cl Kyn; Abcam) and 100 μM D-2-amino-5-phosphonovalerate (D-APV; Abcam) to block NMDARs. All pharmacological agents were prepared in water and kept at -20°C. While in use they were diluted (1:1000) in an external bath solution.

5.2 The Patch-Clamp Technique

The patch-clamp technique is an electrophysiological recording method that allows detailed investigations on a cell of interest, similar to intracellular recording techniques (Hamill et al., 1981). However, unlike intracellular recordings where the pipette penetrates the cell, in patch-clamp recordings the pipette does not penetrate the cell. Instead, a glass micropipette filled with an intracellular solution forms a high-resistance seal with the cell membrane, known as a giga-ohm seal. When the pipette is pulled away, the membrane around the patch breaks while maintaining the seal intact. This occurs because the bond between the pipette glass and the cell membrane is stronger than the membrane itself (Molleman, 2003,

p.2). At this point, a continuous electrical pathway between the cell's interior and the pipette internal solution is established.

In voltage-clamp mode, the membrane potential can be controlled, allowing direct recording of membrane currents. This is achieved through an electronic feedback system, where the measured potential is compared to a predetermined holding potential, and any deviation is corrected by injecting compensatory currents. Conversely, in the current-clamp mode, the current is controlled without a feedback system and the voltage is not clamped (Molleman, 2003, p.29).

Patch-clamp is a versatile technique that can be performed through various configurations, allowing researchers to study ion channels at distinct levels. It can measure the cumulative activity of all ion channels in the whole-cell configuration (Figure 5.1) or focus on individual ion channels either with the inside-out and outside-out configurations. Additionally, it enables easy manipulation of the extracellular or intracellular fluid of the membrane during recordings (Molleman, 2003, p.32).

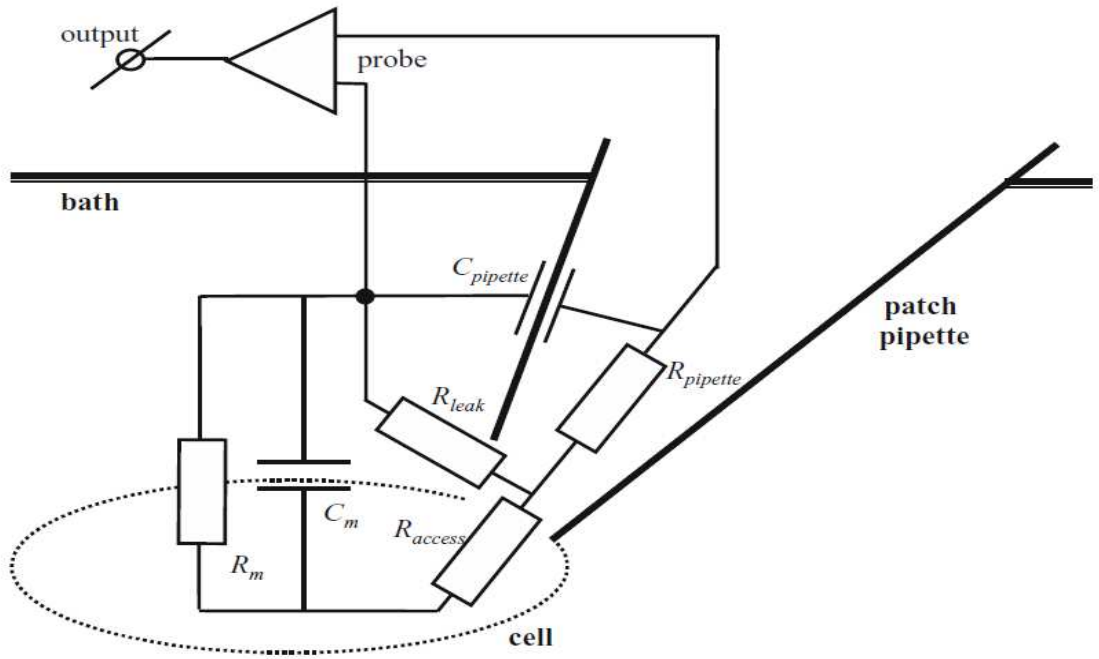

Figure 5.1 The electrical circuit of the whole-cell patch-clamp recording. Representation of a circuit formed by patch pipette and cell's interior consists of the pipette resistance

($R_{pipette)}$, the access resistance ($R_{access,}$), and the membrane resistance (R_m). As R_m is the largest resistor, it enables the observation of whole-cell currents. The leak resistance (R_{leak}) parallel to the circuit, should be as high as possible to minimise short-circuiting of membrane current. The membrane capacitance (C_m) influences the voltage clamp's time characteristics. The picture shows a circuit in the voltage-clamp mode formed by R_{access} and $R_{pipette}$ (their sum known as series resistance), in series with C_m, where the holding potential is set by the experimenter (taken from Molleman, 2003, p.40).

5.2.1 Whole-cell recordings from GoC soma

An upright epifluorescence microscope (Olympus) with a 40X (numerical aperture NA = 0.8) water-immersion objective (Olympus) was used for slice visualisation during electrophysiological recordings. The soma of visually recognized GoC was targeted for whole-cell patch-clamp recordings. A Sutter P-1000 horizontal puller (Sutter Instruments) was used to produce patch pipettes (3-5 MΩ) from standard borosilicate glass capillaries. Later, the patch pipettes were filled with an intracellular solution containing the following: potassium gluconate 145 mM, KCl 5 mM, HEPES 10 mM, EGTA 0.2 mM, MgCl2 4.6 mM, ATP-Na2 4 mM, GTP-Na2 0.4 mM, and pH 7.3 was adjusted with KOH. Using a Multiclamp 700B amplifier and pClamp data acquisition software, whole-cell patch-clamp recordings were acquired. Data sampling at 50 kHz was achieved with a Digidata 1440A interface (Molecular Devices, USA). The pClamp10.7 software from Molecular Devices served for offline signal analysis. A low-pass filter was applied to excitatory postsynaptic currents (EPSCs) at fc = 10 kHz (-3 dB). In line with previous studies (Forti et al., 2006; Locatelli et al., 2021), recordings were eliminated when the baseline current recorded at -70 mV was negative to – 150 pA. Throughout the recording, series resistance (Rs) (3.6 ± 0.2 MΩ, n = 109) was continuously tracked and compensated by 10–60%; accepted recordings were only those with stable Rs (changes < 20%). The values of membrane potential were not corrected for liquid junction potentials.

5.2.2 Voltage-Clamp Modality: Stimulation

STDP induction involved the stimulation of MF and PF using two glass monopolar electrodes (1-2 MΩ, 3-10 μm diameter) filled with Krebs' solution. The electrode for MF stimulation was positioned in the white matter, while the electrode for PF stimulation was placed in the molecular layer (Figure 5.2). Before and after the STDP induction, EPSCs were evoked at -70 mV by stimulating MF bundles with voltage steps at a frequency of 0.1 Hz (test frequency) using a stimulus isolator system. This simulation was conducted for either 10 minutes in the control condition before the STDP induction or 30 minutes in the post-STDP induction condition.

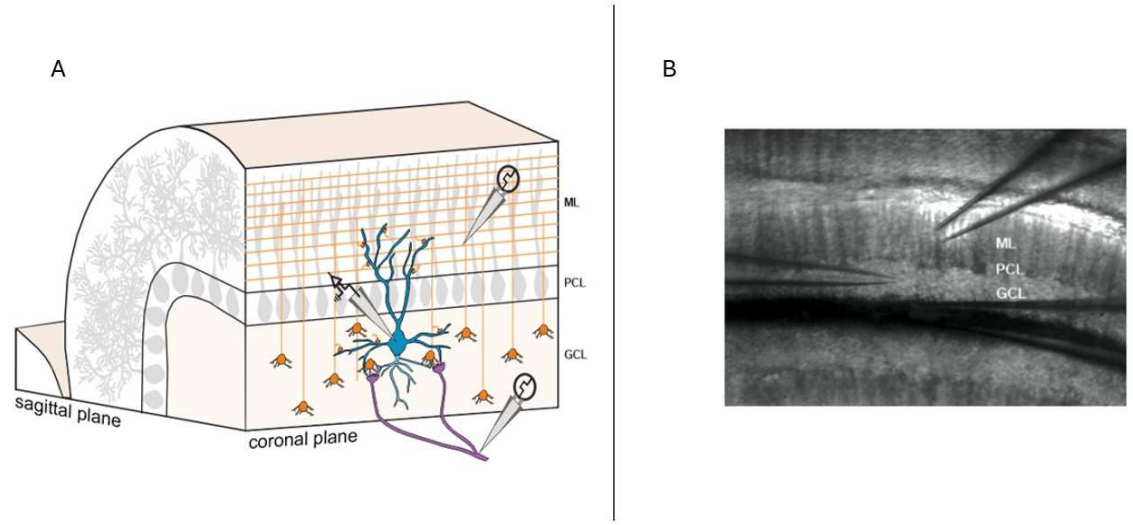

Figure 5.2 The configuration of the whole-cell recordings and electrode placement. A, Schematic representation of the position of a Golgi cell (blue) in the coronal section of the cerebellar cortex. MF bundles are depicted in purple, and granule cells and their axons (parallel fibres) are depicted in orange. (ML: molecular layer; PCL: Purkinje cell layer; GCL: granular cell layer). **B,** Image of an experiment showing the recording pipette located in the GCL. One of the glass monopolar electrodes placed in the ML to stimulate the parallel fibres, and the other placed in the white matter to stimulate mossy fibres.

GoC-evoked EPSCs can exhibit either a short latency response (one peak per stimulus) or a combination of short- and long-latency responses (multiple peaks per stimulus) according to previous studies (Cesana et al., 2013; Tabuchi et al., 2019). In fact, a pipette

placed within the MF bundle stimulates not only GoC basal dendrites via a monosynaptic pathway (MF - GoC) but also GrC dendrites within the glomerulus. These GrC dendrites then create a disynaptic pathway (MF - GrC - GoC) by forming synaptic connections with GoC apical dendrites through PFs.

5.2.3 Current-Clamp Modality: STDP induction protocol

By pairing PF-MF stimulations 60 times at 1, 4, or 10 Hz with a fixed temporal window ($\Delta t = \pm 10, \pm 25, \pm 50$, or ± 100 ms), STDP was elicited from a holding potential (V_{hold}) of approximately −60 mV. The timing window (Δt) was defined as the interval between the peak of the PF-AP (action potential elicited stimulating PF) and the onset of the MF-EPSP (excitatory postsynaptic potential evoked stimulating MF). In accordance with the canonical pair-based STDP criteria, a spike timing interval was considered positive when MF-EPSP arrived after PF-AP and negative when MF-EPSP arrived before PF-AP. Indeed, postsynaptic activity coincided with PF-AP and presynaptic activity coincided with MF-EPSP (Figure 5.3).

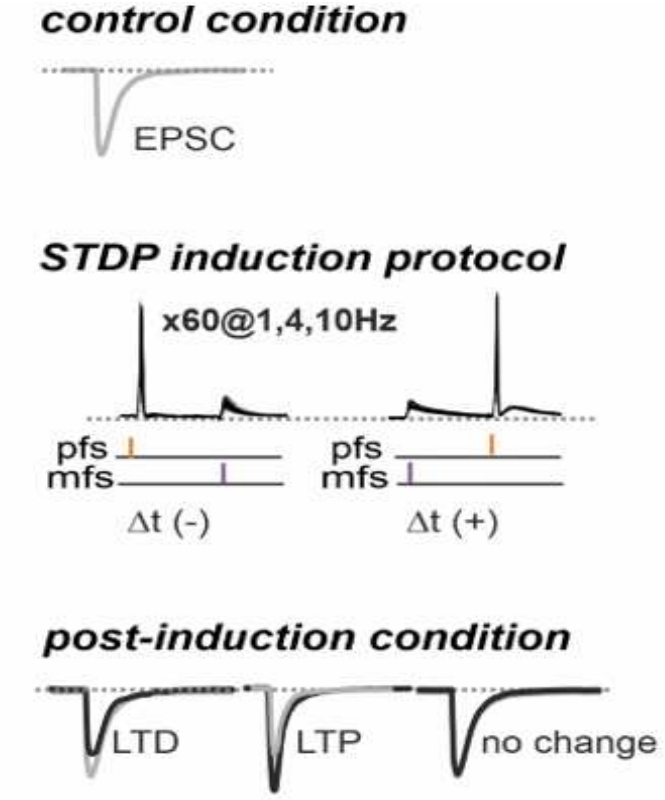

Figure 5.3 Summary scheme of the experimental design. Control condition (up): EPSCs were recorded before STDP induction. STDP induction protocol (middle): the timing window (Δt) is negative when an action potential elicited by stimulating parallel fibres (pfs) arrives before an excitatory postsynaptic potential elicited by stimulating mossy fibres (mfs), and positive when the order is reversed. Paired PF-MF simulations are repeated 60 times at 1, 4, or 10 Hz with a fixed temporal window (Δt = ±10, ±25, ±50, or ±100 ms). Post-induction condition (bottom): EPSCs were recorded for 30 minutes after the STDP induction protocol, to determine whether and to what extent LTD, LTP, or no change in synaptic strength were induced.

5.3 Data Analysis

All EPSCs underwent digital filtering at 1.5 kHz and were subjected to offline analysis with pClamp10.7 software (Molecular Devices, USA). Following the methodology of

previous studies (Cesana et al., 2013; Locatelli et al., 2021), short-latency responses were considered when the time to peak was less than 2.0 ms. The difference between the peak EPSC and the current level immediately prior to stimulation was used to calculate the EPSC amplitude. Changes in long-term synaptic efficacy (percent change, % change) were assessed after 30 minutes during post-induction protocol.

Statistical analyses were performed using OriginPro 8. Data are presented as mean ± SEM. The Shapiro-Wilk test was used to verify the normal distribution of the data. Statistical significance was determined using either student's t-test or one-way parametric ANOVA, with further analysis by Tukey's post hoc test when necessary. The analyses were two-sided with a significance level of $\alpha = 0.05$.

D. Results

6.1 Identification criteria of GoCs

Acute cerebellar slices from juvenile (P16-P21) GlyT2-eGFP mice were used to perform experiments. Whole-cell recordings were conducted on visually identified GFP-positive GoCs, known to represent 86% of total GoC population (Dugué et al., 2005; Simat et al., 2007). To distinguish GoCs from other GFP-positive interneurons located in the granular layer, such as Lugaro cells and their subtype, globular cells, (Simat et al., 2007; Zeilhofer et al., 2005), we used morphological and electrophysiological criteria (Dieudonné & Dumoulin, 2000; Eyre & Nusser, 2016; Hirono et al., 2017): i) based on the typical anatomical location of Lugaro cells directly beneath Purkinje cells (Prestori et al., 2019; Miyazaki et al., 2021), GFP-positive cells primarily positioned in the central region of the granular layer were exclusively selected (Figure 6.1A); ii) cells with a rounded shape and large soma (>15 µm diameter) were exclusively selected (Fig. 6.1A) considering that Lugaro cells have smaller soma and display an elongated shape; iii) assessment of responses to voltage steps revealed that the selected cells exhibited a large membrane capacitance (C_m = 49.5 ± 1.2 pF) and a low input resistance (R_{in} = 119.7 ± 4.9 MΩ, n = 109). These characteristics indicate large neuronal size and an extensive axonal plexus, which are distinctive features of GoCs (Forti et al., 2006; Locatelli et al.,2021); iv) recorded neurons showed spontaneous firing potentials (Figure 6.1B) and exhibited an average resting membrane potential (V_m) consistent with that reported for GoCs (Simat et al., 2007).

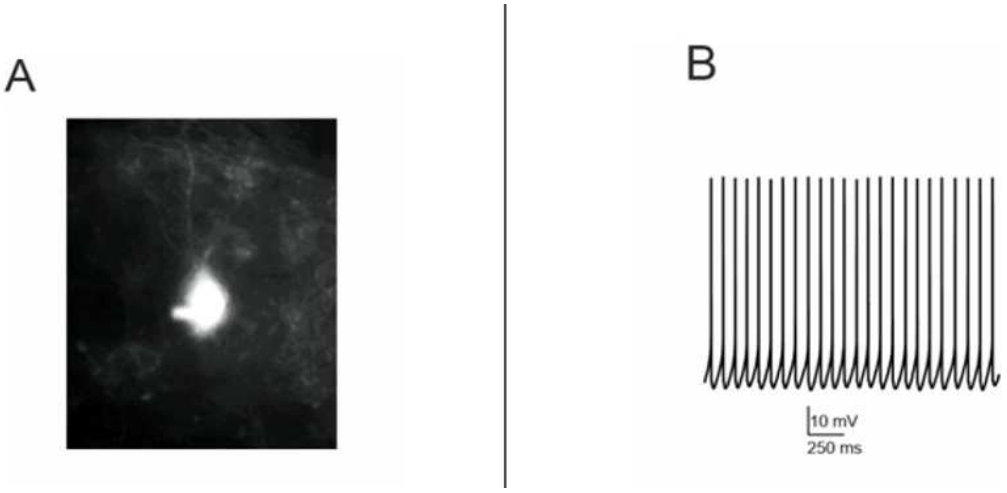

Figure 6.1 Morphological and electrophysiological characterization of GoC. A, Image showing a GFP-positive Golgi cell f during a whole-cell patch-clamp recording. **B,** Example trace of the typical spontaneous firing of a GoC (8.0 Hz) under perfusion with $GABA_A$ and glycine receptor antagonists.

6.2 The phase differences between MF and PF inputs regulate STDP at MF-GoC synapses

STDP involves repeated pairing of EPSPs and APs within a specific time window (Markram et al., 1997). The temporal relationship between synaptic inputs and APs is crucial for determining the sign and magnitude of synaptic changes (Markram et al., 1997; Song et al., 2000; Caporale & Dan, 2008; Sgritta et al., 2017). According to the predictions from the multicompartment GoC model developed by Masoli et al. (2020), inputs from MF and PF that are highly temporally correlated are likely to induce STDP at MF-GoC synapses. To test the prediction of the GoC model, phase-locked PF-AP → MF-EPSP (post-before-pre) or MF-EPSP → PF-AP (pre-before-post) were repeatedly paired 60 times at 4 Hz using time windows of $\Delta t = \pm 10, \pm 25, \pm 50$, or ± 100 ms (Figure 5.3). In line with the STDP rule, pairing PF-AP followed by MF-EPSP at the intervals of 10 or 25 ms induced significant st-LTD (Δt = -10 ms: -34.2 ± 11.3%, n = 6, Student's paired t-test, p = 0.049; Δt = -25 ms: -33.6 ± 4.6%, n = 6, Student's paired t-test, p = 0.006; Figure 6.2), while pairing MF-EPSP followed by a PF-AP at the same intervals (10 or 25 ms) induced significant st-LTP (Δt = 10 ms: 25.4 ± 5.3%, n = 6, Student's paired t-test p = 0.03; Δt = 25 ms: 27.1 ± 7.4%, n = 6,

Student's paired t-test, p = 0.01; Figure 4.2). Both st-LTD and st-LTP remained nearly unchanged for the entire duration of the recordings in all cases (Figure 6.2). Hence, in line with the canonical Hebbian STDP (Dan & Poo, 2004; Caporale et al., 2008; Markram et al., 2011), the plasticity at MF-GoC synapses exhibits bidirectionality and order dependence. Specifically, pre-before-post induction protocol leads to LTP, while post-before-pre induction protocol leads to LTD.

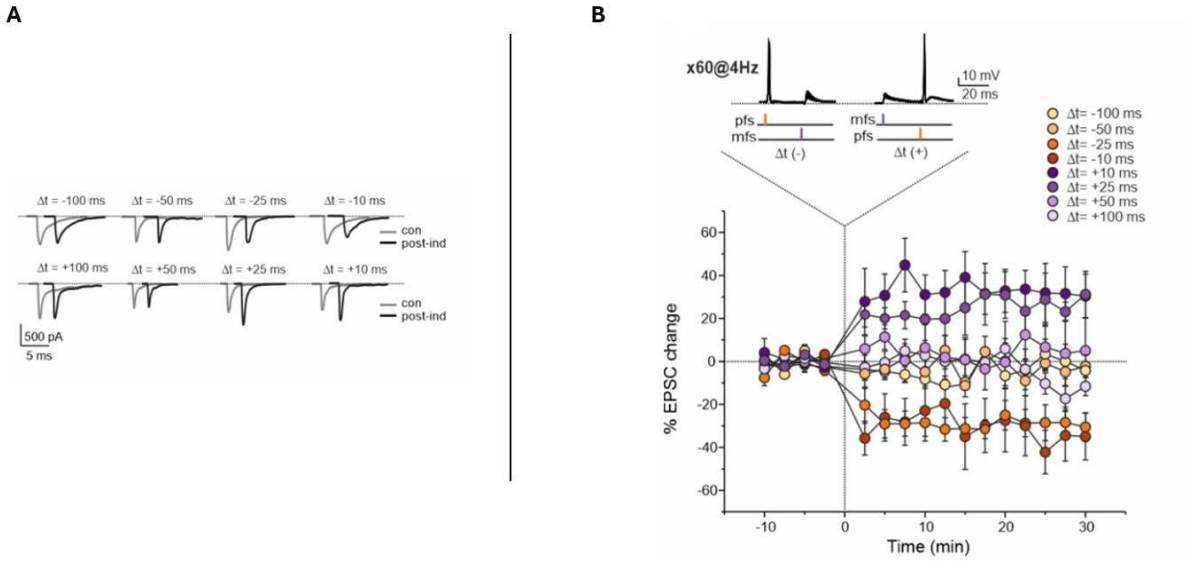

Figure 6.2 Phase differences between MF-PF inputs regulate STDP at MF-GoC synapses. A, Average EPSC traces (average of 30 sweeps) evoked by MF stimulation before (con-, grey traces) and 30 min after STDP induction (post-ind-, black traces) are shown for each time interval (Δt = ± 100 ms). **B,** Using fixed time windows (Δt = ± 10, ± 25, ± 50, or ± 100 ms), pairings of MF-PF inputs (or the reversed) induced STDP at a frequency of 4 Hz (60 repetitions). The plot shows changes in EPSC amplitude over time (percentage increase over baseline) for each Δt. The vertical dashed line indicates STDP induction time. Bars show mean±SEM, and each point represents the average of 30 consecutive EPSC amplitudes.

6.3 The eligible time window for STDP induction at MF-GoC synapses

Either st-LTD or st-LTP vanishes when the temporal window with Δt = -50 ms (Figure 6.2): st-LTD vanished when Δt = -50 (3.5 ± 5.4%, n = 4, Student's paired t-test, p = 0.34), and Δt = -100 ms (-2.1 ± 3.8%, n = 3, Student's paired t-test, p = 0.44); st-LTP disappeared at Δt =

+50 (1.2 ± 7.6%, n = 6, Student's paired t-test, p = 0.92) and Δt = +100 (13.7 ± 3.5%, n = 3, Student's paired t-test, p = 0.13). This relationship between the time window and plasticity changes is represented in the STDP phase-plot, which shows similar but opposite changes in EPSC amplitude for each pair of positive and negative Δt. (Figure 6.3A). Therefore, STDP observed at MF-GoC synapses exhibits an asymmetric nature. Among all the tested time windows, Δt = ± 25 ms was identified as the most effective for inducing st-LTD and st-LTP (Figure 6.3B). Additionally, the temporal order and phase difference between MF and PF inputs are the two crucial factors governing the sign and magnitude of plasticity at the MF-GoC synapses, revealing a bidirectional Hebbian STDP.

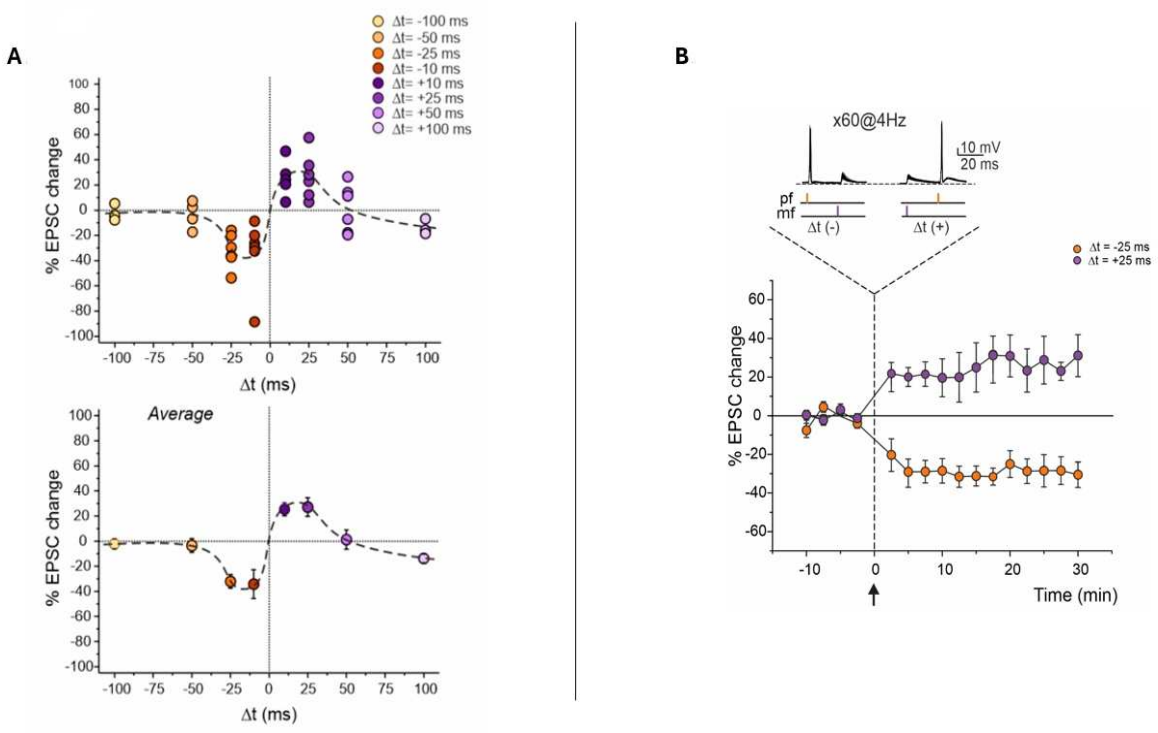

Figure 6.3 STDP timing curve and the most effective timing interval for the STDP induction. A, STDP timing curve shows EPSC amplitude changes in response to MF-PF pairings for each Δt. Bottom: Bars show mean±SEM; each point represents the average of the EPSC amplitude changes displayed above. **B,** the plot shows the changes in EPSC amplitude over time (percentage increase over baseline) for Δt = ± 25 ms, selected as the most effective time window for the STDP induction. Bars show mean±SEM, and each point represents the average of 30 consecutive EPSC amplitudes.

6.4 NMDAR activation is essential for STDP induction at MF-GoC synapses.

The molecular mechanism underlying STDP typically involves NMDARs at many synapses. NMDARs function as a molecular coincidence detector between presynaptic glutamate release and postsynaptic depolarization (Bi & Poo, 1998; Froemke et al., 2005; Caporale & Dan, 2008; Shouval et al., 2010). At MF-GoC synapses, NMDARs play a crucial role in synaptic communication at basal dendrites of GoCs (Cesana et al., 2013), known for their susceptibility to NMDAR-dependent synaptic plasticity (Masoli et al., 2020; Locatelli et al., 2021). To probe the role of NMDAR activation in MF-GoC STDP, NMDAR antagonists D-APV (100 μM) and 7-Cl Kyn (50 μM) were added to the extracellular Krebs' solution. Consequently, the induction of both st-LTP (-7.5 ± 6.0%, n = 4, Student's paired t-test, p = 0.29; Figure 6.4) and st-LTD (-6.1 ± 4.4%, n = 4, Student's paired t-test, p = 0.25; Figure 6.4) was abolished by the bath application of NMDAR antagonists, indicating that MF-GoC STDP relies on NMDAR-dependent mechanisms for both LTP and LTD.

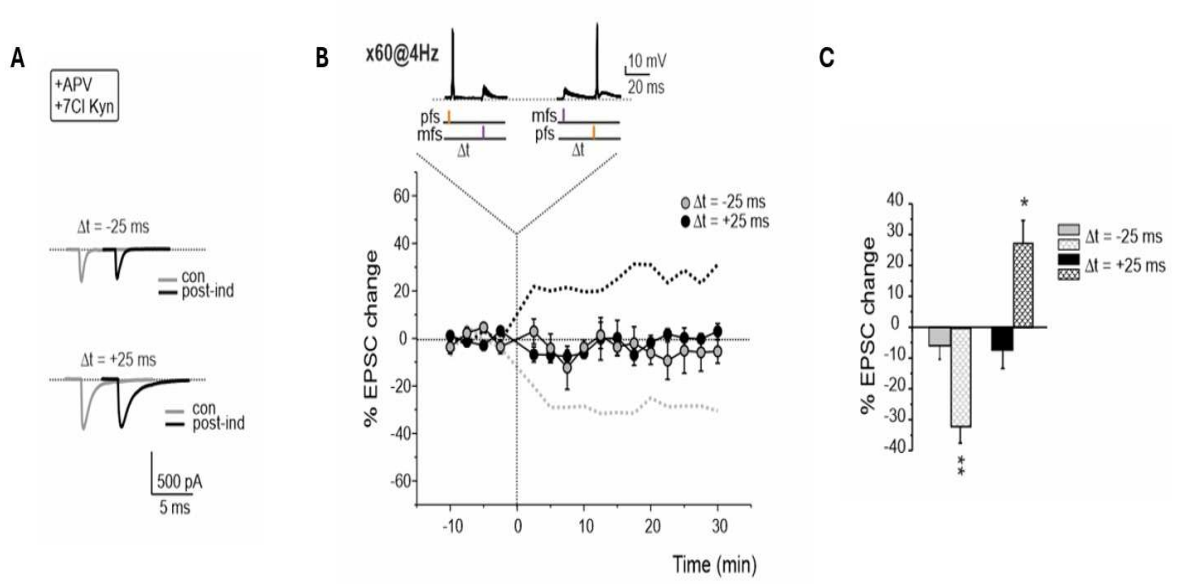

Figure 6.4 NMDAR activation is essential for STDP induction at MF-GoC synapses. A, average traces of EPSC (average of 30 sweeps) evoked by MF stimulation before (con-, grey traces) and 30 min after STDP induction (post-ind-, black traces) awhile bath applying NMDAR blockers, D-APV (100 μM) and 7 Cl Kyn (50 μM). **B,** the plot shows the changes in

EPSC amplitude over time (percentage increase over baseline) for $\Delta t = \pm 25$ ms under bath application of NMDAR blockers. The vertical dashed line indicates the STDP induction time. Bars show mean±SEM, and each point represents the average of 30 consecutive EPSC amplitudes. The dashed lines in black and grey are replotted from Figure 4.2B. NMDAR antagonists prevented both the st-LTP and st-LTD induction. **C,** bar graphs show average EPSC changes after negative spike-timing pairings (grey) and positive spike-timing pairings (black) for $\Delta t = \pm 25$ ms. *, $p<0.05$, **, $p<0.01$, ***, $p<0.001$ Student's unpaired t test.

E. Discussion and Conclusion

Discussion

The cerebellum's ability to process temporal information on a millisecond timescale is crucial for coordinating movements, refining motor control, and integrating sensorimotor inputs (Timmann et al., 1999; Osborne et al., 2007; Jörntell, 2017). Spike-timing plays a crucial role in enhancing information storage and computational efficiency across diverse neuronal networks (Garrido et al., 2013; Markov et al., 2021), and this feature is particularly prominent in the cerebellum, renowned for its precise timing capabilities. Recently, a form of Hebbian STDP has been identified at the MF-GrC synapse (Sgritta et al., 2017), supporting the cerebellar role in learning the appropriate timing of actions (D'Angelo & De Zeeuw 2009; Solinas et al., 2010; Gao et al., 2012; Garrido et al., 2013; D'Angelo, 2014).

At the input stage of the cerebellar cortex, GoCs are the main inhibitory interneurons. They serve an essential role in governing the fast and precise reconfiguration of inputs through feedback, feedforward, and lateral inhibition on GrC activity (D'Angelo & De Zeeuw 2009; Mapelli et al., 2009). Despite the well-characterised inhibitory role of GoCs, the mechanisms governing timing and plasticity at GoC excitatory synapses remain unexplored.

This study provides the first evidence for the existence of STDP at the MF-GoC synapse, confirming predictions from the multicompartment GoC model (Masoli et al., 2020). Experimental findings demonstrate that repeated MF-PF pairings induce a typical bidirectional Hebbian-STDP (Dan & Poo, 2004; Caporale et al., 2008; Markram et al., 2011), where the temporal relationship between PF and MF activations determines whether st-LTP or st-LTD occurs. Specifically, the phase difference and temporal order of MF-PF inputs critically influence the direction and magnitude of MF-GoC STDP.

Interestingly, MF-GoC STDP shares similarities with observed forms of STDP in other brain regions, including the neocortex, hippocampus, and striatum (Bi & Poo, 1998; Debanne et al., 1998; Markram et al., 1997, 2012; Sjöström et al., 2008). Additionally, its Hebbian nature distinguishes MF-GoC STDP from the non-Hebbian and anti-Hebbian STDP observed at cerebellar PC synapses (Bell et al., 1997; Piochon et al., 2012). Moreover, it

should be noted that MF-GoC STDP is not only influenced by spike-timing and firing rate (Bell et al., 1997; Markram et al., 1997; Sjöström et al., 2008; Froemke et al., 2010; Sgritta et al., 2017) but also strongly relies on cooperativity among MF-PF inputs.

GoCs exhibit a diverse array of voltage-gated ion channels, including Na^+, K^+ and Ca^{2+} channels, distributed differentially across apical and basal dendrites, endowing these compartments with distinct biophysical properties. Basal dendrites, enriched with Na^+ channels, show faster kinetics, and are closely coupled to the soma and axon initial segment compared to distal apical dendrites (Locatelli et al., 2021; Masoli et al., 2020). Moreover, the differential distribution of N-type and T-type Ca^{2+} channels further contribute to this asymmetry, with implications for synaptic integration and plasticity mechanisms (Masoli et al., 2020; Locatelli et al., 2021). Computational models of GoC pacemaking and intrinsic electroresponsiveness highlight the role of A-type K^+ channels in regulating AP delay, potentially influencing MF-GoC STDP by modulating the temporal summation of synaptic responses in dendrites (Solinas et al., 2007a). This highlights how the diversity of GoC dendritic channels may shape the amplitude and kinetics of MF-EPSPs during STDP (Vervaeke et al., 2012; Rudolph et al., 2015; Masoli et al., 2020). Interestingly, the complex dendritic conductance in GoCs resembles that observed in pyramidal cells of the neocortex and hippocampus, where basal and apical dendrites play distinct roles in driving STDP (Gordon et al., 2006; Ilan et al., 2011; Masoli et al., 2020). Nevertheless, further research is essential to elucidate the specific contributions of voltage-gated ion channels to MF-GoC STDP.

This study then reveals the key role of NMDARs in the induction of MF-GoC STDP, as evidenced by the prevention of synaptic modification during the bath-application of NMDAR antagonists. According to the BCM rule, the level of Ca^{2+} influx via NMDARs dictates the direction of long-term synaptic plasticity, with high Ca^{2+} levels leading to LTP and low levels inducing LTD (Lisman, 1989; Malenka & Bear, 2004; Gall et al., 2005; Locatelli et al., 2021; Sgritta et al., 2017). Additionally, the observed narrow window for inducing st-LTP and st-LTD ($\Delta t = \pm 25$ ms) aligns with the kinetics of NMDAR activation (D'Angelo et al., 1994; Sgritta et al., 2017). Indeed, according to model predictions, when a PF input follows a MF input, this latter intercepts the upstroke of bAP, causing high membrane depolarization. This, in turn, facilitates NMDAR activation, leading to a significant increase of Ca^{2+} influx in basal dendrites, thus inducing st-LTP (Kampa et al., 2004; Masoli et al., 2020; Sgritta et al.,

2017). On the other hand, when a PF input precedes a MF input, this latter falls in the AHP region of the bAP. NMDAR channels fail to properly unblock, resulting in minimal receptor activation and limited Ca^{2+} influx, leading to st-LTD (Sgritta et al.,2017; Masoli et al., 2020). Taken together these findings suggest that the precise timing of pre- and postsynaptic activity governs Ca^{2+} influx through NMDARs, thereby modulating synaptic plasticity at MF-GoC synapses. However, future investigations are warranted to fully characterise the role of NMDARs and intracellular Ca^{2+} changes in inducing STDP.

Lastly, the induction of MF-GoC STDP at 4 Hz suggests that this plasticity operates within the theta band (4–7.5 Hz). This frequency range aligns with the spontaneous rhythmic discharge observed in GoCs in both awake and anaesthetised animals (Vos *et al*., 1999b; Holtzman *et al*., 2006). Theta-frequency oscillations are prevalent in GoCs as well as in the entire granular layer network. Additionally, GoCs and GrCs exhibit resonance at these frequencies (Forti et al., 2006; Dugue et al., 2009). Gap junctions among GoC apical dendrites promote these oscillations, while feedback inhibition from GoCs contributes to their coherence within the granular layer (Garrido et al., 2016; Solinas et al., 2007a,b). Interestingly, MF- GrC STDP is also optimally induced in the theta band (6 Hz; Sgritta et al., 2017). The confinement of STDP to the theta-band in the granular layer might serve to synchronise cerebellar activity with extracerebellar structures, including the neocortex and hippocampus, during specific functional states such as voluntary movement, resting attentiveness, and memory encoding (Ros et al., 2009; Buzsaki et al., 2006, Cheron et al., 2016). However, the behavioural implications of this STDP confinement to the theta band remain to be proved and require further investigations.

Conclusion

Overall, these findings significantly advance our understanding of cerebellar learning and timing by demonstrating how spatially distinct excitatory inputs can converge onto a single inhibitory cell, driving long-term synaptic changes with precise temporal accuracy. This STDP mechanism might act as a novel and potent regulatory mechanism for controlling GoC activity, which, in turn, influences GrC activity and plasticity within the granular layer. Indeed, GoCs can control GrC activity through various inhibitory loops: i) feed-forward inhibition determines a time-windowing effect over GrC activity; ii) lateral inhibition establishes a centre-surround organisation in the granular layer, with the GoC control of the excitatory-inhibitory balance in GrCs regulating plasticity at the MF-GrC relay; iii) feedback inhibition enhances low-frequency oscillations in the granular layer. Consequently, the regulation of GoC activity by STDP might hold significant implications for GrC signalling, ultimately shaping the PC output to the DCN and thus to extracerebellar areas. Dysregulation of STDP at MF-GoC synapses may therefore contribute to various cerebellar disorders, including motor and cognitive dysfunctions, such as ataxia and autism. To better understand these novel insights and assess their impact, future studies could integrate single-cell models into large-scale cerebellar network models. This approach would provide a thorough examination of how MF-GoC STDP regulates information processing and learning across the entire granular layer, shedding light on its role in regulating information processing and learning within the cerebellar granular layer.

References

Albus, J. (1971) The theory of cerebellar function. Math. Biosci. 10, 25–61.

Apps, R., Hawkes, R., Aoki, S., Bengtsson, F., Brown, A. M., Chen, G., Ebner, T. J., Isope, P., Jörntell, H., Lackey, E. P., Lawrenson, C., Lumb, B., Schonewille, M., Sillitoe, R. V., Spaeth, L., Sugihara, I., Valera, A., Voogd, J., Wylie, D. R., & Ruigrok, T. J. H. (2018). Cerebellar Modules and Their Role as Operational Cerebellar Processing Units: A Consensus paper [corrected]. Cerebellum (London, England), 17(5), 654–682. https://doi.org/10.1007/s12311-018-0952-3

Armano, S., Rossi, P., Taglietti, V., & D'Angelo, E. (2000). Long-term potentiation of intrinsic excitability at the mossy fiber–granule cell synapse of rat cerebellum. *Journal of Neuroscience*, *20*(14), 5208-5216.

Badura, A., & De Zeeuw, C. I. (2017). Cerebellar granule cells: dense, rich and evolving representations. *Current Biology*, *27*(11), R415-R418.

Barmack, N. H., & Yakhnitsa, V. (2008). Functions of interneurons in mouse cerebellum. *Journal of Neuroscience*, *28*(5), 1140-1152.

Bell, C. C., Han, V. &Sawtel,l N. B. (2008). Cerebellum-like structures and their implications for cerebellar function. Annu Rev Neurosci 31: 1–24

Bell, C. C., Han, V. Z., Sugawara, Y., & Grant, K. (1997). Synaptic plasticity in a cerebellum-like structure depends on temporal order. *Nature*, *387*(6630), 278-281.

Bender, V. A., Bender, K. J., Brasier, D. J., & Feldman, D. E. (2006). Two coincidence detectors for spike timing-dependent plasticity in somatosensory cortex. *Journal of Neuroscience*, *26*(16), 4166-4177.

Bi, G. Q., & Poo, M. M. (1998). Synaptic modifications in cultured hippocampal neurons: dependence on spike timing, synaptic strength, and postsynaptic cell type. *Journal of neuroscience*, *18*(24), 10464-10472.

Bienenstock, E. L., Cooper, L. N. & Munro, P. W. (1982). Theory for the development of neuron selectivity: orientation specificity and binocular interaction in visual cortex. J. Neurosci. 2, 32–48.

Bliss, T. V., & Lomo, T. (1973). Long-lasting potentiation of synaptic transmission in the dentate area of the anaesthetized rabbit following stimulation of the perforant path. *The Journal of physiology*, *232*(2), 331–356. https://doi.org/10.1113/jphysiol.1973.sp010273

Blot, A., & Barbour, B. (2014). Ultra-rapid axon-axon ephaptic inhibition of cerebellar Purkinje cells by the pinceau. *Nature neuroscience*, *17*(2), 289–295. https://doi.org/10.1038/nn.3624

Bosman, L. W., Koekkoek, S. K., Shapiro, J., Rijken, B. F., Zandstra, F., Van Der Ende, B., ... & De Zeeuw, C. I. (2010). Encoding of whisker input by cerebellar Purkinje cells. *The Journal of physiology*, *588*(19), 3757-3783.

Braitenberg, V., & Atwood, R. P. (1958). Morphological observations on the cerebellar cortex. *The Journal of comparative neurology*, *109*(1), 1–33. https://doi.org/10.1002/cne.901090102

Brzosko, Z., Mierau, S. B., & Paulsen, O. (2019). Neuromodulation of spike-timing-dependent plasticity: past, present, and future. *Neuron*, *103*(4), 563-581.

Buzsáki, G. (2006). *Rhythms of the Brain*. Oxford University Press. https://doi.org/10.1093/acprof:oso/9780195301069.001.0001

Byrne, J. (1997). *Synaptic Plasticity*. Neuroscience Online. https://nba.uth.tmc.edu/neuroscience/m/s1/chapter07.html

Caporale, N., & Dan, Y. (2008). Spike timing–dependent plasticity: a Hebbian learning rule. *Annu. Rev. Neurosci.*, *31*, 25-46.

Casellato, C., Antonietti, A., Garrido, J. A., Ferrigno, G., D'Angelo, E., & Pedrocchi, A. (2015). Distributed cerebellar plasticity implements generalized multiple-scale memory components in real-robot sensorimotor tasks. *Frontiers in Computational Neuroscience*, *9*, 24.

Catani, M., & Sandrone, S. (2015). *Brain Renaissance: From Vesalius to Modern Neuroscience*. Oxford University Press. https://doi.org/10.1093/med/9780199383832.001.0001

Cerminara, N. L., Lang, E. J., Sillitoe, R. V., & Apps, R. (2015). Redefining the cerebellar cortex as an assembly of non-uniform Purkinje cell microcircuits. *Nature Reviews Neuroscience*, *16*(2), 79-93.

Cesana, E., Pietrajtis, K., Bidoret, C., Isope, P., D'Angelo, E., Dieudonné, S., & Forti, L. (2013). Granule cell ascending axon excitatory synapses onto Golgi cells implement a potent feedback circuit in the cerebellar granular layer. *Journal of Neuroscience*, *33*(30), 12430-12446.

Chao, O. Y., Pathak, S. S., Zhang, H., Augustine, G. J., Christie, J. M., Kikuchi, C., ... & Yang, Y. M. (2023). Social memory deficit caused by dysregulation of the cerebellar vermis. *Nature communications*, *14*(1), 6007.

Chéron, G., Márquez-Ruiz, J., & Dan, B. (2016). Oscillations, timing, plasticity, and learning in the cerebellum. *The Cerebellum*, *15*, 122-138.

Chistiakova, M., Bannon, N. M., Bazhenov, M., & Volgushev, M. (2014). Heterosynaptic plasticity: multiple mechanisms and multiple roles. *The Neuroscientist*, *20*(5), 483-498.

Christie, J. M., & Westbrook, G. L. (2003). Regulation of backpropagating action potentials in mitral cell lateral dendrites by A-type potassium currents. *Journal of neurophysiology*, *89*(5), 2466-2472.

Churchland, P. S., & Sejnowski, T. J. (1992). *The computational brain.* The MIT Press.

Citri, A., & Malenka, R. C. (2008). Synaptic plasticity: multiple forms, functions, and mechanisms. *Neuropsychopharmacology*, *33*(1), 18-41.

Clopath, C. & Gerstner, W. (2010). Voltage and spike timing interact in STDP – a unified model. Front. Synaptic Neurosci. 2:25. doi: 10.3389/fnsyn.2010.00025

Clopath, C., Büsing, L., Vasilaki, E., & Gerstner, W. (2010). Connectivity reflects coding: a model of voltage-based STDP with homeostasis. *Nature neuroscience*, *13*(3), 344-352.

Coesmans, M., Weber, J. T., De Zeeuw, C. I., & Hansel, C. (2004). Bidirectional parallel fiber plasticity in the cerebellum under climbing fiber control. *Neuron*, *44*(4), 691-700.

Cohen, D., & Yarom, Y. (1998). Patches of synchronized activity in the cerebellar cortex evoked by mossy-fiber stimulation: questioning the role of parallel fibers. *Proceedings of the National Academy of Sciences of the United States of America*, *95*(25), 15032–15036. https://doi.org/10.1073/pnas.95.25.15032

Coolidge, F. L. (2020). *Evolutionary neuropsychology: An introduction to the evolution of the structures and functions of the human brain.* (pp. xi, 275). Oxford University Press. https://doi.org/10.1093/oso/9780190940942.001.0001

Cramer, S. W., Gao, W., Chen, G., & Ebner, T. J. (2013). Reevaluation of the beam and radial hypotheses of parallel fiber action in the cerebellar cortex. *Journal of Neuroscience*, *33*(28), 11412-11424.

D'Angelo, E. (2011). Neural circuits of the cerebellum: hypothesis for function. *Journal of Integrative Neuroscience*, *10*(03), 317–352. https://doi.org/10.1142/S0219635211002762

D'Angelo, E. (2016). Granule Cells and Parallel Fibers. In *Essentials of Cerebellum and Cerebellar Disorders: A Primer for Graduate Students* (pp. 177-182*)*. Cham: Springer International Publishing.

D'Angelo, E. (2018). Physiology of the cerebellum. In *Handbook of Clinical Neurology* (Vol. 154, pp. 85–108). Elsevier. https://doi.org/10.1016/B978-0-444-63956-1.00006-0

D'Angelo, E., Mapelli, L., Casellato, C., Garrido, J. A., Luque, N., Monaco, J., ... & Ros, E. (2016). Distributed circuit plasticity: new clues for the cerebellar mechanisms of learning. *The Cerebellum*, *15*, 139-151.

D'Angelo, E., Mazzarello, P., Prestori, F., Mapelli, J., Solinas, S., Lombardo, P., Cesana, E., Gandolfi, D., & Congi, L. (2011). The cerebellar network: From structure to function

and dynamics. *Brain Research Reviews*, *66*(1–2), 5–15. https://doi.org/10.1016/j.brainresrev.2010.10.002

Dan, Y., & Poo, M. M. (2006). Spike timing-dependent plasticity: from synapse to perception. *Physiological reviews*, *86*(3), 1033-1048.

D'Angelo E. (2008). The critical role of Golgi cells in regulating spatio-temporal integration and plasticity at the cerebellum input stage. *Frontiers in neuroscience*, *2*(1), 35–46. https://doi.org/10.3389/neuro.01.008.2008

D'Angelo, E. (2014). The organization of plasticity in the cerebellar cortex: from synapses to control. *Progress in brain research*, *210*, 31-58.

D'Angelo, E., & De Zeeuw, C. I. (2009). Timing and plasticity in the cerebellum: focus on the granular layer. Trends in neurosciences, 32(1), 30–40. https://doi.org/10.1016/j.tins.2008.09.007

D'Angelo, E., Rossi, P., & Taglietti, V. (1994). Voltage‐dependent kinetics of N‐methyl‐D‐aspartate synaptic currents in rat cerebellar granule cells. *European Journal of Neuroscience*, *6*(4), 640-645.

D'Angelo, E., Solinas, S., Mapelli, J., Gandolfi, D., Mapelli, L., & Prestori, F. (2013). The cerebellar Golgi cell and spatiotemporal organisation of granular layer activity. Frontiers in neural circuits, 7, 93. https://doi.org/10.3389/fncir.2013.00093

De Zeeuw, C. I., Koekkoek, S. K. E., Wylie, D. R. W., & Simpson, J. I. (1997). Association between dendritic lamellar bodies and complex spike synchrony in the olivocerebellar system. *Journal of Neurophysiology*, *77*(4), 1747-1758.

Dean, P., Porrill, J., Ekerot, C. F., & Jörntell, H. (2010). The cerebellar microcircuit as an adaptive filter: experimental and computational evidence. *Nature reviews. Neuroscience*, *11*(1), 30–43. https://doi.org/10.1038/nrn2756

Dieudonne S. (1998). Submillisecond kinetics and low efficacy of parallel fibre-Golgi cell synaptic currents in the rat cerebellum. *The Journal of physiology*, *510 (Pt 3)*(Pt 3), 845–866. https://doi.org/10.1111/j.1469-7793.1998.845bj.x

Dieudonné, S. (2016). Golgi neurons. *Essentials of Cerebellum and Cerebellar Disorders: A Primer For Graduate Students*, 201-205.

Dieudonne, S., & Dumoulin, A. (2000). Serotonin-driven long-range inhibitory connections in the cerebellar cortex. *Journal of Neuroscience*, *20*(5), 1837-1848.

Douglas, R. M., & Goddard, G. V. (1975). Long-term potentiation of the perforant path-granule cell synapse in the rat hippocampus. *Brain research*, *86*(2), 205-215.

Doya, K. (1999). What are the computations of the cerebellum, the basal ganglia and the cerebral cortex?. *Neural networks*, *12*(7-8), 961-974.

Dudek, S. M., & Bear, M. F. (1992). Homosynaptic long-term depression in area CA1 of hippocampus and effects of N-methyl-D-aspartate receptor blockade. *Proceedings of the National Academy of Sciences*, *89*(10), 4363-4367.

Dugué, G. P., Brunel, N., Hakim, V., Schwartz, E., Chat, M., Lévesque, M., ... & Dieudonné, S. (2009). Electrical coupling mediates tunable low-frequency oscillations and resonance in the cerebellar Golgi cell network. Neuron, 61(1), 126-139.

Dugué, G. P., Dumoulin, A., Triller, A., & Dieudonné, S. (2005). Target-dependent use of coreleased inhibitory transmitters at central synapses. *Journal of Neuroscience*, *25*(28), 6490-6498.

Duguid, I., Branco, T., London, M., Chadderton, P., & Häusser, M. (2012). Tonic inhibition enhances fidelity of sensory information transmission in the cerebellar cortex. *Journal of Neuroscience*, *32*(32), 11132-11143.

Dumoulin, A., Triller, A., & Dieudonne, S. (2001). IPSC kinetics at identified GABAergic and mixed GABAergic and glycinergic synapses onto cerebellar Golgi cells. Journal of Neuroscience, 21(16), 6045-6057.

Eccles, J. C., & Sherrington, C. S. (1931). Studies on the flexor reflex.-IV. After-discharge. *Proceedings of the Royal Society of London. Series B, Containing Papers of a Biological Character*, *107*(754), 586-596.

Eccles, J. C., Ito, M., & Szentágothai, J. (1967). *The Cerebellum as a Neuronal Machine*. Springer Berlin Heidelberg. https://doi.org/10.1007/978-3-662-13147-3

Eccles, J., Llinàs, R., Sasaki, K. (1964). Golgi cell inhibition in the cerebellar cortex. Nature 204, 1265–1266.

Eccles, J.C. (1973). The cerebellum as a computer: patterns in space and time. J. Physiol. 229, 1–32.

Eyre, M. D., & Nusser, Z. (2016). Only a minority of the inhibitory inputs to cerebellar Golgi cells originate from local GABAergic cells. *eneuro*, *3*(3).

Farrant, M., & Nusser, Z. (2005). Variations on an inhibitory theme: phasic and tonic activation of GABAA receptors. *Nature Reviews Neuroscience*, *6*(3), 215-229.

Forti, L., Cesana, E., Mapelli, J., & D'Angelo, E. (2006). Ionic mechanisms of autorhythmic firing in rat cerebellar Golgi cells. *The Journal of physiology*, *574* (Pt 3), 711–729. https://doi.org/10.1113/jphysiol.2006.110858

Froemke, R. C., Debanne, D. & Bi, G. Q. (2010a). Temporal modulation of spike-timing-dependent plasticity. *Front. Synaptic Neurosci.* 2:19. doi: 10.3389/ fnsyn.2010.00019

Froemke, R. C., Letzkus, J. J., Kampa, B. M., Hang, G. B. & Stuart, G. J. (2010b). Dendritic synapse location and neocortical spike-timing-dependent plasticity. *Front. Synaptic Neurosci.* 2:29. doi: 10.3389/fnsyn.2010.00029

Froemke, R. C., Poo, M. & Dan, Y. (2005). Spike-timing dependent plasticity depends on dendritic location. *Nature* 434, 221–225.

Froemke, R.C. & Dan,Y. (2002). Spike-timing-dependent synaptic modification induced by natural spike trains. Nature 416, 433–438.

Fuenzalida, M., Fernandez de Sevilla, D., Couve, A., & Buno, W. (2010). Role of AMPA and NMDA receptors and back-propagating action potentials in spike timing–dependent plasticity. *Journal of neurophysiology*, *103*(1), 47-54.

Gall, D., Prestori, F., Sola, E., D'Errico, A., Roussel, C., Forti, L., Rossi, P., & D'Angelo, E. (2005). Intracellular calcium regulation by burst discharge determines bidirectional long-term synaptic plasticity at the cerebellum input stage. The Journal of neuroscience: the official journal of the Society for Neuroscience, 25(19), 4813–4822. https://doi.org/10.1523/JNEUROSCI.0410-05.2005

Galliano, E., Baratella, M., Sgritta, M., Ruigrok, T. J. H., Haasdijk, E. D., Hoebeek, F. E., D'Angelo, E., Jaarsma, D., & De Zeeuw, C. I. (2013). Anatomical investigation of potential contacts between climbing fibers and cerebellar Golgi cells in the mouse. Frontiers in Neural Circuits, 7. https://doi.org/10.3389/fncir.2013.00059

Galliano, E., Mazzarello, P., & D'Angelo, E. (2010). Discovery and rediscoveries of Golgi cells. The Journal of physiology, 588(Pt 19), 3639–3655. https://doi.org/10.1113/jphysiol.2010.189605

Gao, W., Chen, G., Reinert, K. C., & Ebner, T. J. (2006). Cerebellar cortical molecular layer inhibition is organised in parasagittal zones. The Journal of neuroscience : the official journal of the Society for Neuroscience, 26(32), 8377–8387. https://doi.org/10.1523/JNEUROSCI.2434-06.2006

Gao, Z., Van Beugen, B. J., & De Zeeuw, C. I. (2012). Distributed synergistic plasticity and cerebellar learning. *Nature Reviews Neuroscience*, *13*(9), 619-635.

Garrido, J. A., Luque, N. R., Tolu, S., & D'Angelo, E. (2016). Oscillation-driven spike-timing dependent plasticity allows multiple overlapping pattern recognition in inhibitory interneuron networks. *International journal of neural systems*, *26*(05), 1650020.

Garrido, J. A., Ros, E., & D'Angelo, E. (2013). Spike timing regulation on the millisecond scale by distributed synaptic plasticity at the cerebellum input stage: a simulation study. *Frontiers in computational neuroscience*, *7*, 64.

Garwicz, M., & Andersson, G. (1992). Spread of synaptic activity along parallel fibres in cat cerebellar anterior lobe. *Experimental brain research*, *88*, 615-622.

Gerard, R. W. (1930). Delayed action potentials in nerve. *American Journal of Physiology-Legacy Content*, *93*(1), 337-341.

Geurts, F. J., De Schutter, E., & Dieudonné, S. (2003). Unraveling the cerebellar cortex: cytology and cellular physiology of large-sized interneurons in the granular layer. *The Cerebellum*, *2*, 290-299.

Glickstein, M., Strata, P., & Voogd, J. (2009). Cerebellum: History. *Neuroscience*, *162*(3), 549–559. https://doi.org/10.1016/j.neuroscience.2009.02.054

Golgi, C. (1874). Sulla fine anatomia del cervelletto umano: Archivio Italiano per le Malattie Nervose, 2, pp. 90–107.

Gordon, U., Polsky, A., & Schiller, J. (2006). Plasticity compartments in basal dendrites of neocortical pyramidal neurons. *Journal of Neuroscience*, *26*(49), 12717-12726.

Grangeray, A., Dorgans, K., Roux, S. & Bossu, L., J. (2016). The Purkinje Cell: As an Integrative Machine. In *Essentials of Cerebellum and Cerebellar Disorders: A Primer for Graduate Students* (pp. 183-188*)*. Cham: Springer International Publishing.

Gruol, D. L., Koibuchi, N., Manto, M., Molinari, M., Schmahmann, J. D., & Shen, Y. (Eds.). (2016). *Essentials of Cerebellum and Cerebellar Disorders*. Springer International Publishing. https://doi.org/10.1007/978-3-319-24551-5

Hamann, M., Rossi, D. J., & Attwell, D. (2002). Tonic and spillover inhibition of granule cells control information flow through cerebellar cortex. *Neuron*, *33*(4), 625-633.

Hamill, O. P., Marty, A., Neher, E., Sakmann, B., & Sigworth, F. J. (1981). Improved patch-clamp techniques for high-resolution current recording from cells and cell-free membrane patches. *Pflügers Archiv*, *391*, 85-100.

Han, K. S., Guo, C., Chen, C. H., Witter, L., Osorno, T., & Regehr, W. G. (2018). Ephaptic coupling promotes synchronous firing of cerebellar Purkinje cells. *Neuron*, *100*(3), 564-578.

Hansel, C., & Linden, D. J. (2000). Long-term depression of the cerebellar climbing fiber–Purkinje neuron synapse. *Neuron*, *26*(2), 473-482.

Hansel, C., Linden, D. J., & D'Angelo, E. (2001). Beyond parallel fiber LTD: the diversity of synaptic and non-synaptic plasticity in the cerebellum. *Nature neuroscience*, *4*(5), 467-475.

Harvey, R. J., & Napper, R. M. A. (1991). Quantitatives studies on the mammalian cerebellum. *Progress in neurobiology*, *36*(6), 437-463.

Hashimotodani, Y., Ohno-Shosaku, T., & Kano, M. (2007). Ca2+-assisted receptor-driven endocannabinoid release: mechanisms that associate presynaptic and postsynaptic activities. *Current opinion in neurobiology*, *17*(3), 360-365.

Hebb, D. O. (1949). The Organization of Behavior. New York: Wiley.

Hirono, M. (2016). Lugaro Cells. In *Essentials of Cerebellum and Cerebellar Disorders: A Primer for Graduate Students* (pp. 207-211). Cham: Springer International Publishing.

Hirono, M., Nagao, S., Yanagawa, Y., & Konishi, S. (2017). Monoaminergic modulation of GABAergic transmission onto cerebellar globular cells. *Neuropharmacology*, *118*, 79-89.

Hirono, M., Watanabe, S., Karube, F., Fujiyama, F., Kawahara, S., Nagao, S., ... & Misonou, H. (2018). Perineuronal nets in the deep cerebellar nuclei regulate GABAergic transmission and delay eyeblink conditioning. *Journal of Neuroscience*, *38*(27), 6130-6144.

Holtzman, T., Rajapaksa, T., Mostofi, A., & Edgley, S. A. (2006). Different responses of rat cerebellar Purkinje cells and Golgi cells evoked by widespread convergent sensory inputs. *The Journal of physiology*, *574*(2), 491-507.

Huguenard, J. R., Hamill, O. P., & Prince, D. A. (1989). Sodium channels in dendrites of rat cortical pyramidal neurons. *Proceedings of the National Academy of Sciences of the United States of America*, *86*(7), 2473–2477. https://doi.org/10.1073/pnas.86.7.2473

Hull, C., & Regehr, W. G. (2012). Identification of an inhibitory circuit that regulates cerebellar Golgi cell activity. Neuron, 73(1), 149–158. https://doi.org/10.1016/j.neuron.2011.10.030

Hull, C., & Regehr, W. G. (2022). The Cerebellar Cortex. Annual review of neuroscience, 45, 151–175. https://doi.org/10.1146/annurev-neuro-091421-125115

Ilan, L. B., Gidon, A., & Segev, I. (2011). Interregional synaptic competition in neurons with multiple STDP-inducing signals. *Journal of neurophysiology*.

Ito M. (2008). Control of mental activities by internal models in the cerebellum. Nat Rev Neurosci 9: 304–313

Ito, M. (2013). Error detection and representation in the olivo-cerebellar system. *Frontiers in neural circuits*, *7*, 1.

Ito, M., Shiida, T., Yagi, N., & Yamamoto, M. (1974). Visual influence on rabbit horizontal vestibulo-ocular reflex presumably effected via the cerebellar flocculus. *Brain research*, *65*(1), 170–174. https://doi.org/10.1016/0006-8993(74)90344-8

Ivry, R. B., & Keele, S. W. (1989). Timing Functions of The Cerebellum. *Journal of Cognitive Neuroscience*, *1*(2), 136–152. https://doi.org/10.1162/jocn.1989.1.2.136

Jacobson, G. A., Rokni, D., & Yarom, Y. (2008). A model of the olivo-cerebellar system as a temporal pattern generator. *Trends in neurosciences*, *31*(12), 617-625.

Jaeger, D. (2021). Cerebellar nuclei and cerebellar learning. In *Handbook of the Cerebellum and Cerebellar Disorders* (pp. 1251-1274). Cham: Springer International Publishing.

James, W. (1890). The Principles of Psychology. New York: Henry Holt and Company the Principles of Psychology.http://dx.doi.org/10.1037/11059-000

Jörntell, H. (2017). Cerebellar physiology: links between microcircuitry properties and sensorimotor functions. *The Journal of physiology*, *595*(1), 11-27.

Kandel, E. R., & Tauc, L. (1964). Mechanism of prolonged heterosynaptic facilitation. *Nature*, *202*(4928), 145-147.

Kandel, E. R., Schwartz, J. H., Jessell, T. M., Siegelbaum, S., Hudspeth, A. J., & Mack, S. (Eds.). (2000). *Principles of neural science* (Vol. 4, pp. 1227-1246). New York: McGraw-hill.

Katz, B. (1969). The release of neural transmitter substances. *Liverpool University Press*, 5-39.

Kawato, M., Ohmae, S., Hoang, H., & Sanger, T. (2021). 50 Years Since the Marr, Ito, and Albus Models of the Cerebellum. *Neuroscience*, *462*, 151–174. https://doi.org/10.1016/j.neuroscience.2020.06.019

Kitazawa, S., Kimura, T., & Yin, P. B. (1998). Cerebellar complex spikes encode both destinations and errors in arm movements. *Nature*, *392*(6675), 494-497.

Konorski, J. (1948). Conditioned Reflexes and Neuron Organization. Cambridge: Cambridge University Press.

Levy, W. B. & Steward, O. (1983). Temporal contiguity requirements for long- term associative potentiation/depression in the hippocampus. Neuroscience 8, 791–797

Levy, W. B., & Steward, O. (1979). Synapses as associative memory elements in the hippocampal formation. *Brain research*, *175*(2), 233-245.

Lisman, J. (1989). A mechanism for the Hebb and the anti-Hebb processes underlying learning and memory. *Proceedings of the National Academy of Sciences*, *86*(23), 9574-9578.

Lisman, J. (2017). Glutamatergic synapses are structurally and biochemically complex because of multiple plasticity processes: long-term potentiation, long-term depression, short-term potentiation and scaling. *Philosophical Transactions of the Royal Society B: Biological Sciences*, *372*(1715), 20160260.

Liu, S. J., & Dubois, C. J. (2016). Stellate cells. In *Essentials of Cerebellum and Cerebellar Disorders: A Primer for Graduate Students* (pp. 189-193*)*. Cham: Springer International Publishing.

Llinás, R., & Yarom, Y. (1986). Oscillatory properties of guinea-pig inferior olivary neurones and their pharmacological modulation: an in vitro study. *The Journal of physiology*, *376*, 163–182. https://doi.org/10.1113/jphysiol.1986.sp016147

Locatelli, F., Soda, T., Montagna, I., Tritto, S., Botta, L., Prestori, F., & D'Angelo, E. (2021). Calcium Channel-Dependent Induction of Long-Term Synaptic Plasticity at Excitatory Golgi Cell Synapses of Cerebellum. The Journal of neuroscience : the official journal of the Society for Neuroscience, 41(15), 3307–3319. https://doi.org/10.1523/JNEUROSCI.3013-19.2020

Lugaro E. (1898). Le resistenze nell'evoluzione della vita. Rivista moderna di cultura 1, 29–60

Luo, Y., & Sugihara, I. (2016). The Olivocerebellar Tract. In *Essentials of Cerebellum and Cerebellar Disorders: A Primer for Graduate Students* (pp. 55-61*)*. Cham: Springer International Publishing.

Lüscher, C., & Malenka, R. C. (2012). NMDA receptor-dependent long-term potentiation and long-term depression (LTP/LTD). *Cold Spring Harbor perspectives in biology*, *4*(6), a005710.

Maex, R., & De Schutter, E. (1998). Synchronization of golgi and granule cell firing in a detailed network model of the cerebellar granule cell layer. *Journal of neurophysiology*, *80*(5), 2521–2537. https://doi.org/10.1152/jn.1998.80.5.2521

Maffei, A., Prestori, F., Shibuki, K., Rossi, P., Taglietti, V., & D'Angelo, E. (2003). NO enhances presynaptic currents during cerebellar mossy fiber—granule cell LTP. *Journal of Neurophysiology*, *90*(4), 2478-2483.

Magee, J. C., & Johnston, D. (1997). A synaptically controlled, associative signal for Hebbian plasticity in hippocampal neurons. *Science*, *275*(5297), 209-213.

Malacarne, M. V. G. (1776) Nuova esposizione della vera struttura del cervelletto umano. Torino: Briolo.

Malenka, R. C. (1994). Synaptic plasticity in the hippocampus: LTP and LTD. *Cell*, *78*(4), 535-538.

Malenka, R. C., & Bear, M. F. (2004). LTP and LTD: an embarrassment of riches. *Neuron*, *44*(1), 5-21.

Manto, M. (2008). The cerebellum, cerebellar disorders, and cerebellar research—two centuries of discoveries. *The Cerebellum*, *7*(4), 505-516.

Mapelli, J., & D'Angelo, E. (2007). The Spatial Organization of Long-Term Synaptic Plasticity at the Input Stage of Cerebellum. *The Journal of Neuroscience*, *27*(6), 1285–1296. https://doi.org/10.1523/JNEUROSCI.4873-06.2007

Mapelli, J., Boiani, G. M., D'Angelo, E., Bigiani, A., & Gandolfi, D. (2022). Long-term synaptic plasticity tunes the gain of information channels through the cerebellum granular layer. *Biomedicines*, *10*(12), 3185.

Mapelli, L., Pagani, M., Garrido, J. A., & D'Angelo, E. (2015). Integrated plasticity at inhibitory and excitatory synapses in the cerebellar circuit. *Frontiers in cellular neuroscience*, *9*, 169.

Mapelli, L., Rossi, P., Nieus, T., & D'Angelo, E. (2009). Tonic Activation of GABA $_B$ Receptors Reduces Release Probability at Inhibitory Connections in the Cerebellar Glomerulus. *Journal of Neurophysiology*, *101*(6), 3089–3099. https://doi.org/10.1152/jn.91190.2008

Mapelli, L., Solinas, S., & D'Angelo, E. (2014). Integration and regulation of glomerular inhibition in the cerebellar granular layer circuit. Frontiers in cellular neuroscience, 8, 55. H https://doi.org/10.3389/fncel.2014.00055

Markov, D. A., Petrucco, L., Kist, A. M., & Portugues, R. (2021). A cerebellar internal model calibrates a feedback controller involved in sensorimotor control. *Nature communications*, *12*(1), 6694.

Markram, H. & Sakmann, B. (1995). Action potentials propagating back into dendrites trigger changes in efficacy of single-axon synapses between layer V pyramidal cells. Soc. Neurosci. Abstr. 21, 2007.

Markram, H., Gerstner, W. & Sjöström, P. J. (2011). A history of spike-timing dependent plasticity. Front. Synaptic Neurosci. 3:4. doi:10.3389/fnsyn.2011.00004

Markram, H., Gerstner, W., & Sjöström, P. J. (2012). Spike-Timing-Dependent Plasticity: A Comprehensive Overview. *Frontiers in Synaptic Neuroscience*, *4*. https://doi.org/10.3389/fnsyn.2012.00002

Markram, H., Lübke, J., Frotscher, M. & Sakmann, B. (1997). Regulation of synaptic efficacy by coincidence of postsynaptic APs and EPSPs. Science 275, 213–215.

Marr, D. (1969). A theory of cerebellar cortex. J. Physiol. 202, 437–470.

Martin, S. J., Grimwood, P. D., & Morris, R. G. (2000). Synaptic plasticity and memory: an evaluation of the hypothesis. *Annual review of neuroscience*, *23*(1), 649-711.

Masoli, S., Ottaviani, A., Casali, S., & D'Angelo, E. (2020). Cerebellar Golgi cell models predict dendritic processing and mechanisms of synaptic plasticity. PLoS computational biology, 16(12), e1007937. https://doi.org/10.1371/journal.pcbi.1007937

Mayer, M. L., Westbrook, G. L., & Guthrie, P. B. (1984). Voltage-dependent block by Mg2+ of NMDA responses in spinal cord neurones. *Nature*, *309*(5965), 261-263.

McCulloch, W. S., & Pitts, W. (1943). A logical calculus of the ideas immanent in nervous activity. *The bulletin of mathematical biophysics*, *5*, 115-133.

Miyazaki, T., Yamasaki, M., Tanaka, K. F., & Watanabe, M. (2021). Compartmentalized input–output organization of Lugaro cells in the cerebellar cortex. *Neuroscience*, *462*, 89-105.

Molleman, A. (2003). *Patch clamping: an introductory guide to patch clamp electrophysiology*. John Wiley & Sons.

Mulkey, R. M., & Malenka, R. C. (1992). Mechanisms underlying induction of homosynaptic long-term depression in area CA1 of the hippocampus. *Neuron*, *9*(5), 967-975.

Nicoll, R. A. (2017). A brief history of long-term potentiation. *neuron*, *93*(2), 281-290

Nicoll, R. A., Kauer, J. A., & Malenka, R. C. (1988). The current excitement in long term potentiation. *Neuron*, *1*(2), 97-103.

Nieus, T., Sola, E., Mapelli, J., Saftenku, E., Rossi, P., & D'Angelo, E. (2006). LTP regulates burst initiation and frequency at mossy fiber–granule cell synapses of rat cerebellum: experimental observations and theoretical predictions. *Journal of neurophysiology*, *95*(2), 686-699.

Osborne, K. J., Damme, K. S., Gupta, T., Dean, D. J., Bernard, J. A., & Mittal, V. A. (2021). Timing dysfunction and cerebellar resting state functional connectivity abnormalities in youth at clinical high-risk for psychosis. Psychological medicine, 51(8), 1289-129

Oscarsson, O. (1979) Functional units of the cerebellum; sagittal zones and microzones. Trends Neurosci 2:143–145.

Palay, S.L., & Chan-Palay, V. (1974). Cerebellar cortex: cytology and organisation. Springer-Verlag, New York.

Paulsen, O., & Sejnowski, T. J. (2000). Natural patterns of activity and long-term synaptic plasticity. *Current opinion in neurobiology*, *10*(2), 172-180.

Person, A. L., & Raman, I. M. (2012). Synchrony and neural coding in cerebellar circuits. Frontiers in neural circuits, 6, 97. https://doi.org/10.3389/fncir.2012.00097

Piochon, C., Kruskal, P., MacLean, J., & Hansel, C. (2013). Non-Hebbian spike-timing-dependent plasticity in cerebellar circuits. *Frontiers in Neural Circuits*, *6*, 124.

Prestori, F., Bonardi, C., Mapelli, L., Lombardo, P., Goselink, R., De Stefano, M. E., ... & D'Angelo, E. (2013). Gating of long-term potentiation by nicotinic acetylcholine receptors at the cerebellum input stage. *PloS one*, *8*(5), e64828.

Prestori, F., Mapelli, L., & D'Angelo, E. (2019). Diverse neuron properties and complex network dynamics in the cerebellar cortical inhibitory circuit. *Frontiers in molecular neuroscience*, *12*, 267.

Pugh, J. R., & Raman, I. M. (2006). Potentiation of mossy fiber EPSCs in the cerebellar nuclei by NMDA receptor activation followed by postinhibitory rebound current. *Neuron*, *51*(1), 113-123.

Ramon y Cajal, S., & Azoulay, L. (1955). Histologie du système nerveux de l'homme et des vertébrés. In *Histologie du système nerveux de l'homme et des vertébrés* (pp. 2v-2v).

Rancz, E. A., Ishikawa, T., Duguid, I., Chadderton, P., Mahon, S., & Häusser, M. (2007). High-fidelity transmission of sensory information by single cerebellar mossy fibre boutons. *Nature*, *450*(7173), 1245–1248. https://doi.org/10.1038/nature05995

Regehr, W., Kehoe, J., Ascher, P., & Armstrong, C. (1993). Synaptically triggered action potentials in dendrites. *Neuron*, *11*(1), 145-151.

Retzius, G. (1892). Kleinere Mittheilungen von den Gebiete der Nervenhistologie. Biologische Untersuchungen (Neue Folge) IV, 57–66.

Robberechts, Q., Wijnants, M., Giugliano, M., & De Schutter, E. (2010). Long-term depression at parallel fiber to Golgi cell synapses. *Journal of neurophysiology*, *104*(6), 3413-3423.

Rokni, D., Tal, Z., Byk, H., & Yarom, Y. (2009). Regularity, variabilty and bi-stability in the activity of cerebellar Purkinje cells. *Frontiers in Cellular Neuroscience*, *3*, 822.

Ros, H., Sachdev, R. N., Yu, Y., Sestan, N., & McCormick, D. A. (2009). Neocortical networks entrain neuronal circuits in cerebellar cortex. *The Journal of neuroscience : the official journal of the Society for Neuroscience*, *29*(33), 10309–10320. https://doi.org/10.1523/JNEUROSCI.2327-09.2009

Roš, H., Sachdev, R. N., Yu, Y., Šestan, N., & McCormick, D. A. (2009). Neocortical networks entrain neuronal circuits in cerebellar cortex. *Journal of Neuroscience*, *29*(33), 10309-10320.

Rudolph, S., Hull, C., & Regehr, W. G. (2015). Active Dendrites and Differential Distribution of Calcium Channels Enable Functional Compartmentalization of Golgi Cells. The Journal of neuroscience : the official journal of the Society for Neuroscience, 35(47), 15492–15504. https://doi.org/10.1523/JNEUROSCI.3132-15.2015

Sakmann, B., & Neher, E. (1984). Patch clamp techniques for studying ionic channels in excitable membranes. *Annual review of physiology*, *46*, 455–472. https://doi.org/10.1146/annurev.ph.46.030184.002323

Schmahmann, J. D., & Sherman, J. C. (1998). The cerebellar cognitive affective syndrome. *Brain: a journal of neurology*, *121*(4), 561-579.

Schröder, H., Moser, N., & Huggenberger, S. (2020). *Neuroanatomy of the Mouse: An Introduction*. Springer International Publishing. https://doi.org/10.1007/978-3-030-19898-5

Sgritta, M., Locatelli, F., Soda, T., Prestori, F., & D'Angelo, E. U. (2017). Hebbian spike-timing dependent plasticity at the cerebellar input stage. Journal of Neuroscience, 37(11), 2809-2823.

Shatz, C. J. (1992). The developing brain. *Scientific American*, *267*(3), 60-67.

Shouval, H. Z., Wang, S. S. H., & Wittenberg, G. M. (2010). Spike timing dependent plasticity: a consequence of more fundamental learning rules. *Frontiers in computational neuroscience*, *4*, 19.

Sillitoe R V, Chung S-H, Fritschy J-M, Hoy M, Hawkes R (2008) Golgi cell dendrites are restricted by Purkinje cell stripe boundaries in the adult mouse cerebellar cortex. J Neurosci 28:2820–2826.

Simat, M., Parpan, F., & Fritschy, J. M. (2007). Heterogeneity of glycinergic and gabaergic interneurons in the granule cell layer of mouse cerebellum. Journal of Comparative Neurology, 500(1), 71-83.

Singh, R. (2021). Cerebellum: Its Anatomy, Functions and Diseases. In N. Ersoy Tunalı (Ed.), *Neurodegenerative Diseases—Molecular Mechanisms and Current Therapeutic Approaches*. IntechOpen. https://doi.org/10.5772/intechopen.93064

Sjöström, P. J., Rancz, E. A., Roth, A., & Hausser, M. (2008). Dendritic excitability and synaptic plasticity. *Physiological reviews*, *88*(2), 769-840.

Sjöström, P. J., Turrigiano, G. G., & Nelson, S. B. (2001). Rate, timing, and cooperativity jointly determine cortical synaptic plasticity. *Neuron*, *32*(6), 1149-1164.

Sokolov, A. A., Miall, R. C., & Ivry, R. B. (2017). The cerebellum: adaptive prediction for movement and cognition. *Trends in cognitive sciences*, *21*(5), 313-332.

Solinas, S., Forti, L., Cesana, E., Mapelli, J., De Schutter, E., & D'Angelo, E. (2007a). Computational reconstruction of pacemaking and intrinsic electroresponsiveness in cerebellar Golgi cells. Frontiers in cellular neuroscience, 1, 2. https://doi.org/10.3389/neuro.03.002.2007

Solinas, S., Forti, L., Cesana, E., Mapelli, J., De Schutter, E., & D'Angelo, E. (2007b). Fast-reset of pacemaking and theta-frequency resonance patterns in cerebellar Golgi cells: simulations of their impact in vivo. Frontiers in cellular neuroscience, 1, 4. https://doi.org/10.3389/neuro.03.004.2007

Solinas, S., Nieus, T., & D'Angelo, E. (2010). A realistic large-scale model of the cerebellum granular layer predicts circuit spatio-temporal filtering properties. Frontiers in cellular neuroscience, 4, 12. https://doi.org/10.3389/fncel.2010.00012

Song, S., Miller, K. D., & Abbott, L. F. (2000). Competitive Hebbian learning through spike-timing-dependent synaptic plasticity. *Nature neuroscience*, *3*(9), 919-926.

Stent, G. S. (1973). A physiological mechanism for Hebb's postulate of learning. *Proceedings of the National Academy of Sciences*, *70*(4), 997-1001.

Stoodley, C. J., & Tsai, P. T. (2021). Adaptive prediction for social contexts: the cerebellar contribution to typical and atypical social behaviors. *Annual review of neuroscience*, *44*(1), 475-493.

Strata, P. (2015). The emotional cerebellum. *The Cerebellum*, *14*, 570-577.

Stuart, G. J., & Sakmann, B. (1994). Active propagation of somatic action potentials into neocortical pyramidal cell dendrites. *Nature*, *367*(6458), 69–72. https://doi.org/10.1038/367069a0

Sudhakar, S. K., Hong, S., Raikov, I., Publio, R., Lang, C., Close, T., ... & De Schutter, E. (2017). Spatiotemporal network coding of physiological mossy fiber inputs by the cerebellar granular layer. *PLoS computational biology*, *13*(9), e1005754.

Szoboszlay, M., Lőrincz, A., Lanore, F., Vervaeke, K., Silver, R. A., & Nusser, Z. (2016). Functional properties of dendritic gap junctions in cerebellar golgi cells. Neuron, 90(5), 1043-1056.

Tabuchi, S., Gilmer, J. I., Purba, K., & Person, A. L. (2019). Pathway-specific drive of cerebellar golgi cells reveals integrative rules of cortical inhibition. *Journal of Neuroscience*, *39*(7), 1169-1181.

Takahashi, M., & Shinoda, Y. (2021). Neural circuits of inputs and outputs of the cerebellar cortex and nuclei. *Neuroscience*, *462*, 70-88.

Tanzi, E. (1893). I fatti e la induzioni nell 'odierna istologia del sistema nervoso. *Revista Sperimentale di Freniatria e Medicine Legale della Alienazioni Mentali*, *19*, 419-72.

Timmann, D., & Daum, I. (2007). Cerebellar contributions to cognitive functions: a progress report after two decades of research. *The cerebellum*, *6*, 159-162.

Timmann, D., Watts, S., & Hore, J. (1999). Failure of cerebellar patients to time finger opening precisely causes ball high-low inaccuracy in overarm throws. *Journal of neurophysiology*, *82*(1), 103-114.

Valera, A. (2013). *Spatial and Temporal Integration of Granular Inputs in the Cerebellar Cortex*. Université de Strasbourg.

Vervaeke, K., Lorincz, A., Gleeson, P., Farinella, M., Nusser, Z., & Silver, R. A. (2010). Rapid desynchronization of an electrically coupled interneuron network with sparse excitatory synaptic input. Neuron, 67(3), 435–451. https://doi.org/10.1016/j.neuron.2010.06.028

Vesalius, A. (1543) De humani corporis fabrica libris septem. Basel: Oporini.

Voogd, J., & Marani, E. (2016). Gross Anatomy of the Cerebellum. In DL. Gruol, N. Koibuchi, M. Manto, M. Molinari, JD. Schmahmann, & Y. Shen (Eds.), *Essentials of Cerebellum and Cerebellar Disorders: A Primer For Graduate Students* (pp. 33-38). Springer-Verlag.

Vos, B. P., Maex, R., Volny-Luraghi, A., & De Schutter, E. (1999a). Parallel fibers synchronize spontaneous activity in cerebellar Golgi cells. The Journal of neuroscience, 19(11), RC6.

Vos, B.P., Volny- Luraghi, A. & De Schutter, E. (1999b). Cerebellar Golgi cells in the rat: receptive fields and timing of responses to facial stimulation. Eur. J. Neurosci. 11, 2621–2634.

Wang, J., Dam, G., Yildirim, S., Rand, W., Wilensky, U., & Houk, J. C. (2008). Reciprocity between the cerebellum and the cerebral cortex: Nonlinear dynamics in microscopic modules for generating voluntary motor commands. *Complexity*, *14*(2), 29-45.

Watanabe, D., & Nakanishi, S. (2003). mGluR2 Postsynaptically Senses Granule Cell Inputs at Golgi Cell Synapses. Neuron, 39(5), 821–829. https://doi.org/10.1016/S0896-6273(03)00530-0

Watanabe, D., Inokawa, H., Hashimoto, K., Suzuki, N., Kano, M., Shigemoto, R., ... & Nakanishi, S. (1998). Ablation of cerebellar Golgi cells disrupts synaptic integration involving GABA inhibition and NMDA receptor activation in motor coordination. Cell, 95(1), 17-27.

Watanabe, M. (2016). Basket cells. In *Essentials of Cerebellum and Cerebellar Disorders: A Primer For Graduate Students, 195-199*.

Waters, J., & Helmchen, F. (2004). Boosting of action potential backpropagation by neocortical network activity in vivo. *Journal of Neuroscience*, *24*(49), 11127-11136.

Williams, S. R., Christensen, S. R., Stuart, G. J., & Häusser, M. (2002). Membrane potential bistability is controlled by the hyperpolarization‐activated current IH in rat cerebellar Purkinje neurons in vitro. *The Journal of physiology*, *539*(2), 469-483.

Zeilhofer, H. U., Studler, B., Arabadzisz, D., Schweizer, C., Ahmadi, S., Layh, B., ... & Fritschy, J. M. (2005). Glycinergic neurons expressing enhanced green fluorescent protein in bacterial artificial chromosome transgenic mice. *Journal of Comparative Neurology*, *482*(2), 123-141.

Zhang, W., & Linden, D. J. (2006). Long-term depression at the mossy fiber–deep cerebellar nucleus synapse. *Journal of Neuroscience*, *26*(26), 6935-6944.

Zucker, R. S., & Regehr, W. G. (2002). Short-term synaptic plasticity. *Annual review of physiology*, *64*(1), 355-405.

Abbreviations

AC1: Ca sensitive adenylyl cyclase 1

AHP: after depolarization phase

AMP: adenosine monophosphate

AMPA:α-amino-3-hydroxy-5-methyl-4-isoxazolepropionic acid receptors

AMPAR: α-amino-3-hydroxy-5-methyl-4-isoxazole propionic acid receptors

AP: action potential

ATP-Na2: Adenosine 5'-triphosphate, disodium salt

bAP: backpropagating action potential

Ca^{2+}: calcium ions

$CaCl_2$: Calcium chloride

CaMKII: calcium/calmodulin-dependent protein kinase II

CB1: cannabinoid1

CF: climbing fibre

CICR: calcium-induced calcium release

C_m: membrane capacitance

CO_2: carbon dioxide

DAG: diacylglycerol

D-APV: D-2-amino-5-phosphonovalerate

dB: decibel

DCN: the deep cerebellar nuclei

eGFP: enhanced green fluorescent protein

EGTA: ethylene glycol-bis (β-aminoethyl ether) N,N,N',N'-tetraacetic acid

EPSC: excitatory postsynaptic currents

EPSP: excitatory postsynaptic potential

GABA: Gamma-aminobutyric acid

GABAR: Gamma-aminobutyric acid receptor

GFP: green fluorescent protein

GlyT2: glycine transporter type 2

GoC: Golgi cell

GrC: granule cell

GTP-Na2: Guanosine 5′-triphosphate sodium salt hydrate

Hepes: N-2-hydroxyethyl piperazine-N-2-ethanesulphonic acid

Hz: hertz

I_H: slow inward-rectifier H-current

I_{K-AHP} :Ca^{2+} dependent K^+ current mediated by SK-type channels

I_{K-slow}: K^+ current mediated by M-type channels

I_{Na}–p: persistent Na^+ current

ION: inferior olive

IP3: Inositol 1,4,5-trisphosphate receptors

K^+: potassium ions

KCl: potassium chloride

$KH2PO_4$: Monopotassium phosphate

KOH: potassium hydroxide

LTD: long-term synaptic depression

LTP: long-term synaptic potential

MF: mossy fibre

MF-EPSP: excitatory postsynaptic potential evoked stimulating MF

MgCl2: magnesium dichloride

$MgSO_4$: magnesium sulphate

ml:millilitre

MLI: molecular layer interneurons

mM: millimolar

ms:millisecond

mV: millivolt

MΩ: megaohm

Na^+: sodium ions

nAChRs: a7-nicotinic acetylcholine receptors

NaCl: sodium chloride

$NaHCO_3$: sodium bicarbonate

NaOH: sodium hydroxide

NMDA: N-methyl-D-aspartate

NMDAR: N-methyl-D-aspartate receptors

NO: nitric oxide

O_2: oxygen

pA: picoamper

PC: Purkinje cell

PF: parallel fibre

PF-AP: action potential elicited stimulating PF

pH: potential of hydrogen

PKA: protein kinase A

PKC: Protein kinase C

PP1: protein phosphatase1

R_{in}: input resistance

Rs: serial resistance

SEM: standard error

STDP: spike-timing dependent plasticity

st-LTD: spike-timing-dependent long-term synaptic depression

st-LTP: spike-timing-dependent long-term synaptic potentiation

STSP: short- term synaptic plasticity

TBS: theta burst stimulation.

The BCM rule: The Bienenstock-Cooper-Munro rule

UBC: unipolar brush cell

VGCC: voltage-gated calcium channels

V_{hold}: holding potential

VOR: vestibulo-ocular reflex

Δt: time window

μm: micrometre

μM: micron

°C: degree Celsius

7-Cl Kyn: μM 7-chlorokynurenic acid sodium salt